ANALYSES OF TIMOSHENKO THIN - WALLED BEAMS AND FRAMES BY FEM

by

R. V. V. G. KRISHNA MURTY

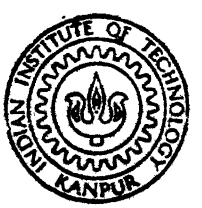

DEPARTMENT OF MECHANICAL ENGINEERING

INDIAN INSTITUTE OF TECHNOLOGY, KANPUR

NOVEMBER, 1988

ANALYSES OF TIMOSHENKO THIN - WALLED BEAMS AND FRAMES BY FEM

A Thesis Submitted
In Partial Fulfilment of the Requirements
for the Degree of
MASTER OF TECHNOLOGY

by

R. V. V. G. KRISHNA MURTY

to the

DEPARTMENT OF MECHANICAL ENGINEERING
INDIAN INSTITUTE OF TECHNOLOGY, KANPUR
NOVEMBER, 1988

DEDICATED

TO

MY PARENTS

CERTIFICATE

This is to certify that the present work Analyses of Timoshenko thin-walled beams and frames by FEM has been carried out by Mr. R.V.V.G. Krishna Murthy under my supervision and it has not been submitted elsewhere for a degree.

Bhupinder Pal Singh. Nov. 18, 88

(BHUPINDER PAL SINGH)
Professor
Department of Mechanical Engineering
I.I.T. KANPUR-208016

November, 1988

ACKNOWLEDGEMENTS

I take the previlage to express my deep sense of gratitude to Prof. B.P. Singh for his guidance and constant encouragement throughout the course of my work. I would be in great debt to Mr. Koppaka Venugopala Rao, who stood on my side in many a difficult situations and made me feel comfortable. I do not find any words to express my gratitude to him and to Mr. Doji Samson. I am very much greatful to my friends, Pokuri, Ramarao, Karra, Raju, Saravan, P.V. Kishore, Vinay Kumar and many other good friends who made my stay here a memorable one. I express my special thanks to Mr. V.K. Mahendraker for his help and encouragement in many ways. My sincere thanks are to Mr. H.V.C. Srivastava for his patient typing and cooperation. I also thank Mr. Bharatwal for oblising my request and making neat drawings.

R.V.V.G. Krishna Murthy

CONTENTS

LIST OF TABLES

LIST OF FIGURES

NOMENCLATURE

The following is the list of some important symbols and notations used in this work.

$u(z,s)$	=	out-of-plane displacement i.e. longitudinal displacement in z- direction.
$v(z,s)$	=	in-plane tangential displacement.
$w(z,s)$	=	in-plane normal displacement.
u_a	=	uniform longitudinal extention of the cross-section
u_x, u_y	=	displacement of a point B(Fig.2) along x and y axes
θ_x, θ_y	=	rotations at the point B about x and y axes
θ_z	=	angle of twist of the cross-section
ϕ	=	θ'_{z_b} and is a measure of warping
x,y	=	coordinates of point A
p,q	=	perpendicular distances from the point B to the tangent and normal at point A respectively.
ω	=	warping function (sectorial coordinate).
t	=	thickness of the profile
Ψ	=	torsional function
T	=	shear flow
G	=	shear modulus

$(')$	=	differentiation wrt z-coordinate
$(-)$	=	differentiation wrt s-coordinate
T	=	kinetic energy of the beam
U	=	strain energy of the beam
σ_z	=	normal stress
τ_{zs}	=	shear stress
$(.)$	=	differentiation wrt time
ρ	=	mass density of the beam
E	=	modulus of elasticity
A	=	area of the cross-section
I_{yy}	=	second moment of area about y-axis
I_{xx}	=	second moment of area about x-axis
$I_{\omega\omega}$	=	sectorial moment of inertia
I_d	=	torsional constant
I_{rr}	=	warping rotational moment of inertia
I_{pp}	=	shear area about x-axis
I_{qq}	=	shear area about y-axis
I_{rp}	=	shear area moment about x-axis
I_{rq}	=	shear area moment about y-axis
I_{pq}	=	mixed shear area

I_B	=	polar moment of inertia of the cross section about the center of shear
δ	=	variation
(e)	=	denotes the typical element
$\lfloor \ \rfloor$	=	row vector
$\{ \}$	=	column vector
(ne)	=	at the nodes of typical element
$[\ ]$	=	square matrix
$[\ ]^T$	=	transpose of matrix
$\lfloor N \rfloor$	=	interpolation functions
$\lceil M \rceil^{(e)}$	=	mass matrix of the element
$[K]^{(e)}$	=	stiffness matrix of the element
$\{U\}^{(ne)}$	=	displacement vector of the element
$\{F\}^{(ne)}$	=	boundary force vector of the element
U_e	=	work done by external forces
q_x, q_y and q_z	=	line loads per unit length of the beam in the x,y and z directions respectively
m_t, m_x, m_y, m_ω	=	applied torsional moment bending moment (about x),bending moment (about y) and bimoments per unit length of the beam.

Θ_x, Θ_y and Θ_z	=	concentrated load in the x,y and z directions respectively
M_t, M_x, M_y and M_ω	=	concentrated torsional torsional moment, bending moment (about x), bending moment (about y) , and bimoments.
$\delta(z-\bar{z})$	=	Dirac delta function for concentrated loads and moments.
$\{Q\}^{(ne)}$	=	load vector of the element
u_{x_B}, u_{y_B}	=	the displacements of pole B in the x and y-directions respectively
x_B, y_B	=	coordinates of the pole B
α	=	angle of tangent at A with the x-axis
p_o	=	the perpendicular distance from the point O to the targent at point A
q_o	=	the perpendicular distance from the point O to the normal at point A
x_A, y_A	=	coordinates of the point A
(x_q, y_q)	=	coordinates of the point of loading
$[T]$	=	transformation matrix
M_{xx}	=	bending moment
M_ω	=	bimoment
$\omega(s_E)$	=	warping function

Q_y = shear force

I_x = statical moment about x-axis

t = thickness of the profile

M_t = warping twisting moment or flexural twist

$I_\omega(s_E)$ = statical sectorial moment

M_{st} = Saint Venant twisting moment

J_s = Saint venant torsional constant of the section

σ_ω = warping normal stress

τ_ω = warping shear stress

SYNOPSIS

In this work free vibration, static and buckling analyses of thin-walled beams are done. The effects of warping, rotary inertia and shear deformation on the frequencies and displacements are studied. Effect of warping on the critical buckling loads is studied. Monosymmetric and unsymmetric cross sectional beams are considered. Torsional analysis of a box section and tapered I-section beams is also done. Plane frames are analysed for static and free vibration cases.

The governing differential equations are derived from the variational principles, and are non-dimensionalised. The finite element method is used to solve these equations. The field variables are approximated over the elements by polynomials The residues obtained are minimized by the Galerkin method. Gauss quadrature is used for obtaining the elemental matrices. The elemental matrices are assembled to get the global matrices and these are solved for frequencies, displacements and critical buckling loads, for various boundary conditions. Equations of the plane frames in the global coordinates are obtained by using transformation matrices.

While considering shear effects, FEM solutions are obtained from six coupled second order differential equations as this enabled to satisfy the geometrical and natural boundary conditions.Three coupled fourth order differential equations are used when the shear effects are neglected.

The effect of warping, rotary inertia, and shear on the frequencies of vibration is studied. A little parametric study is done with the non-dimensionalised parameters. In the case of tapered beams the effect of taper on the displacements is studied.

In the case of plane frames the effect of warping and configuration of the beams on the displacements and stresses is studied. Frequencies of vibration of plane frames are obtained, when the effects of warping and rotary inertia are taken into account.

CHAPTER- I

INTRODUCTION

It is very difficult to define precisely a thin walled beam. One may say that it is an assembly of thin plates joined along their edges. The plate thicknesses are small compared to the cross-sectional dimensions, and cross sectional dimensions inturn are small compared to the length of the beam. Thin walled beams have lot of applications in the field of engineering owing to their high strenth to low weight ratio.

The major application of the thin-walled beams is in the aircraft industry, ship structures, cranes, bridge construction, storage racks, railway wagons and coaches. Thin-walled beams can be used for different purposes depending upon the design requirements. The beams can be used as closed section box girders to give more torsional rigidity and as open section plate girders to give low torsional rigidity.

In thin-walled beams the shear stresses and strains are relatively much larger than those in solid beams. When a thin-walled beam is twisted, there is an out of plane distortion of the cross section of the beam in the direction of the beam axis, called warping. This violates the Bernoulli'

hypothesis (plane sections remain plane over the entire cross section). If the warping of the cross section is restraine it results in producing normal stresses in the axial direction and shear stresses in the cross section. These stresses are called the warping normal stress (σ_ω) and warping shear stress (τ_ω) or in short warping stresses. These warping stresses are as large as or even larger than the bending stresses and can not be ignored. Thus the thin-walled beams have to be treated in a special manner and a separate theory has been developed to analyse these beams, i.e., Vlasov's theory for the th walled beams. It is more general theory than the Bernoulli's theory and is based on the law of sectorial areas and treats the plane sections case as a special case. Two new concepts, bimoment and warping twisting moment, were introduced by Vlasov's theory to explain the warping phenomena and the stresse developed there in.

In the case of thin-walled beams there can be a local buckling, if the inplane stresses reach their critical values. This changes the geometry of the cross section of the beam in contrast to the over all buckling where the geometry of the cross section is retained. If the thin-walled beam is sufficient long then over all buckling occurs before local buckling can occur. In some cases these two bucklings can interact and in those cases the buckling load will be less than the individu buckling loads. Thus the thin-walled beams have to be designed for both overall and local bucklings.

There is an important phenomena of coupled flexure and torsion which occurs in the thin-walled beams of mono and unsymmetric cross section beams. This phenomena can be explained with respect to the shear center. Shear center is a point through which the transverse shear loads and supports should act, rather than through the centroid of the cross section, if no torsion is to result. Hence if the shear center does not coincide with the centroid of the cross section (e.g. mono-symmetric and unsymmetric cross sections) and if the transverse loads act through the centroid, then there exists a coupling between flexure and torsion.

1.1 PREVIOUS WORK :

The coupled flexure and torsion, which is an interesting phenomena of thin-walled beams, has been studied by many workers and researchers in this field.

Lot of work was done on the static analysis of thin-walled beams. Number of books are available in the literature. Vlasov [1] in his very comprehensive famous book "Thin-Walled Elastic Beams" developed his theory for static, stability and dynamics for thin-walled straight and curved beams. Among the some other important books dealing with static analyses are Murray [2] , Gjelsvik [3], Megson [4] and Zbirohowski [5].

In his book, Murray [2] derived the equilibrium equations for bending and torsion of thin-walled beams by first order theory. The equations were derived by both equilibrium and energy methods. Some examples on torsional analysis of thin-walled beams were solved.

Gjelsvik [3] discussed the torsion and flexure of thin-walled bars of open and closed cross sections. The section properties and important features of regular sections were discussed.

The books by Megson [4] and Zbirohowski [5] also discussed many aspects of thin-walled beams, under static loading.

A finite element formulation for thin-walled beams was given by Gunnlaugsson [6] . In this work the governing equilibrium equations were drived by including the deformation due to shear. A transformation matrix was given in the work to change the local nodal parameters to the global nodal parameters in order to achieve the compatibility between the two adjacent elements, whose centroidal axes and axes of twist do not coincide.

A torsional stiffness matrix was derived by Chen and Hu [7] , for a thin-walled beam based on the warping displacement assumption. Also the general stiffness matrix for a beam under simultaneous torsion, bending and tension was derived for the coupled torsion-bending analysis.

A transformation matrix to change the local coordinates of an element to the global system was given in their work. The correctness of this was checked for a thin walled beam of rectangular box cross section under uniform distributed torque.

Wekezer [8] applied the finite element method to the theory of thin-walled bars of variable cross sections in torsional analysis. The solution of the problem was based on the linear membrane shell theory with the application of Vlasov's assumptions. He divided the bar into elements along its longitudinal axis and then approximated the shell mid surface of the element by arbitrary triangular sub-elements.

There has been little work in the dynamic analysis of thin-walled beams under coupled flexure and torsion. Vlasov [1], did work on coupled flexural torsional vibrations of thin walled beams including the effects of warping and rotary inertia. The applicability of this coupled flexure and torsion to many practical problems was considered by many researchers using analytical as well as numerical methods. The tripled coupled flexural and torsional vibrations of thin-walled beams were derived by Gere and Lin [9] based on the development given by Timoshenko [10] for double coupling. The effects of rotary inertia and shear deformation were neglected. The effect of warping was taken into account.

Bishop and Price [15] solved the equation of coupled bending and twisting of a Timoshenko beam. The effects of shear deflection and rotary inertia in bending for an unsymmetric beam were included. The mode shapes and the orthogonality conditions were obtained.

The effects of shear deformation, rotary inertia and warping were considered by Tso [16], in the coupled flexural torsional vibrations of thin-walled beams. The governing equations of motion were derived by variational principles. The coupled frequencies of vibrations of a monosymmetric cross section beam were obtained by analytical methods. Tso discussed the effect of shear and rotary inertia on the frequencies.

The coupled flexural torsional buckling of thin walled columns has been considered by many workers. The books dealing this topic are Timoshenko and Gere [17], Vlasov [1] and Murray [2]. These obtained the governing equations for the coupled flexural torsional buckling by the equilibrium method. The equations for monosymmetric and unsymmetric section beams were solved by exact methods. Critical load equations for monosymmetric and unsymmetric section beams, with any end conditions were given, as functions of uncoupled critical buckling loads in flexure and torsion.

The analysis of a plane frame was considered by many workers in the past. Martin [18], gave the transformation matrices for Euler beam elements, in order to change the local coordinates to the global system. The static problem

solved by direct stiffness and flexibility methods.

Nosseir and Dickinson [19] applied the finite element method to the free vibration analysis of a model of a car body. They approximated the chassis, under body and full body of a car with ordinary beam elements and panels. The out of plane vibrations were considered. Because of the symmetry of the frame, only one half of the model was analysed with appropriate boundary conditions along the axis of symmetry.

Finite element techniques were applied by Ali, Hedges, Mills, Norville and Gurdogan[20] to the analysis of an automobile structure. The static, stress and dynamic analyses were done on an automobile chassis frame. Ordinary beam elements were used in the approximation of the frame.

1.2 PRESENT WORK :

In the present work the Galerkin finite element method is used to solve the more familiar differential equation of the thin-walled beams and frames. First the equations of motion of a thin-walled beam of unsymmetric cross section with variable area were derived by variational principles, including the effects of warping, rotary inertia and shear for completeness sake. The effect of these quantities on the coupled frequencies of vibration is studied, for various end

conditions. Non-dimensionalisation is done for the governing equations and a limited parametric study is done with respect to these non-dimensionalised parameters. Results for both monosymmetric and unsymmetric cross section beams are obtained in this work.

Static equilibrium equations for a general unsymmetric section of a thin walled beam are derived for completeness sake, including the effects of warping and shear. The coupled equations are solved for various end conditions, to get the coupled displacements and rotations of thin-walled beams of monosymmetric as well as unsymmetric sections. Torsional analysis of a cantilever of a rectangular box section and a tapered cantilever of I-section is done. In the case of tapered cantilever, the equations of equilibrium derived for a variable area are used.

Coupled flexural torsional buckling equation for an unsymmetric section with variable area are derived by variational principles. The coupled equations are solved for an unsymmetric section column with various end conditions.

A transformation matrix is derived for transforming displacements in local coordinates to the displacements in global coordinates for using in the plane frame analyses. A plane frame is analysed for static and free vibration cases.

Thus the principal objective of this work is to study the effects of rotary inertia and shear deformation in thin-walled beams and frames in static, free vibration and buckling cases.

CHAPTER- II

BASIC AND FEM EQUATIONS

In this chapter governing differential equations of thin walled beams for the following cases are derived from the variational principle.

Free vibrations

Static analysis

Buckling analysis

Plane frame

These equations are for variable cross-sections and are non dimensionalised. The equations account for warping, rotatory inertia and shear deformation. Their FEM equations are obtained using Galerkin method.

2.1 FREE VIBRATIONS OF THIN WALLED BEAMS :

Equations of motion have been drived for a thin-walled beam as shown in Fig. 1. The origin of the axes is at the center of gravity (C.G) of the cross-sections and xy-axes are its principal axes. The z- axis is in the direction of the beam axis.

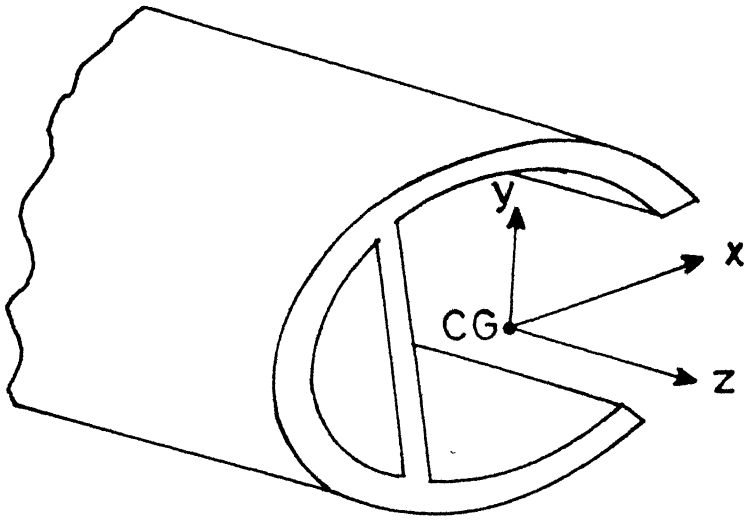

Fig.1 Thin-Walled Beam.

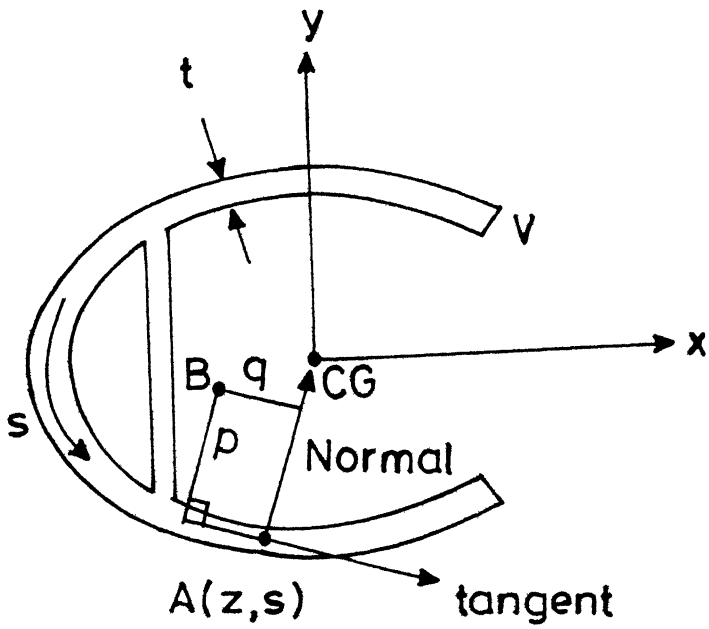

Fig. 2 Thin-Walled Beam Cross-Section.

The following are the assumptions made in deriving the Equations [2,6,16,21]

1. The deformations are small compared with the structural dimensions.
2. The beam is straight before loading and there is no local buckling.
3. The thickness of the cross section of the beam is small compared to the cross sectional dimensions.
4. When a thin-walled beam is bent and twisted its cross section remains undeformed in its own plane, but rotates about the flexural axis (locus of the centres of shear) as a rigid body.

2.1.1 <u>The in plane and out-of-plane displacements of a point on the cross-section</u> :

Based on the assumptions made above, the displacement field for a point A on the cross-section (Fig. 2) is, Eqns. (A-34), [2,6]

$$u(z,s) = u_a - \theta_y\, x + \theta_x y - \phi\omega \qquad \ldots\ (1)$$

$$v(z,s) = u_x\, \bar{x} + u_y\, \bar{y} + p\theta_z \qquad \ldots\ (2)$$

$$w(z,s) = -u_x\, \bar{y} + u_y\, \bar{x} + q\theta_z \qquad \ldots\ (3)$$

Here

$u(z,s)$ = out-of-plane displacement i.e. longitudinal displacement in z-direction,

$v(z,s)$ = in-plane tangential displacement,

$w(z,s)$ = in-plane normal displacement,

u_a = uniform longitudinal extention of the cross-section

u_x, u_y = displacement of a point B (Fig. 2) along x and y axes,

θ_x, θ_y = rotations at the point B about x and y axes,

θ_z = angle of twist of the cross-section,

ϕ = θ'_{z_b} and is a measure of warping

x,y = coordinates of point A

p,q = perpendicular distances from the point B to the tangent and normal at point A respectively.

ω = warping function (sectorial coordinate) and is, Eqns. (A-31), [2].

$$\omega = \int_0^s \left(p - \frac{\Psi}{t}\right) ds \quad \text{for closed profiles} \qquad \ldots\ (4)$$

$$\omega = \int_0^s p\, ds \quad \text{for open profiles}$$

t = thickness of the profile

Ψ = torsional function and is, Eqns. (A-29), [2]

or $$\Psi = \frac{T}{G\,\theta'_z} \qquad \ldots\ (5)$$

T = shear flow

G = shear modulus

In the above a prime ($'$) denotes differentiation wrt. z-coordinate and over dash ($-$) indicates differentiation wrt. s-coordinate.

2.1.2 The Kinetic and strain energies of the beam :

In obtaining the expresions for kinetic and strain energies the following assumptions are made

(i) The material of the beam is isotropic, homogeneous and linearly elastic.

(ii) The longitudinal stress σ_z and the in-plane shear stress τ_{zs} are the only significant stresses in the beam. Other stresses σ_{nn}, σ_{ss}, τ_{zn} and τ_{sn} are negligible.

These expressions and the corresponding fourth order differential equations were derived by [16] for uniform cross-sections . Here second order differential equations are derived for variable cross-sections.

The kinetic energy of the beam can be written as

$$T = \frac{1}{2} \int_0^l \int_A \rho \left(\left(\frac{\partial u}{\partial t}\right)^2 + \left(\frac{\partial v}{\partial t}\right)^2 + \left(\frac{\partial w}{\partial t}\right)^2 \right) dA\, dz \quad .... (6)$$

where ρ is the mass density of the beam.

With the above assumptions in the mind, the strain energy of the beam can be written as

$$U = \frac{1}{2} \int_0^l \int_A \left(E\left(\frac{\partial u}{\partial z}\right)^2 + G\left(\frac{\partial v}{\partial z} + \frac{\partial u}{\partial s}\right)^2 \right) dA\, dz \quad .... (7)$$

Where E is the modulus of elasticity and G is the modulus of rigidity.

Substituting the expressions of u,v and w from the Eqns. (1) to (3) in the Eqns. (6) and (7), one gets

$$T-U= \frac{1}{2}\int_0^l \Big\{ \rho \Big[\int_A \dot{u}_a^2\, dA + \dot{\theta}_y^2 \int_A x^2 dA - 2\dot{u}_a \dot{\theta}_y \int_A x\, dA + \dot{\theta}_x^2 \int_A y^2 dA$$

$$+ \dot{\phi}^2 \int_A \omega^2 dA - 2\dot{\theta}_x \dot{\phi} \int_A y\omega dA + 2\dot{u}_a \dot{\theta}_x \int_A y dA$$

$$-2\dot{\theta}_x \dot{\theta}_y \int_A xy\, dA - 2\dot{u}_a \dot{\phi} \int_A \omega dA + 2\dot{\theta}_y \dot{\phi} \int_A x\omega dA + \dot{u}_x^2 \int_A (\bar{x}^2+\bar{y}^2) dA$$

$$+ \dot{u}_y^2 \int_A (\bar{x}^2+\bar{y}^2) dA + \dot{\theta}_z^2 \int_A (p^2+q^2) dA + 2\dot{u}_y \dot{\theta}_z \int_A (x-x_B) dA$$

$$-2\dot{u}_x \dot{\theta}_z \int_A (y-y_B) dA \Big] \Big]$$

$$-E \Big[u_a'^2 \int_A dA + \theta_y'^2 \int_A x^2 dA - 2u_a' \theta_y' \int_A x dA + \theta_x'^2 \int_A y^2 dA + \phi'^2 \int_A \omega^2 dA$$

$$-2\theta_x' \phi' \int_A y\omega dA + 2u_a' \theta_x' \int_A y dA - 2\theta_x' \theta_y' \int_A xy dA -$$

$$-2u_a' \phi' \int_A w dA + 2\theta_y' \phi' \int_A x\omega dA \Big]$$

$$-G \Big[(u_x'-\theta_y)^2 \int_A \bar{x}^2 dA + (u_y'+\theta_x)^2 \int_A \bar{y}^2 dA + (\theta_z'-\phi)^2 \int_A p^2 dA$$

$$+ 2(u_x'-\theta_y)(u_y'+\theta_x) \int_A \bar{x}\bar{y}\, dA + 2(u_y'+\theta_x)(\theta_z'-\phi) \int_A \bar{y}\, p\, dA$$

$$+ 2(\theta_z'-\phi)(u_x'-\theta_y) \int_A \bar{x}\, p\, dA + \phi^2 \int_A \frac{\Psi^2}{t^2} dA + 2(u_x'-\theta_y)\phi \int_A \frac{\Psi}{t} \bar{x}\, dA$$

$$+2(u_y'+\theta_x)\phi \int_A \frac{\Psi}{t} \bar{y}\, dA + 2(\theta_z'-\phi)\phi \int_A \frac{\Psi}{t} \Big(\bar{\omega} + \frac{\Psi}{t}\Big) dA \Big] \Big\} dz$$

.... (8)

Dot (.) represents differentiation wrt time

As the origin of the principal axes, xy, is at the centroid of the cross-section, of the beam, one has

$$\text{First moment of area about y-axis} = I_y = \int_A x\, dA = 0$$

$$\text{First moment of area about x-axis} = I_x = \int_A y\, dA = 0$$

$$\text{Product moment of inertia} = I_{xy} = \int_A xy\, dA = 0 \qquad \ldots\ (9)$$

If point B (Fig. 2) is centre of shear, then the following quantities are zero [3] , see Appendix II.

$$\text{Sectorial product area about x-axis} = I_{\omega x} = \int \omega y\, dA = 0$$

$$\text{Sectorial product area about y-axis} = I_{\omega x} = \int \omega x\, dA = 0 \qquad \ldots\ (10)$$

Since in the calculation of the warping function (sectional coordinate) the starting point V (Fig. 2) is arbitrary, it can be chosen such that

$$\text{First moment of sectorial area about center of shear} = I_\omega = \int_A \omega dA = 0 \qquad \ldots\ (11)$$

By Leibnitz rule [22] and using Eqns. (9) and (11), the following three integrals of Eqn. (8) become zero

$$\int_A \frac{\Psi}{t} \bar{x}\, dA = \frac{\Psi}{t} \int_A \frac{dx}{ds} dA = \frac{\Psi}{t} \frac{d}{ds} \int_A x\, dA = 0$$

$$\int_A \frac{\Psi}{t} \bar{y}\, dA = \frac{\Psi}{t} \int_A \frac{dy}{ds} dA = \frac{\Psi}{t} \frac{d}{ds} \int_A y\, dA = 0 \qquad \ldots\ (12)$$

$$\int_A \frac{\Psi}{t} \bar{\omega}\, dA = \frac{\Psi}{t} \int_A \frac{dw}{ds} dA = \frac{\Psi}{t} \frac{d}{ds} \int_A \omega\, dA = 0$$

Various quantities of Eqn. (8) are defined as follow

Area of the cross-section = $A = \int_A dA$

Second moment of Area about y-axis= $I_{yy} = \int_A x^2 dA$

Second moment of Area about x-axis = $I_{xx} = \int_A y^2\, dA$

Sectorial moment of inertia = $I_{\omega\omega} = \int_A \omega^2 dA$ .... (13)

Torsional constant = $I_d = \int_A \frac{\Psi^2}{t^2} dA$

Warping rotational moment of inertia= $I_{rr} = \int_A p^2 dA$

Shear area about x-axis = $I_{pp} = \int_A \bar{y}^2\, dA$

Shear area about y-axis = $I_{qq} = \int_A \bar{x}^2\, dA$

Shear area moment about x-axis= $I_{rp} = I_{pr} = \int_A p\bar{y}\, dA$

Shear area moment about y-axis= $I_{rq} = I_{qr} = \int_A p\, \bar{x}\, dA$

Mixed shear area = $I_{pq} = I_{qp} = \int_A \bar{x}\, \bar{y}\, dA$

Polar moment of inertia of the cross section about the center of shear = $I_B = \int_A (p^2+q^2)\, dA$

Using Eqns. (9) to (13), Eqn. (8) becomes

$$T-U=\frac{1}{2}\int_0^1 \{\rho[A\,\dot{u}_a^2+I_{yy}\dot{\theta}_y^2+I_{xx}\dot{\theta}_x^2+I_{\omega\omega}\dot{\phi}^2+A\,\dot{u}_x^2+A\,\dot{u}_y^2+I_B\,\dot{\theta}_z^2$$

$$-2A\,x_B\dot{u}_y\dot{\theta}_z+2A\,y_B\dot{u}_x\dot{\theta}_z\,]-E\,[A\,u_a'^2+I_{yy}\theta_y'^2+I_{xx}\theta_x'^2+I_{\omega\omega}\phi'^2]$$

$$-G\,[I_{qq}(u_x'-\theta_y)^2+I_{pp}(u_y'+\theta_x)^2+I_{rr}(\theta_z'-\phi)^2$$

$$+2I_{pq}(u_x'-\theta_y)(u_y'+\theta_x)$$

$$+2I_{rp}(u_y'+\theta_x)(\theta_z'-\phi)+2I_{rq}(\theta_z'-\phi)(u_x'-\theta_y)+I_d\,\phi^2$$

$$+2I_d(\theta_z'-\phi)\,\phi]\}dz \quad \ldots\ (14)$$

2.1.3 Basic Equations :

Applying Hamilton's principle to Eqn. (14) and taking the variation one gets the seven equations of motion associated, with δu_a, δu_x, $\delta\theta_y$, δu_y, $\delta\theta_x$, $\delta\theta_z$, $\delta\phi$ and the corresponding boundary conditions, as

$$\frac{\partial}{\partial z}(EA\,u_a')-\frac{\partial}{\partial t}(\rho A\,\dot{u}_a)=0 \quad \ldots\ (15)$$

$$\frac{\partial}{\partial z}(G\,I_{qq}(u_x'-\theta_y))+\frac{\partial}{\partial z}(G\,I_{qp}(u_y'+\theta_x))$$

$$+\frac{\partial}{\partial z}(GI_{qr}(\theta_z'-\phi))-\frac{\partial}{\partial t}(\rho A\dot{u}_x)-\frac{\partial}{\partial t}(\rho A\,y_B\dot{\theta}_z)$$

$$=0 \quad \ldots\ (16)$$

$$\frac{\partial}{\partial z}(EI_{yy}\theta_y')+GI_{qq}(u_x'-\theta_y)+GI_{qp}(u_y'+\theta_x)+GI_{qr}(\theta_z'-\phi)-\frac{\partial}{\partial t}(\rho I_{yy}\dot{\theta}_y) = 0$$

.... (17)

$$\frac{\partial}{\partial z}(GI_{pp}(u_y'+\theta_x))+\frac{\partial}{\partial z}(GI_{pq}(u_x'-\theta_y))+\frac{\partial}{\partial z}(GI_{pr}(\theta_z-\phi))$$

$$-\frac{\partial}{\partial t}(\rho A\,\dot{u}_y)+\frac{\partial}{\partial t}(\rho A\,x_B\dot{\theta}_z) = 0$$

.... (18)

$$\frac{\partial}{\partial z}(EI_{xx}\theta_x')-GI_{pp}(u_y'+\theta_x)-GI_{pq}(u_x'-\theta_y)-GI_{pr}(\theta_z'-\phi)-\frac{\partial}{\partial t}(\rho I_{xx}\dot{\theta}_x) = 0$$

.... (19)

$$\frac{\partial}{\partial z}(GI_{rr}(\theta_z'-\phi))+\frac{\partial}{\partial z}(GI_{rp}(u_y'+\theta_x))+\frac{\partial}{\partial z}(GI_{rq}(u_x'-\theta_y))+\frac{\partial}{\partial z}(GI_d\phi)$$

$$-\frac{\partial}{\partial t}(\rho I_B\dot{\theta}_z)+\frac{\partial}{\partial t}(\rho A\,x_B\dot{u}_y)-\frac{\partial}{\partial t}(\rho A\,y_B\dot{u}_x) = 0$$

.... (20)

$$\frac{\partial}{\partial z}(E\,I_{\omega\omega}\,\phi')+GI_{rr}(\theta_z'-\phi)+GI_{rp}(u_y'+\theta_x)+GI_{rq}(u_x'-\theta_y)-GI_d(\theta_z'-\phi)$$

$$-\frac{\partial}{\partial t}(\rho I_{\omega\omega}\,\phi) = 0$$

.... (21)

and boundary conditions as

$$EA\,u_a'\,\delta u_a\Big|_o^l = 0 \qquad \text{.... (22)}$$

$$[\,G\,I_{qq}(u_x'-\theta_y)+G\,I_{qp}(u_y'+\theta_x)+G\,I_{qr}(\theta_z'-\phi)\,]\,\delta u_x\Big|_o^l = 0$$

.... (23)

$$EI_{yy}\,\theta_y'\,\delta\theta_y\Big|_o^l = 0 \qquad \text{.... (24)}$$

$$[GI_{pp}(u_y'+\theta_x) + G I_{pq}(u_x'-\theta_y) + G I_{pr}(\theta_z'-\phi)]\delta u_y \Big|_o^l = 0$$

.... (25)

$$E I_{xx}\,\theta_x'\,\delta\theta_x \Big|_o^l = 0 \qquad \text{.... (26)}$$

$$[G I_{rr}(\theta_z'-\phi) + G I_{rp}(u_y'+\theta_x) + G I_{rq}(u_x'-\theta_y) + GI_d\,\phi]\delta\theta_z \Big|_o^l = 0$$

.... (27)

$$EI_{ww}\,\phi'\delta\phi \Big|_o^l = 0 \qquad \text{.... (28)}$$

In the case of open profiles Saint Venant torsional constant is to be used for I_d in Eqns (20), (21) and (28).

In the above equations

EAu_a' = Extensional force

$[GI_{qq}(u_x'-\theta_y)+GI_{qp}(u_y'+\theta_x)+GI_{qr}(\theta_z'-\phi)]$ = Shear force in x-directio

$EI_{yy}\,\theta_y'$ = Bending moment about y-axis

$[GI_{pp}(u_y'+\theta_x)+GI_{pq}(u_x'-\theta_y)+GI_{pr}(\theta_z'-\phi)]$ = Shear force in y-direction

$EI_{xx}\,\theta_x'$ = Bending moment about x-axis

$[GI_{rr}(\theta_z'-\phi)+GI_{rp}(u_y'+\theta_x)+GI_{rq}(u_x'-\theta_y)+GI_d\phi]$ = warping twisting moment.

$EI_{ww}\,\phi'$ = Bimoment

2.1.4 Non-Dimensionalisation of equations and B.C.

The following parameters (denoted by capital letters) are used to non-dimensionalise the equations of motion, Eqns. (15) to (21)

$$\frac{z}{l} = Z \; ; \; \frac{u_a}{l} = U_a \; ; \; \frac{u_x}{l} = U_x$$

$$\frac{u_y}{l} = U_y \; ; \; \frac{u_z}{l} = U_z \; ; \; l\phi = \bar{\Phi} \; ; \; \frac{y_B}{l} = Y_B \; ; \; \frac{x_B}{l} = X_B$$

$$t\sqrt{\frac{E}{\rho l^2}} = T \; ; \; \frac{A}{A_o} = A_n \; ; \; I_{yy_n} = \frac{I_{yy}}{I_{yy_o}} \; ; \; I_{xx_n} = \frac{I_{xx}}{I_{xx_o}}$$

$$I_{qq_n} = \frac{I_{qq}}{I_{qq_o}} \; ; \; I_{qp_n} = \frac{I_{qp}}{I_{qp_o}} \; ; \; I_{qr_n} = \frac{I_{qr}}{I_{qr_o}}$$

$$I_{pp_n} = \frac{I_{pp}}{I_{pp_o}} \; ; \; I_{pq_n} = \frac{I_{pq}}{I_{pq_o}} \; ; \; I_{pr_n} = \frac{I_{pr}}{I_{pr_o}} \qquad \ldots\ (29)$$

$$I_{rr_n} = \frac{I_{rr}}{I_{rr_o}} \; ; \; I_{rp_n} = \frac{I_{rp}}{I_{rp_o}} \; ; \; I_{rq_n} = \frac{I_{rq}}{I_{rq_o}}$$

$$I_{\omega\omega_n} = \frac{I_{\omega\omega}}{I_{\omega\omega_o}} \; ; \; I_{dn} = \frac{I_d}{I_{d_o}} \; ; \; I_{B_n} = \frac{I_B}{I_{B_o}}$$

Here the quantities with subscript o represent the section properties at z = o (one extreme end of the beam) and the quantities with subscript n are the non-dimensionalised section properties.

With these parameters equations of motion become

$$\frac{\partial}{\partial z}(A_n U_a') - A_n \ddot{U}_a = 0 \qquad \ldots\ (30)$$

$$\frac{Re_{yy}^2}{Se_{qq}^2} \frac{\partial}{\partial z}(I_{qq_n}(u_x' - \theta_y)) + \frac{Re_{yy}^2}{Se_{qp}^2} \frac{\partial}{\partial z}(I_{qp_n}(u_y' + \theta_x)) + \frac{Re_{yy}^2}{Se_{qr}^2} \frac{\partial}{\partial z}(I_{qr_n}(\theta_z - \bar{\Phi})) - A_n \ddot{U}_x - Y_B A_n \ddot{\theta}_z = 0 \qquad \ldots\ (31)$$

$$\frac{\partial}{\partial z}(I_{yy_n}\theta'_y)+\frac{1}{Se^2_{qq}}I_{qq_n}(U'_x-\theta_y)+\frac{1}{Se^2_{qp}}I_{qp_n}(U'_y+\theta_x)$$

$$+\frac{1}{Se^2_{qr}}I_{qr_n}(\theta'_z-\Phi)-I_{yy_n}\ddot{\theta}_y = 0$$

.... (32)

$$\frac{Re^2_{xx}}{Se^2_{pp}}\frac{\partial}{\partial z}(I_{pp_n}(U'_y+\theta_x))+\frac{Re^2_{xx}}{Se^2_{pq}}\frac{\partial}{\partial z}(I_{pq_n}(U'_x-\theta_y))$$

$$+\frac{Re^2_{xx}}{Se^2_{pr}}\cdot\frac{\partial}{\partial z}(I_{pr_n}(\theta'_z-\Phi))-A_n\ddot{U}_y+X_B A_n\ddot{\theta}_z = 0$$

.... (33)

$$\frac{\partial}{\partial z}(I_{xx_n}\theta'_x)-\frac{1}{Se^2_{pp}}I_{pp_n}(U'_y+\theta_x)-\frac{1}{Se^2_{pq}}I_{pq_n}(U'_x-\theta_y)$$

$$-\frac{1}{Se^2_{pr}}I_{pr_n}(\theta'_z-\Phi)-I_{xx_n}\ddot{\theta}_x = 0$$

.... (34)

$$\frac{Re^2_{\omega\omega}}{Se^2_{rr}}\frac{\partial}{\partial z}(I_{rr_n}(\theta'_z-\Phi))+\frac{Re^2_{\omega\omega}}{Se^2_{rp}}\frac{\partial}{\partial z}(I_{rp_n}(U'_y+\theta_x))$$

$$+\frac{Re^2_{\omega\omega}}{Se^2_{rq}}\frac{\partial}{\partial z}(I_{rq_n}(U'_x-\theta_y))+\frac{Re^2_{\omega\omega}}{\omega e^2}\frac{\partial}{\partial z}(I_{d_n}\Phi)$$

$$-Re^2_B I_{B_n}\ddot{\theta}_z+X_B A_n\ddot{U}_y-Y_B A_n\ddot{U}_x = 0$$

.... (35)

$$\frac{\partial}{\partial z}(I_{\omega\omega_n}\Phi') + \frac{1}{Se_{rr}^2} I_{rr_n}(\theta_z' - \Phi) + \frac{1}{Se_{rp}^2} I_{rp_n}(U_y' + \theta_x)$$

$$+ \frac{1}{Se_{rq}^2} I_{rq_n}(U_x' - \theta_y) - \frac{1}{\omega_e^2} I_{d_n}(\theta_z' - \Phi) - I_{\omega\omega_n}\ddot{\Phi} = 0$$

.... (36)

where

$$Re_{yy}^2 = \frac{I_{yy_o}}{A_o l^2} \; ; \; Se_{qq}^2 = \frac{EI_{yy_o}}{GI_{qq_o} l^2}$$

$$Se_{qp}^2 = \frac{EI_{yy_o}}{GI_{qp_o} l^2} \; ; \; Se_{qr}^2 = \frac{EI_{yy_o}}{GI_{qr_o} l^2}$$

$$Re_{xx}^2 = \frac{I_{xx_o}}{A_o l^2} \; ; \; Se_{pp}^2 = \frac{EI_{xx_o}}{GI_{pp_o} l^2}$$

$$Se_{pq}^2 = \frac{EI_{xx_o}}{GI_{pq_o} l^2} \; ; \; Se_{pr}^2 = \frac{EI_{xx_o}}{GI_{pr_o} l^2} \quad .... (37)$$

$$Re_{\omega\omega}^2 = \frac{I_{ww_o}}{A_o l^4} \; ; \; Se_{rr}^2 = \frac{EI_{\omega\omega_o}}{GI_{rr_o} l^2}$$

$$Se_{rp}^2 = \frac{EI_{\omega\omega_o}}{GI_{rp_o} l^3} \; : \; Se_{rq}^2 = \frac{EI_{\omega\omega_o}}{GI_{rq_o} l^3}$$

$$\omega e^2 = \frac{EI_{\omega\omega_o}}{GI_{do} l^2} \; ; \; Re_B^2 = \frac{I_{B_o}}{A_o l^2}$$

Similarly using the Eqns. (29), the boundary conditions (Eqns. (22) to (28)) become

$$A_n \, U_a' \, \delta U_a \Big|_0^1 = 0 \quad \ldots\ldots (38)$$

$$\left[\frac{1}{Se_{qq}^2} I_{qq_n}(U_x' - \theta_y) + \frac{1}{Se_{qp}^2} I_{qp_n}(U_y' + \theta_x) + \frac{1}{Se_{qr}^2} I_{qr_n}(\theta_z' - \Phi) \right] \delta U_x \Big|_0^1 = 0 \quad \ldots\ldots (39)$$

$$I_{yy_n} \, \theta_y' \, \delta\theta_y \Big|_0^1 = 0 \quad \ldots\ldots (40)$$

$$\left[\frac{1}{Se_{pp}^2} I_{pp_n}(U_y' + \theta_x) + \frac{1}{Se_{pq}^2} I_{pq_n}(U_x' - \theta_y) + \frac{1}{Se_{pr}^2} I_{pr_n}(\theta_z' - \Phi) \right] \delta U_y \Big|_0^1 = 0 \quad \ldots\ldots (41)$$

$$I_{xx_n} \, \theta_x' \, \delta\theta_x \Big|_0^1 = 0 \quad \ldots\ldots (42)$$

$$\left[\frac{1}{Se_{rr}^2} I_{rr_n}(\theta_z - \Phi) + \frac{1}{Se_{rp}^2} I_{rp_n}(U_y' + \theta_x) + \frac{1}{Se_{rq}^2} I_{rq_n}(U_x' - \theta_y) + \frac{1}{\omega e^2} I_{d_n} \Phi \right] \delta\theta_z \Big|_0^1 = 0$$

$$\ldots\ldots (43)$$

$$I_{\omega\dot{\varphi}_n} \Phi' \, \delta\Phi \Big|_0^1 = 0 \quad \ldots\ldots (44)$$

For a prismatic beam (uniform in cross section) the quantities with subscript n will all be equal to unity. Equation of axial motion (30) is independent of other equations and its solution is well known. So here onward this equation is not considered in the analysis.

2.1.5 FEM Equations :

Equations (31) to (36) are the six coupled governing differential eauations of motion for thin-walled beams. Solution of these coupled equations is obtained by Galerkin finite element method in this work.

Beam is divided into number of elements called finite elements, Fig.3 . The displacements over the typical finite element, e , Fig. 3 are approximated as

$$
\begin{aligned}
U_x^{(e)} &= a_o + a_1 Z + \ldots\ldots\ldots = \lfloor L \rfloor \{U_x\}^{(ne)} \\
U_y^{(e)} &= c_o + c_1 Z + \ldots\ldots\ldots = \lfloor M \rfloor \{U_y\}^{(ne)} \\
\theta_x^{(e)} &= c_o + c_1 Z + \ldots\ldots\ldots = \lfloor N \rfloor \{\theta_x\}^{(ne)} \qquad \ldots.(45) \\
\theta_y^{(e)} &= d_o + d_1 Z + \ldots\ldots\ldots = \lfloor O \rfloor \{\theta_y\}^{(ne)} \\
\theta_z^{(e)} &= e_o + e_1 Z + \ldots\ldots\ldots = \lfloor P \rfloor \{\theta_z\}^{(ne)} \\
\Phi^{(e)} &= f_o + f_1 Z + \ldots\ldots\ldots = \lfloor Q \rfloor \{\Phi\}^{(ne)}
\end{aligned}
$$

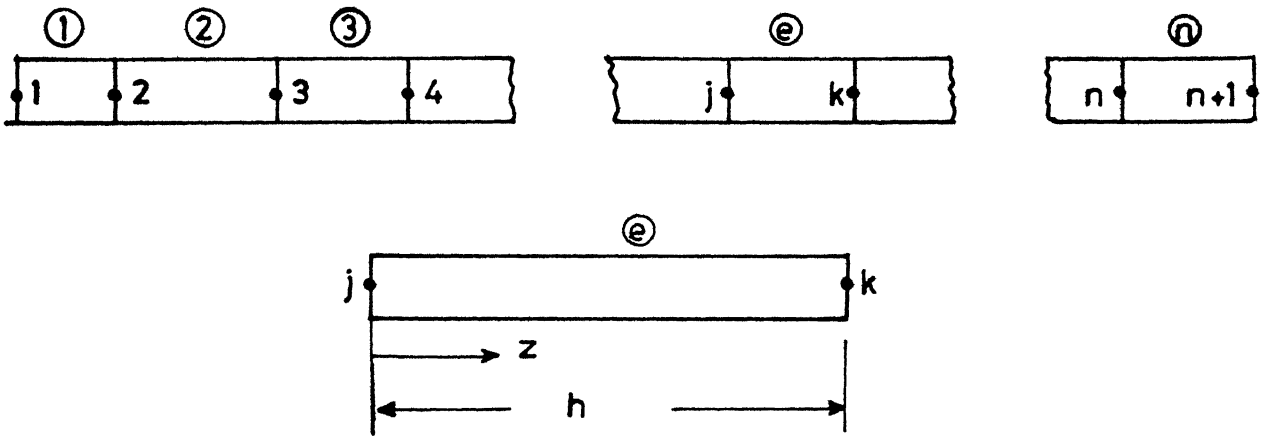

Fig. 3 Finite Element Divison and the Typical Element of a Beam.

Substituting these in Eqns. (31)to (36), six residues Re^{U_x}, Re^{θ_y}, Re^{U_y}, Re^{θ_x}, Re^{θ_z}, $Re^{\bar{\Phi}}$ are obtained. These six residues are minimized by the Galerkin method, i.e. six residues are multiplied by L_i, M_i, N_i, O_i, P_i and Q_i and integrated by parts to reduce the order of derivatives wherever possible. For brevity sake, this operation is shown here only for Eqn. (31), thus

$$L_i \frac{Re^2_{yy}}{Se^2_{qq}}(I_{qq_n}(U_x'^{(e)} - \theta_y^{(e)}))\Big|_o^h - \int_o^h \frac{Re^2_{yy}}{Se^2_{qq}} L_i'(I_{qq_n}(U_x'^{(e)} - \theta_y^{(e)})dz$$

$$+ L_i \frac{Re^2_{yy}}{Se^2_{qp}}(I_{qp_n}(U_y'^{(e)} + \theta_x^{(e)}))\Big|_o^h - \int_o^h L_i' \frac{Re^2_{yy}}{Se^2_{qp}}(I_{qp_n}(U_y'^{(e)} + \theta_x^{(e)}))dz$$

$$+ L_i \frac{Re^2_{yy}}{Se^2_{qr}}(I_{qr_n}(\theta_z'^{(e)} - \Phi^{(e)}))\Big|_o^h - \int_o^h L_i' \frac{Re^2_{yy}}{Se^2_{qr}}(I_{qr_n}(\theta_z^{(e)} - \Phi^{(e)}))\,dz$$

$$- \int_o^h L_i A_n \ddot{U}_x^{(e)}\,dz - \int_o^h L_i Y_o A_n \ddot{\theta}_z^{(e)}\,dz = 0$$

.... (46)

Observing Eqn. (46) and five similar equations, it is seen that highest order of derivatives of displacements U_x, U_y, θ_x, θ_y, θ_z and $\bar{\Phi}$ in the integrals are of first order. Thus compatibility of these displacements is needed at the nodes of the element. It is also seen that highest order of derivatives of these displacements in these six equations are of

first order. Thus completeness of these displacements and their first derivatives is needed. Hence the compatibility, and completeness requirements for all displacements are identical, and

$$[L] = [M] = [N] = [O] = [P] = [Q] = [N] \quad \ldots\ (47)$$

The above requirements are satisfied with C_o elements. But it has been seen that this element leads to ill-conditioning in beams and plates with shear effects, [23,24] To avoid this ill-conditioning C_1 elements are used in this work. For this C_1 element, shape functions are

$$[N] = [N_1 \quad N_2 \quad N_3 \quad N_4] \quad \ldots\ (48)$$

where

$$N_1 = 1 - 3\frac{z^2}{h^2} + 2\frac{z^3}{h^3}$$

$$N_2 = z - 2\frac{z^2}{h} + \frac{z^3}{h^2} \quad \ldots\ (49)$$

$$N_3 = 3\frac{z^2}{h^2} - 2\frac{z^3}{h^3}$$

$$N_4 = \frac{z^3}{h^2} - \frac{z^2}{h}$$

and the nodal variables are U_x, U_x' and similarly for other displacements.

Equation (46) and five other similar equations are put in the matrix form, using Eqn. (45), thus

$$
\begin{bmatrix}
[M_1] & [0] & [0] & [0] & [M_2] & [0] \\
 & [M_3] & [0] & [0] & [0] & [0] \\
 & & [M_1] & [0] & [M_4] & [0] \\
 & & & [M_5] & [0] & [0] \\
 & & & & [M_6] & [0] \\
 & & & & & [M_7]
\end{bmatrix}
\begin{Bmatrix}
\{\ddot{U}_x\}^{(ne)} \\
\{\ddot{\theta}_y\}^{(ne)} \\
\{\ddot{U}_y\}^{(ne)} \\
\{\ddot{\theta}_x\}^{(ne)} \\
\{\ddot{\theta}_z\}^{(ne)} \\
\{\ddot{\Phi}\}^{(ne)}
\end{Bmatrix}
+
\begin{bmatrix}
[K_1] & [K_2] & [K_3] & [K_4] & [K_5] & [K_6] \\
 & [K_7] & [K_8] & [K_9] & [K_{10}] & [K_{11}] \\
 & & [K_{12}] & [K_{13}] & [K_{14}] & [K_{15}] \\
 & & & [K_{16}] & [K_{17}] & [K_{18}] \\
 & & & & [K_{19}] & [K_{20}] \\
 & & & & & [K_{21}]
\end{bmatrix}
\begin{Bmatrix}
\{U_x\}^{(ne)} \\
\{\theta_y\}^{(ne)} \\
\{U_y\}^{(ne)} \\
\{\theta_x\}^{(ne)} \\
\{\theta_z\}^{(ne)} \\
\{\Phi\}^{(ne)}
\end{Bmatrix}
=
$$

Symmetrical

Symmetrical

.... (50)

Where

$$[M_1] = \int_o^h A_n \{N\}[N]\,dz \; ; \; [M_2] = \int_o^h A_n Y_b \{N\}[N]\,dz \; ;$$

$$[M_3] = Re_{yy}^2 \int_o^h I_{yy_n} \{N\}[N]\,dz$$

$$[M_4] = -\int_o^h A_n X_b \{N\}[N]\,dz \; ; \; [M_5] = Re_{xx}^2 \int_o^h I_{xx_n} \{N\}[N]\,dz;$$

$$[M_6] = Re_B^2 \int_o^h I_{B_n} \{N\}[N]\,dz \; ; \; [M_7] = Re_{\omega\omega}^2 \int_o^h I_{\omega\omega_n} \{N\}[N]\,dz$$

.... (51)

and

$$[K_1] = \frac{Re_{yy}^2}{Se_{qq}^2} \int_o^h I_{qq_n} \{\acute{N}\}[\acute{N}]\,dz \; ; \; [K_2] = -\frac{Re_{yy}^2}{Se_{qq}^2} \int_o^h I_{qq_n} \{\acute{N}\}[N]\,dz;$$

$$[K_3] = \frac{Re_{yy}^2}{Se_{qp}^2} \int_o^h I_{qp_n} \{\acute{N}\}[\acute{N}]\,dz; \; [K_4] = \frac{Re_{yy}^2}{Se_{qp}^2} \int_o^h I_{qp_n} \{\acute{N}\}[N]\,dz \; ;$$

$$[K_5] = \frac{Re_{yy}^2}{Se_{qr}^2} \int_o^h I_{qr_n} \{\acute{N}\}[\acute{N}]\,dz \; ; \; [K_6] = \frac{-Re_{yy}^2}{Se_{qr}^2} \int_o^h I_{qr_n} \{\acute{N}\}[N]\,dz \; ;$$

$$[K_7] = \frac{Re_{yy}^2}{Se_{qq}^2} \int_o^h I_{qq_n} \{N\}[N]\,dz + Re_{yy}^2 \int_o^h I_{yy_n} \{\acute{N}\}[\acute{N}]\,dz \; ;$$

$$[K_8] = \frac{-Re_{yy}^2}{Se_{qp}^2} \int_o^h I_{qp_n} \{N\}[\acute{N}]\,dz \; ; \; [K_9] = \frac{-Re_{yy}^2}{Se_{qp}^2} \int_o^h I_{qp_n} \{N\}[N]\,dz \; ;$$

$$[K_{10}] = \frac{-Re_{yy}^2}{Se_{qr}^2} \int_o^h I_{qr_n} \{N\}[\acute{N}]\,dz \; ; [K_{11}] = \frac{Re_{yy}^2}{Se_{qr}^2} \int_o^h I_{qr_n} \{N\}[N]\,dz \; ;$$

$$[K_{12}] = \frac{Re_{xx}^2}{Se_{pp}^2} \int_o^h I_{pp_n} \{N'\}[N'] dz \; ; \; [K_{13}] = \frac{Re_{xx}^2}{Se_{pp}^2} \int_o^h I_{pp_n} \{N'\} [N] dz \; ;$$

$$[K_{14}] = \frac{Re_{xx}^2}{Se_{pr}^2} \int_o^h I_{pr_n} \{N'\}[N'] dz \; ; \; [K_{15}] = \frac{-Re_{xx}^2}{Se_{pr}^2} \int_o^h I_{prn} \{N'\} [N] dz \; ;$$

$$[K_{16}] = \frac{Re_{xx}^2}{Se_{pp}^2} \int_o^h I_{pp_n} \{N\} [N] dz + Re_{xx}^2 \int_o^h I_{xx_n} \{N'\} [N'] dz \; ;$$

$$[K_{17}] = \frac{Re_{xx}^2}{Se_{pr}^2} \int_o^h I_{pr_n} \{N\}[N'] dz \; ; \; [K_{18}] = \frac{-Re_{xx}^2}{Se_{pr}^2} \int_o^h I_{pr_n} \{N\} [N] dz \; ;$$

$$[K_{19}] = \frac{Re_{\omega\omega}^2}{Se_{rr}^2} \int_o^h I_{rr_n} \{N'\} [N'] dz \; ; [K_{20}] = \frac{Re_{\omega\omega}^2}{\omega e^2} \int_o^h I_{d_n} \{N'\} [N] dz$$

$$- \frac{Re_{\omega\omega}^2}{Se_{rr}^2} \int_o^h I_{rr_n} \{N'\} [N] dz \; ;$$

$$[K_{21}] = \frac{Re_{\omega\omega}^2}{Se_{rr}^2} \int_o^h I_{rr_n} \{N\} [N] dz - \frac{Re_{\omega\omega}^2}{We^2} \int_o^h I_{d_n} \{N\} [N] dz$$

$$+ Re_{\omega\omega}^2 \int_o^h I_{\omega\omega_n} \{N'\} [N'] dz$$

.... (52)

and

$$\{F_1\} = Re_{yy}^2 \begin{Bmatrix} -\left(\frac{1}{Se_{qq}^2} I_{qq_n}(U_x' - \theta_y) + \frac{1}{Se_{qp}^2} I_{qp_n}(U_y' + \theta_x) + \frac{1}{Se_{qr}^2} I_{qr_n}(\theta_z' - \Phi)\right)\Big|_j \\ \frac{1}{Se_{qq}^2} I_{qq_n}(U_x' - \theta_y) + \frac{1}{Se_{qp}^2} I_{qp_n}(U_y' + \theta_x) + \frac{1}{Se_{qr}^2} I_{qr_n}(\theta_z' - \Phi)\Big|_k \\ 0 \end{Bmatrix}$$

$$\{F_2\} = Re_{yy}^2 \begin{Bmatrix} -I_{yy_n}\ \theta_y'\Big|_j \\ 0 \\ I_{yy}\ \theta_y'\Big|_k \\ 0 \end{Bmatrix}$$

$$\{F_3\} = Re_{xx}^2 \begin{Bmatrix} -\left(\frac{1}{Se_{pp}^2} I_{pp_n}(U_y' + \theta_x) + \frac{1}{Se_{pq}^2} I_{pq_n}(U_x' - \theta_y) + \frac{1}{Se_{pr}^2} I_{pr_n}(\theta_z - \Phi)\right)\Big|_j \\ 0 \\ \left(\frac{1}{Se_{pp}^2} I_{pp_n}(U_y' + \theta_x) + \frac{1}{Se_{pq}^2} I_{pq_n}(U_x' - \theta_y) + \frac{1}{Se_{pr}^2} I_{pr_n}(\theta_z' - \Phi)\right)\Big|_k \\ 0 \end{Bmatrix}$$

$$\{F_4\} = Re_{xx}^2 \begin{Bmatrix} -I_{xx_n}\ \theta_x'\Big|_j \\ I_{xx_n}\ \theta_x'\Big|_k \\ 0 \end{Bmatrix}$$

$$= Re^2_{\omega\omega} \begin{Bmatrix} -\left(\frac{1}{Se^2_{rr}} I_{rr_n} (\theta'_z - \bar{\phi}) + \frac{1}{Se^2_{rp}} I_{rp_n} (U'_y + \theta_x) + \frac{1}{Se^2_{rq}} I_{rq_n} (U'_x - \theta_y) + \frac{1}{\omega_e^2} I_{d_n} \bar{\phi}\right)\Big|_j \\ 0 \\ \left(\frac{1}{Se^2_{rr}} I_{rr_n} (\theta'_z - \bar{\phi}) + \frac{1}{Se^2_{rp}} I_{rp_n} (U'_y + \theta_x) + \frac{1}{Se^2_{rq}} I_{rq_n} (U'_x - \theta_y) + \frac{1}{\omega_e^2} I_{d_n} \bar{\phi}\right)\Big|_k \\ 0 \end{Bmatrix}$$

$$= Re^2_{\omega\omega} \begin{Bmatrix} -I_{\omega\omega_n} \bar{\phi}' \Big|_j \\ 0 \\ I_{\omega\omega_n} \bar{\phi}' \Big|_k \\ 0 \end{Bmatrix} \quad \ldots\ (53)$$

quation (50) in a concise form is

$$[M]^{(e)} \{\ddot{U}\}^{(ne)} + [K]^{(e)} \{U\}^{(ne)} = \{F\}^{(ne)} \quad \ldots\ (54)$$

here

$[M]^{(e)}$ = mass matrix of the element

$[K]^{(e)}$ = stiffness matrix of the element

$\{U\}^{(ne)}$ = displacement vector of the element

$\{F\}^{(ne)}$ = boundary force vector of the element

Assembling for all elements and applying the boundary conditions, equation of motion become

$$[M]\{\ddot{U}\}^{(n)} + [K]\{U\}^{(n)} = \{0\} \qquad \ldots. (55)$$

2.2 STATIC ANALYSIS :

2.2.1 Basic Equations :

The governing equations for the static analysis are derived (including shear deformation effects).

For this case potential to be minimised is

$$V = U - U_e \qquad \ldots. (56)$$

Where U is the strain energy given by Eqn. (7), U_e is the work done by external forces and is

$$U_e = \int_0^l (q_z u_a + q_y u_y + q_x u_x + m_t \theta_z + m_y \theta_y + m_x \theta_x - m_\omega \phi) dz + \int_0^l (Q_z u_a \delta(z - \bar{z}_{u_a})$$

$$+ Q_y u_y \delta(z - \bar{z}_{u_y}) + Q_x u_x \delta(z - \bar{z}_{u_x}) + M_t \theta_z \delta(z - \bar{z}_{\theta_z}) + M_y \theta_y \delta(z - \bar{z}_{\theta_y})$$

$$+ M_x \theta_x \delta(z - \bar{z}_{\theta_x}) - M_\omega \phi (z - \bar{z}_\phi)) dz.$$

Where

q_x, q_y and q_z = line loads per unit length of the beam in the x,y and z directions respectively.

m_t, m_x, m_y, m_ω = applied torsional moment bending moment (about x), bending moment (about y) and bimoments per unit length of the beam.

Q_x, Q_y and Q_z = concentrated load in the x,y and z directions respectively

M_t, M_x, M_y and M_ω = concentrated torsional moment, bending moment (about x), bending moment (about y), and bimoments.

$\delta (z - \bar{z})$ = Dirac delta function for concentrated loads and moments

Minimising the potential, Eqn. (56), one gets the governing equilibrium equations as

$$\frac{\partial}{\partial z}(EAu_a') + q_z + Q_z \delta(z - \bar{z}_{u_a}) = 0 \quad \ldots.(58)$$

$$\frac{\partial}{\partial z}(GI_{qq}(u_x' - \theta_y)) + \frac{\partial}{\partial z}(GI_{qp}(u_y' + \theta_x)) + \frac{\partial}{\partial z}(GI_{qr}(\theta_z' - \phi)) + q_x + Q_x \delta(z - \bar{z}_{u_x}) = 0 \quad \ldots.(59)$$

$$\frac{\partial}{\partial z}(EI_{yy}\theta_y') + GI_{qq}(u_x' - \theta_y) + GI_{qp}(u_y' + \theta_x) + GI_{qr}(\theta_z' - \phi) + m_y + M_y \delta(z - \bar{z}_{\theta_y}) = 0 \quad \ldots.(60)$$

$$\frac{\partial}{\partial z}(GI_{pp}(u_y' + \theta_x)) + \frac{\partial}{\partial z}(GI_{pq}(u_x' - \theta_y)) + \frac{\partial}{\partial z}(GI_{pr}(\theta_z' - \phi)) + q_y + Q_y \delta(z - \bar{z}_{u_y}) = 0 \quad \ldots.(61)$$

$$\frac{\partial}{\partial z}(EI_{xx}\theta_x') - GI_{pp}(u_y'+\theta_x) - GI_{pq}(u_x' - \theta_y) - GI_{pr}(\theta_z' - \phi)$$

$$+ m_x + M_x^{\delta}(z - \bar{z}_{\theta_x}) = 0 \quad \ldots.(62)$$

$$\frac{\partial}{\partial z}(GI_{rr}(\theta_z' - \phi)) + \frac{\partial}{\partial z}(GI_{rp}(u_y'+\theta_x)) + \frac{\partial}{\partial z}(GI_{rq}(u_x' - \theta_y))$$

$$+ \frac{\partial}{\partial z}(GI_d\phi) + m_t + M_t^{\delta}(z - \bar{z}_{\theta_z}) = 0 \quad \ldots.(63)$$

$$\frac{\partial}{\partial z}(EI_{\omega\omega}\phi') + GI_{rr}(\theta_z' - \phi) + GI_{rp}(u_y'+\theta_x) + GI_{rq}(u_x' - \theta_y)$$

$$- GI_d(\theta_z' - \phi) - m_\omega - M_\omega^{\delta}(z - \bar{z}_{\phi}) = 0 \quad \ldots.(64)$$

2.2.2 Nondimensionalisation :

The governing equations (58) to (64) are nondimensionalised, using the parameters of Eqn. (29), and are

$$\frac{\partial}{\partial z}(A_n U_a') + q_z + Q_z = 0 \quad \ldots.(65)$$

$$\frac{1}{Se_{qq}^2}\frac{\partial}{\partial z}(I_{qq_n}(U_x' - \theta_y)) + \frac{1}{Se_{qp}^2}\frac{\partial}{\partial z}(I_{qp_n}(U_y' + \theta_x))$$

$$+ \frac{1}{Se_{qr}^2}\frac{\partial}{\partial z}(I_{qr_n}(\theta_z' - \Phi)) + q_x + Q_x = 0 \quad \ldots.(66)$$

$$\frac{\partial}{\partial z}(I_{yy_n}\theta_y) + \frac{1}{Se_{qq}^2}(U_x' - \theta_y) + \frac{1}{Se_{qp}^2}I_{qp_n}(U_y' + \theta_x)$$

$$+ \frac{1}{Se_{qr}^2}I_{qr_n}(\theta_z' - \Phi) + m_Y + M_Y = 0 \quad \ldots.(67)$$

$$\frac{1}{Se_{pp}^2}\frac{\partial}{\partial z}(I_{pp_n}(U_y'+\theta_x))+\frac{1}{Se_{pq}^2}\frac{\partial}{\partial z}(I_{pq_n}(U_x'-\theta_y))$$

$$+\frac{1}{Se_{pr}^2}\frac{\partial}{\partial z}(I_{pr_n}(\theta_z'-\dot{\phi}))+q_Y+Q_Y = 0 \quad ....(68)$$

$$\frac{\partial}{\partial z}(I_{xx_n}\theta_x')-\frac{1}{Se_{pp}^2}I_{pp_n}(U_y'+\theta_x)-\frac{1}{Se_{pq}^2}I_{pq_n}(U_x'-\theta_y)$$

$$-\frac{1}{Se_{pr}^2}I_{pr_n}(\theta_z'-\dot{\phi})+m_X+M_X = 0 \quad ....(69)$$

$$\frac{1}{Se_{rr}^2}\frac{\partial}{\partial z}(I_{rr_n}(\theta_z'-\dot{\phi}))+\frac{1}{Se_{rp}^2}\frac{\partial}{\partial z}(I_{rp_n}(U_y'+\theta_x))$$

$$+\frac{1}{Se_{rq}^2}\frac{\partial}{\partial z}(I_{rq_n}(U_x'-\theta_y))+\frac{1}{\omega e^2}\frac{\partial}{\partial z}(I_{d_n}\dot{\phi})+m_T+M_T = 0 \quad ....(70)$$

$$\frac{\partial}{\partial z}(I_{\omega\omega_n}\dot{\phi}')+\frac{1}{Se_{rr}^2}I_{rr_n}(\theta_z'-\dot{\phi})+\frac{1}{Se_{rp}^2}I_{rp_n}(U_y'+\theta_x)$$

$$+\frac{1}{Se_{rq}^2}I_{rq_n}(U_x'-\theta_y)-\frac{1}{\omega e^2}I_{d_n}(\theta_z'-\dot{\phi})-m_Q-M_Q = 0 \quad ....(71)$$

Where Se_{qq}^2, Se_{qp}^2, Se_{qr}^2, Se_{pp}^2, Se_{pq}^2, Se_{rr}^2, Se_{rp}^2, Se_{rq}^2

and ωe^2 are defined by Eqn. (37) and

$$q_Z = \frac{q_z l}{EA_o} \; ; \qquad Q_Z = \frac{Q_z l \; \delta(z-\bar{z}_{u_a})}{EA_o}$$

$$q_X = \frac{q_x l^3}{EI_{yy_o}} \; ; \qquad Q_X = \frac{Q_x l^3 \; \delta(z-\bar{z}_{u_x})}{EI_{yy_o}}$$

$$m_Y = \frac{m_y l^2}{EI_{yy_o}} \; ; \quad M_Y = \frac{M_y l^2 \delta(z-\bar{z}_{\theta_y})}{EI_{yy_o}}$$

$$q_Y = \frac{q_y l^3}{EI_{xx_o}} \; ; \quad Q_Y = \frac{Q_y l^3 \delta(z-\bar{z}_{u_y})}{EI_{xx_o}} \qquad \ldots\ldots (72)$$

$$m_X = \frac{m_x l^2}{EI_{xx_o}} \; ; \quad M_X = \frac{M_x l^2 \; \delta(z-\bar{z}_{\theta_x})}{EI_{xx_o}}$$

$$m_T = \frac{m_t l^4}{EI_{\omega\omega_o}} \; ; \; M_T = \frac{M_t l^4 \; \delta(z-\bar{z}_{\theta_z})}{EI_{\omega\omega_o}}$$

$$m_\varrho = \frac{m_\omega l^3}{EI_{\omega\omega_o}} \; ; \; M_\varrho = \frac{M_\omega l^3 \; \delta(z-\bar{z}_{\phi})}{EI_{\omega\omega_o}}$$

2.2.3 FEM Equations :

Equations (66) to (71) are the six coupled governing differential equations for the static case. Solution of these coupled equations is obtained by Galerkin finite element method in this work.

The displacements over the typical element, Fig.3 , are approximated as in Eqn. (45). Substituting Eqns.(45) in Eqns. (66) to (71), six residues Re^{U_x} , Re^{θ_y} , Re^{U_y}, Re^{θ_x}, Re^{θ_z} and Re^{ϕ} are obtained. These six residues are minimized by the Galerkin method. For brevity sake this is shown here only for Eqn. (66), thus

$$N_i \frac{1}{Se^2_{qq}} (I_{qq_n}(U_x^{'(e)} - \theta_y^{(e)}))\Big|_o^h - \int_o^h \frac{1}{Se^2_{qq}} N_i'(I_{qq_n}(U_x^{(e)} - \theta_y^{(e)}))dz$$

$$N_i \frac{1}{Se^2_{qp}}(I_{qp_n}(U_y^{'(e)} + \theta_x^{(e)}))\Big|_o^h - \int_o^h \frac{1}{Se^2_{qp}} N_i'(I_{qp_n}(U_y^{'(e)} + \theta_x^{(e)}))dz$$

$$+N_i \frac{1}{Se^2_{qr}}(I_{qr_n}(\theta_z^{'(e)} - \phi^{(e)}))\Big|_o^h - \int_o^h \frac{1}{Se^2_{qr}} N_i'(I_{qr_n}(\theta_z^{'(e)} - \phi^{(e)}))dz$$

$$+ \int_o^h N_i\, q_X\, dz + \int_o^h N_i\, Q_X\, dz = 0 \qquad \ldots\ (73)$$

By observing Eqn. (73) and five similar equation for compatibility and completeness, one can see that C_o elements can satisfy the requirements. But it has been seen that this element leads to ill-conditioning in beams and plates with shear effects, [23, 24] . To avoid this ill conditioning C_1 element are used in this work. So the interpolation functions of Eqn.(48) are used. The modal variables are U_x, U_x' and similarly for other displacements.

Equation (73) and five other similar equations are put in the matrix form using Eqn. (45),

$$[K]^{(e)} \{U\}^{(ne)} = \{Q\}^{(ne)} + \{F\}^{(ne)} \quad \ldots\ (74)$$

where $[K]^{(e)}$ = stiffness matrix of the element

$\{U\}^{(ne)}$ = displacement vector of the element

$\{Q\}^{(ne)}$ = Load vector of the element

$\{F\}^{(ne)}$ = Boundary force matrix of the element

Matrices $[K]^{(e)}$ and $\{F\}^{(ne)}$ are obtained from Eqn. (50), by substituting $Re_{xx}^2 = Re_{yy}^2 = Re_{\omega\omega}^2 = 1$.

And load matrix $\{Q\}^{(ne)}$ is

$$\{Q\}^{(ne)} = \begin{Bmatrix} \{Q_1\} \\ \{Q_2\} \\ \{Q_3\} \\ \{Q_4\} \\ \{Q_5\} \\ \{Q_6\} \end{Bmatrix} = \begin{bmatrix} \int_o^h \{N\}\, q_x\, dz + \int_o^h \{N\}\, Q_x\, dz \\ \int_o^h \{N\}\, m_Y\, dz + \int_o^h \{N\}\, M_Y\, dz \\ \int_o^h \{N\}\, q_Y\, dz + \int_o^h \{N\} Q_Y\, dz \\ \int_o^h \{N\}\, m_X\, dz + \int_o^h \{N\} M_X\, dz \\ \int_o^h \{N\}\, m_T\, dz + \int_o^h \{N\}\, M_T\, dz \\ -\int_o^h \{N\} m_Q\, dz - \int_o^h \{N\}\, M_Q\, dz \end{bmatrix} \quad \ldots\ (75)$$

Assembling for all elements and applying the boundary conditions, the governing equations for static case become,

$$[K]\{U\}^{(n)} = \{Q\}^{(n)} \qquad \ldots\ (76)$$

2.3 BUCKLING ANALYSIS :

2.3.1 Basic Equations :

In this section coupled flexural-torsional buckling equations of a thin walled column are derived from variational principles. These equations are classical equations and have been derived using equilibrium method by many researches See [17,2] .

The inplane displacement, v and w of a point A on the cross-section of a thin-walled column, Fig. A-2, are given by Eqn. (A-9).

Using Eqns. (A-3) to (A-6), Eqns.(A-9) become

$$v = (u_{x_B} + y_B\,\theta_z)\cos\alpha + (u_{y_B} - x_B\,\theta_z)\sin\alpha + p_o\,\theta_z$$

$$w = -(u_{x_B} + y_B\theta_z)\sin\alpha + (u_{y_B} - x_B\,\theta_z)\cos\alpha + q_o\,\theta_z \qquad \ldots(77)$$

where

u_{x_B}, u_{y_B} = the displacements of pole B in the x and y-directions respectively

x_B, y_B = coordinates of the pole B.

α = angle of tangent at A with the x-axis

p_o = the perpendicular distance from the point O to the targent at point A

$= (x_A \sin \alpha - y_A \cos \alpha)$

q_o = The perpendicular distance from the point O to the normal at point A.

$= (x_A \cos \alpha + y_A \sin \alpha)$

x_A, y_A = Coordinates of the point A

The out of plane displacement of point A is given by Eqn. (A-22). Neglecting the effect of shear strain, it becomes,

$$u = u_a - u'_{x_B} x_A - u'_{y_B} y_A - \theta'_z \omega_B \qquad \ldots. (78)$$

Here the subscript b has been dropped.
The point O is taken at the centroid of the cross section and the point B as the shear center in this work, Fig. (A-2). Here onwards subscripts B of the displacements and their derivatives of the shear centre B are dropped.

Normal strain is

$$\varepsilon_{zz} = \frac{\partial u}{\partial z} + \frac{1}{2} \left[\left(\frac{\partial u}{\partial z}\right)^2 + \left(\frac{\partial v}{\partial z}\right)^2 + \left(\frac{\partial w}{\partial z}\right)^2 \right]$$

The contribution of $\frac{1}{2} \left(\frac{\partial u}{\partial z}\right)^2$ to the ε_{zz} is negligible compared to others, thus

$$\varepsilon_{zz} = \frac{\partial u}{\partial z} + \frac{1}{2} \left[\left(\frac{\partial v}{\partial z}\right)^2 + \left(\frac{\partial w}{\partial z}\right)^2 \right] \qquad \ldots.(79)$$

With this strain energy becomes

$$U = \frac{1}{2} \int_v (E\ \varepsilon_{zz}^2 + G\ \gamma_{zs}^2)\ dv$$

$$= \frac{1}{2} \int_0^1 \int_A \left\{ E\left[\frac{\partial u}{\partial z} + \frac{1}{2}\left(\left(\frac{\partial v}{\partial z}\right)^2 + \left(\frac{\partial w}{\partial z}\right)^2\right)\right]^2 + G\left(\frac{\partial u}{\partial s} + \frac{\partial v}{\partial z}\right)^2 \right\} dA dz$$

.... (80)

Substituting the Eqns. (77) and (78) in Eqn. (80) and neglecting the terms having higher order powers of the derivatives one gets,

$$U = \frac{1}{2} \int_0^1 [\ E(Au_a'^2 + I_{yy}u_x''^2 + I_{xx}u_y''^2 + I_{\omega\omega}\theta_z''^2 + Au_a'\ u_x'^2 + I_B\ u_a'\ \theta_z'^2$$

$$+ Au_a'\ u_y'^2 + 2y_B\ Au_x'\ \theta_z'\ u_a' - 2x_B\ Au_y'\ \theta_z' u_a')$$

$$+ GI_d\ \theta_z'^2\ ]\ dz \qquad \text{.... (81)}$$

Terms I_{xx}, I_{yy}, $I_{\omega\omega}$, I_B and I_D are defined in Eqn. (13). Now treating EAu_a' as a constant, axial compressive force, $-p$, Eqn. (81) becomes

$$U = \frac{1}{2} \int_0^1 [E(Au_a'^2 + I_{yy}u_x''^2 + I_{xx}\ u_y''^2 + I_{\omega\omega}\ \theta_z''^2) - pu_x'^2 - p\frac{I_B}{A}\ \theta_z'^2 - pu_y'^2$$

$$- 2py_B\ u_x'\theta_z' + 2px_B\ u_y'\ \theta_z' + GI_d\ \theta_z'^2\ ]\ dz$$

.... (82)

Minimizing this potential U, one gets the four buckling equations associated with δu_z, δu_x, δu_y, $\delta \theta_z$ as

$$\frac{\partial}{\partial z}(EA\ u_a') = 0 \quad .... (83)$$

$$\frac{\partial^2}{\partial z^2}(EI_{yy}\ u_x'') + \frac{\partial}{\partial z}(pu_x') + \frac{\partial}{\partial z}(py_B\ \theta_z') = 0 \quad .... (84)$$

$$\frac{\partial^2}{\partial z^2}(EI_{xx}\ u_y'') + \frac{\partial}{\partial z}(pu_y') - \frac{\partial}{\partial z}(px_B\ \theta_z') = 0 \quad .... (85)$$

$$\frac{\partial^2}{\partial z^2}(EI_{\omega\omega}\theta_z'') - \frac{\partial}{\partial z}(GI_d\ \theta_z') + \frac{\partial}{\partial z}\left(\frac{pI_B}{A}\ \theta_z'\right) - \frac{\partial}{\partial z}(px_B\ u_y') + \frac{\partial}{\partial z}(py_B\ u_x') = 0 \quad .... (86)$$

and the boundary conditions

$$EAu_a\ \delta u_a' \Big|_o^1 = 0 \ ; \quad .... (87)$$

$$EI_{yy}\ u_x''\ \delta u_x' \Big|_o^1 = 0 \ ; \ \left(\frac{\partial}{\partial z}(EI_{yy}u_x'') + pu_x' + py_B\ \theta_z'\right)\delta u_x \Big|_o^1 = 0 \quad .... (88)$$

$$EI_{xx}\ u_y''\ \delta u_y \Big|_o^1 = 0 \ ; \ \left(\frac{\partial}{\partial z}(EI_{xx}u_y'') + pu_y' - px_B\ \theta_z'\right)\delta u_y \Big|_o^1 = 0 \quad .... (89)$$

$$EI_{\omega\omega}\theta_z'' \delta\theta_z' \Big|_o^1 = 0 \; ; \; \left(\frac{\partial}{\partial z}(EI_{\omega\omega}\,\theta_z'') + \frac{pI_B}{A}\,\theta_z' + py_B\,u_x'\right.$$

$$\left. -px_B\,u_y' - GI_d\theta_z'\right)\delta\theta_z \Big|_o^1 = 0 \qquad \ldots.(90)$$

2.3.2 Non-dimensionalisation :

The buckling equations Eqns(83)to(85) are non-dimensionalised, using the parameters of Eqn. (29)

and $\frac{p}{EA_o} = P$ .... (91)

These become

$$\frac{\partial}{\partial Z}(A_n\,U_a') = 0 \qquad \ldots.(92)$$

$$Re_{yy}^2 \frac{\partial^2}{dZ^2}(I_{yy_n}U_x'') + \frac{\partial}{\partial Z}(PU_x') + \frac{\partial}{\partial Z}(P\,Y_B\,\theta_z') = 0 \qquad \ldots.(93)$$

$$Re_{xx}^2 \frac{\partial^2}{\partial Z^2}(I_{xx_n}U_y'') + \frac{\partial}{\partial Z}(PU_y') - \frac{\partial}{\partial Z}(PX_B\,\theta_z') = 0 \qquad \ldots.(94)$$

$$Re_{\omega\omega}^2 \frac{\partial^2}{\partial Z^2}(I_{\omega\omega_n}\theta_z'') - \frac{Re_{\omega\omega}^2}{\omega e^2\partial Z}(I_{d_n}\,\theta_z') + Re_B^2 \frac{\partial}{\partial Z}\left(P\frac{I_{Bn}}{A_n}\,\theta_z'\right)$$

$$- \frac{\partial}{\partial Z}(PX_B\,U_y') + \frac{\partial}{\partial Z}(PY_B\,U_x') = 0 \qquad \ldots.(95)$$

Where Re_{xx}^2, Re_{yy}^2, $Re_{\omega\omega}^2$, ωe^2 and Re_B^2 are defined in Eqns. (37).

The boundary conditions are

$$A_n U_a' \delta U_a \Big|_0^1 = 0 \quad ; \qquad \ldots(96)$$

$$I_{yy_n} U_x'' \delta U_x' \Big|_0^1 = 0 \quad ; \quad (Re_{yy}^2 \frac{\partial}{\partial Z}(I_{yy_n} U_x'') + PU_x' + PY_B \theta_z') \delta U_x \Big|_0^1 = 0$$

$$\ldots.(97)$$

$$I_{xx_n} U_y'' \delta U_y' \Big|_0^1 = 0 \quad ; \quad (Re_{xx}^2 \frac{\partial}{\partial z}(I_{xx_n} U_y'') + PU_y' - PX_B \theta_z') \delta U_y \Big|_0^1 = 0$$

$$\ldots.(98)$$

$$I_{\omega\omega_n} \theta_z \delta\theta_z' \Big|_0^1 = 0 \quad ; \quad (Re_{\omega\omega}^2 \frac{\partial}{\partial z}(I_{\omega\omega_n} \theta_z'') + Re_B^2 \frac{PI_{B_n}}{A_n} \theta_z + PY_B U_x' - PX_B U_y' - \frac{Re_{\omega\omega}^2}{\omega e^2} I_{d_n} \theta_z') \delta\theta_z \Big|_0^1 = 0$$

$$\ldots.(99)$$

2.3.3 FEM Equations :

Equations (93) to (95) are the three coupled governing differential equation of buckling of a thin walled column. Solution of these coupled equations is obtained by the Galerkin finite element method.

The displacements U_x, U_y and θ_z over the typical element, Fig. 3, are approximated as in Eqn. (45). Substituting Eqns. (45) in Eqns. (93) to (95), three residues Re^{u_x}, Re^{u_y} and Re^{θ_z} are obtained. These three residues are minimized by the Galerkin method. For brevity sake this is shown here only for Eqn. (93) thus.

$$N_i \, Re^2_{yy} \frac{\partial}{\partial Z} \left(I_{yy_n} U_x^{''(e)}\right)\Big|_o^h - Re^2_{yy} N_i' \, I_{yy_n} U_x^{''(e)} \Big|_o^h +$$

$$+ Re^2_{yy} \int_o^h N_i'' \, I_{yy_n} \, U_x^{''(e)} dz + N_i \, PU_x^{'(e)} \Big|_o^h - \int_o^h N_i \, PU_x^{'(e)} dz$$

$$+ N_i \, PY_B \, \theta_z^{'(e)} \Big|_o^h - \int_o^h N_i' \, PY_B \, \theta_z^{'(e)} dz = 0 \qquad \ldots\ (100)$$

By observing Eqn. (100) and two similar equations for compatibility and completeness, one can see that C_1 elements for U_x, U_y, and θ_z satisfy the requirements. The interpolation functions of Eqn. (48) are used. The nodal variables are U_x, U_x', U_y, U_y', θ_z and θ_z' for each node.

Equations (100) and two other similar equation are put in the matrix form using Eqn. (45),

$$\begin{bmatrix} [K_1] & [0] & [0] \\ [0] & [K_2] & [0] \\ [0] & [0] & [K_3] \end{bmatrix} \begin{Bmatrix} \{U_x\}^{(ne)} \\ \{U_y\}^{(ne)} \\ \{\theta_z\}^{(ne)} \end{Bmatrix} - P \begin{bmatrix} [L_1] & [0] & [L_2] \\ [0] & [L_1] & [L_3] \\ [L_2] & [L_3] & [L_4] \end{bmatrix} \begin{Bmatrix} \{U_x\}^{(ne)} \\ \{U_y\}^{(ne)} \\ \{\theta_z\}^{(ne)} \end{Bmatrix} = \begin{Bmatrix} \{F_1\} \\ \{F_2\} \\ \{F_3\} \end{Bmatrix}$$

$$\ldots\ (101)$$

Where

$$[K_1] = Re_{yy}^2 \int_o^h I_{yy_n} \{\ddot{N}\} [\ddot{N}]\, dz \quad ; \quad [K_2] = Re_{xx}^2 \int_o^h I_{xx_n} \{\ddot{N}\} [\ddot{N}]\, dz$$

$$[K_3] = Re_{\omega\omega}^2 \int_o^h I_{\omega\omega_n} \{\ddot{N}\} [\ddot{N}]\, dz + \frac{Re_{\omega\omega}^2}{\omega_e^2} \int_o^h I_{d_n} \{\dot{N}\} [\dot{N}]\, dz$$

$$[L_1] = \int_o^h \{\dot{N}\} [\dot{N}]\, dz \quad ; \quad [L_2] = \int_o^h Y_B \{N\} [\dot{N}]\, dz \qquad \ldots.(102)$$

$$[L_3] = -\int_o^h X_B \{\dot{N}\} [N]\, dz \quad ; \quad [L_4] = Re_B^2 \int_o^h \frac{I_{B_n}}{A_n} \{\dot{N}\} [\dot{N}]\, dz$$

and

$$\{F_1\} = \begin{Bmatrix} (Re_{yy}^2 \frac{\partial}{\partial Z} (I_{yy_n} \ddot{U}_x) + P\dot{U}_x + P\, Y_B \dot{\theta}_z) \Big|_j \\ Re_{yy}^2\, I_{yy_n}\, \ddot{U}_x \Big|_j \\ -(Re_{yy}^2 \frac{\partial}{\partial Z} (I_{yy_n} \ddot{U}_x) + P\, \dot{U}_x + P\, Y_B \dot{\theta}_z) \Big|_k \\ -Re_{yy}^2\, I_{yy_n}\, \ddot{U}_x \Big|_k \end{Bmatrix}$$

$$\{F_2\} = \begin{Bmatrix} (Re_{xx}^2 \frac{\partial}{\partial Z} (I_{xx_n} \ddot{U}_y) + P\, \dot{U}_y - PX_B \dot{\theta}_z) \Big|_j \\ -Re_{xx}^2\, I_{xx_n}\, \ddot{U}_y \Big|_j \\ -(Re_{xx}^2 \frac{\partial}{\partial Z} (I_{xx_n} \ddot{U}_y) + P\, \dot{U}_y - P\, X_B\, \dot{\theta}_z) \Big|_k \\ -Re_{xx}^2\, I_{xx_n}\, \ddot{U}_y \Big|_k \end{Bmatrix} \qquad \ldots.(103)$$

$$\{F_3\} = \left\{ \begin{array}{l} \left(Re^2_{\omega\omega} \frac{\partial}{\partial Z}(I_{\omega\omega_n} \theta'_z) - \frac{Re^2_{\omega\omega}}{\omega e^2} I_{d_n} \theta'_z + Re^2_B \frac{IB_n}{A_n} p\ \theta'_z \right. \\ \qquad \left. - P\ X_B\ U'_y + P\ Y_B\ U'_x \right) \Big|_j \\ \\ - Re^2_{\omega\omega}\ I_{\omega\omega_n} \theta''_z \Big|_j \\ \\ \left(-Re^2_{\omega\omega} \frac{\partial}{\partial Z}(I_{\omega\omega_n}\ \theta''_z) + \frac{Re_{\omega\omega}}{\omega e^2} I_{d_n}\ \theta'_z - Re^2_B \frac{I_{B_n}}{A_n} P\ \theta'_z \right. \\ \qquad \left. + P\ X_B\ U'_y - P\ Y_B\ U'_x \right) \Big|_k \\ \\ Re^2_{\omega\omega}\ I_{\omega\omega_n}\ \theta''_z \Big|_k \end{array} \right\}$$

Assembling for all elements and applying the boundary conditions, Eqn. (101) is solved for the critical buckling loads.

2.4 PLANE FRAME :

In this work plane frames (lying in zx plane) subjected to transverse loads (y-directions) are considered. Plane frames are formed by joining thin walled beams. FEM equations for a typical element are first obtained in the local coordinates ($\bar{z}$ $\bar{x}$) and then in the global coordinates (zx) using a transformation matrix. Shear effects are neglected in the frame analysis. Frames are studied for static and free vibration cases.

2.4.1 Static analysis:

2.4.1.1 Basic Equations :

As the plane frames subjected to transverse loading are under study, the governing equations for the beams of these frames are Eqns. (61) to (64). Neglecting shear, these four second order differential equations are combined to two fourth order differential equations,

$$EI_{xx} \frac{\partial^4 \bar{u}_y}{\partial \bar{z}^4} = \bar{q}_y + \bar{Q}_y \, \delta(z-\bar{z}u_y) + \frac{\partial \bar{m}_x}{\partial \bar{z}} \quad \ldots\ldots (104)$$

$$EI_{\omega\omega} \frac{\partial^4 \bar{\theta}_z}{\partial \bar{z}^4} - GI_d \frac{\partial^2 \theta_z}{\partial \bar{z}^2} = \bar{m}_t + \bar{M}_t \, \delta(z-\bar{z}_{\theta_z}) + \frac{\partial \bar{m}_\omega}{\partial \bar{z}} \quad \ldots\ldots (105)$$

The over dash refers to the displacements and rotations in the local axes.

The above equations are valid when the loading is at the shear center of the beams. When the loading is at the centroid of the cross section of the beam, the equations (104) and (105) become [2].

$$EI_{xx}\frac{\partial^4 \bar{u}_y}{\partial \bar{z}^4} = \bar{q}_y + \bar{Q}_y \delta(z-\bar{z}_{u_y}) + \frac{\partial \bar{m}_x}{\partial \bar{z}} \quad \ldots\ (106)$$

$$EI_{\omega\omega}\frac{\partial^4 \bar{\theta}_z}{\partial \bar{z}^4} - GI_d\frac{\partial^2 \bar{\theta}_z}{\partial \bar{z}^2} = \bar{m}_t + \bar{M}_t\,\delta(z-\bar{z}_{\theta_z}) + \frac{\partial \bar{m}_\omega}{\partial \bar{z}} - \bar{q}_x(y_q - y_B) + \bar{q}_y(x_q - x_B) \quad \ldots\ (107)$$

where (x_q, y_q) the coordinates of the point of loading and (x_B, y_B) are the coordinates of the shear center.

2.4.1.2 FEM Equations :

Equations (106) and (107) are the two differential equations for the static analysis of a beam of a plane frame.

The displacements over the typical finite element, e , Fig. 3 are approximated as

$$\bar{u}_y^{(e)} = [N]\{\bar{u}_y\}^{(ne)}$$
$$\bar{\theta}_z^{(e)} = [M]\{\bar{\theta}_z\}^{(ne)} \quad \ldots\ (108)$$

Substituting these in Eqns. (106) and (107), two residues $Re^{\bar{u}_y}$, $Re^{\bar{\theta}_z}$ are obtained. These two residues are minimized by the Galerkin method.

Study of compatibility and completeness requirements shows that C_1 elements are needed for displacements $\bar{u}_y^{(e)}$ and $\bar{\theta}_z^{(e)}$, thus

$$[N] = [M] = [N] \quad \ldots\ (109)$$

$$\{\bar{F}_1\}^{(ne)} = \begin{Bmatrix} EI_{xx}\, u_y'''\,|_j \\ -EI_{xx}\, \bar{u}_y''\,|_j \\ -EI_{xx}\, \bar{u}_y'''\,|_k \\ EI_{xx}\, \bar{u}_y''\,|_k \end{Bmatrix} \quad \ldots\ldots (113)$$

$$\{\bar{F}_2\}^{(ne)} = \begin{Bmatrix} (EI_{\omega\omega}\, \bar{\theta}_z''' - G\, I_d\, \bar{\theta}_z')\,|_j \\ -EI_{\omega\omega}\, \bar{\theta}_z''\,|_j \\ (-EI_{\omega\omega}\bar{\theta}_z''' + G\, I_d\, \bar{\theta}_z')\,|_k \\ EI_{\omega\omega}\, \bar{\theta}_z''\,|_k \end{Bmatrix}$$

where

$EI_{xx}\, \bar{u}_y''$ = Bending moment ; $-EI_{xx}\, \bar{u}_y'''$ = Shear force.

$-EI_{\omega\omega}\bar{\theta}_z''$ = Bimoment ; $-EI_{\omega\omega}\bar{\theta}_z''' + G\, I_d \bar{\theta}_z'$ = Warping Twisting moment +St Venant tisting moment

= Total twisting moment

Equation (110) in a more concise form is

$$[\bar{K}]^{(e)} \{\bar{u}\}^{(ne)} = \{\bar{Q}\}^{(ne)} + \{\bar{F}\}^{(ne)} \quad \ldots\ldots (114)$$

where

$[\bar{K}]^{(e)}$ = Stiffness matrix of the element in the local axes.

$\{\bar{u}\}^{(ne)}$ = Displacement vector of the element in the local axes.

$\{\bar{Q}\}^{(ne)}$ = Load vector of the element in the local axes.

$\{\bar{F}\}^{(ne)}$ = Boundary force vector of the element in the local axes.

2.4.1.3 Transformation to the Global axes.

The displacements and their derivatives of a beam element of the plane frame in the local axes $(\bar{x},\bar{z})$, Fig. 4, are transformed to the global zes (xz) as [18,6]

$$\begin{Bmatrix} \bar{u}_y \\ \bar{u}_y' \\ \bar{\theta}_z \\ \bar{\theta}_z' \\ \bar{u}_y \\ \bar{u}_y' \\ \bar{\theta}_z \\ \bar{\theta}_z' \end{Bmatrix}_j \\ \bar{\theta}_z' \Big|_k = \begin{bmatrix} 1 & 0 & 0 & 0 & 0 & 0 & 0 & 0 \\ 0 & \cos\alpha & -\sin\alpha & 0 & 0 & 0 & 0 & 0 \\ 0 & \sin\alpha & \cos\alpha & 0 & 0 & 0 & 0 & 0 \\ 0 & 0 & 0 & 1 & 0 & 0 & 0 & 0 \\ 0 & 0 & 0 & 0 & 1 & 0 & 0 & 0 \\ 0 & 0 & 0 & 0 & 0 & \cos\alpha & -\sin\alpha & 0 \\ 0 & 0 & 0 & 0 & 0 & \sin\alpha & \cos\alpha & 0 \\ 0 & 0 & 0 & 0 & 0 & 0 & 0 & 1 \end{bmatrix} \begin{Bmatrix} u_y \\ u_y' \\ \theta_z \\ \theta_z' \\ u_y \\ u_y' \\ \theta_z \\ \theta_z' \end{Bmatrix}_j \\ \theta_z' \Big|_k$$

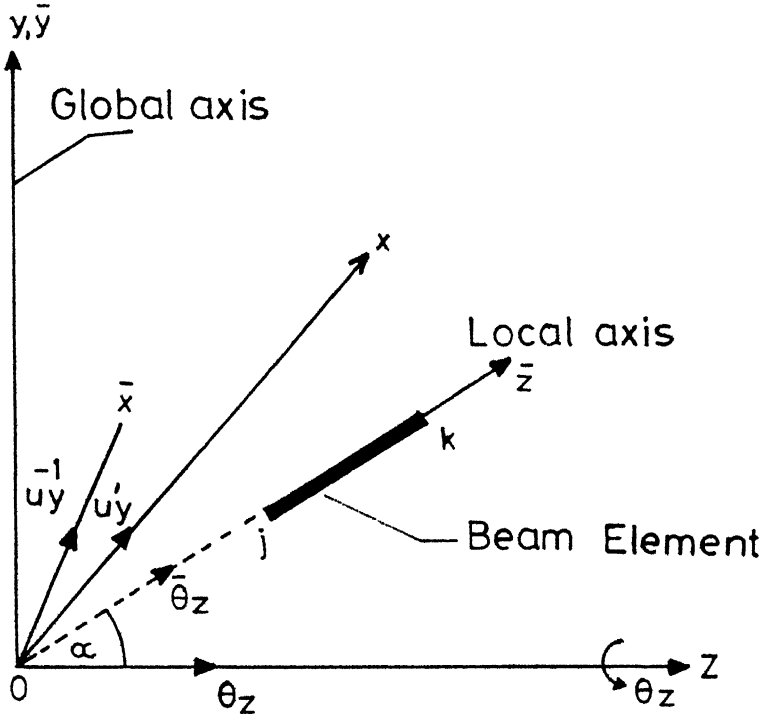

Fig. 4 Local and Global Axes of a Beam Element.

or $\{\bar{u}\}^{(ne)} = [T]\ \{u\}^{(ne)}$ .... (115)

where α is the angle between the element jk and global axis z.

Matrix $\{\bar{u}\}^{(ne)}$ = displacement matrix in local axes,

$[T]$ = transformation matrix,

$\{u\}^{(ne)}$ = displacement matrix in global axes.

Similarly forces in local axes are related to forces in global axes,

$$\{\bar{F}\}^{(ne)} = [T]\ \{F\}^{(ne)} \quad \text{.... (116)}$$

Using the Eqns. (115) and (116) , Equation (114) becomes,

$$[K]^{(e)}\ \{u\}^{(ne)} = \{Q\}^{(ne)} + \{F\}^{(ne)} \quad \text{.... (117)}$$

where

$[K]^{(e)} = [T]^{T}\ [\bar{K}]^{(e)}\ [T]$ = Stiffness matrix of the element in the global axes,

$\{Q\}^{(ne)}$ = load matrix of the element in global axes,

$\{F\}^{(ne)}$ = boundary force matrix of the element in global axe

After assembling for all the elements, using the Eqn. (117) and applying the following boundary conditions,

Pined end $u_y = 0$; $EI_{xx}\ u_y'' = 0$; $\theta_z = 0$; $EI_{\omega\omega}\theta_z'' = 0$ ....(118)

Fixed end $u_y = 0$; $u_y' = 0$; $\theta_z = 0$; $\theta_z' = 0$ ....(119)

Free end $EI_{xx}u_y'' = 0$; $EI_{xx}\ u_y''' = 0$; $EI_{\omega\omega}\theta_z'' = 0$;

$$(ET_{\omega\omega}\ \theta_z''' - GI_d\ \theta_z') = 0 \quad \text{....(120)}$$

one gets,

$$[K]\{u\}^n = \{Q\}^n \qquad \ldots\ (121)$$

Equation (121) is solved for the displacements in the global axes.

2.4.1.4 Stresses in the plane frame.

After solving the Eqn. (121) for displacements, one can find out the nodal forces and moments $\{F\}^{(ne)}$ from the Eqn. (117) as

$$\{F\}^{(ne)} = [K]^{(e)} \{u\}^{(ne)} - \{Q\}^{(ne)} \qquad \ldots\ (122)$$

Using these moments and forces, the total stresses (Normal and shear) at the nodes are calculated as [2,5]

$$\text{Total normal stress} = \sigma_z = \frac{M_{xx} y}{I_{xx}} + \frac{M_\omega\, \omega(s_E)}{I_{\omega\omega}} \qquad \ldots\ (123)$$

$$\text{Total shear stress} = \tau_{zs} = \frac{Q_y I_x}{t\, I_{xx}} + \frac{M_t I_\omega(s_E)}{t\, I_{\omega\omega}} + \frac{M_{st}\, t}{I_d} \qquad \ldots\ (124)$$

where

M_{xx} = Bending moment = $E\, I_{xx}\, u_y''$

M_ω = Bimoment = $-E\, I_{\omega\omega}\, \theta_z''$

$\omega(s_E)$ = Warping function, see Appendix III and [5]

Q_y = Shear force = $-E\, I_{xx}\, u_y'''$

I_x = Statical moment about x-axis = $\int_A y \, dA$

t = Thickness of the profile

M_t = Warping twisting moment or flexural twist $= -EI_{\omega\omega}\theta_z'''$

$I_\omega(s_E)$ = Statical sectorial moment = $\int_A \omega(s_E)dA$, see Appendix III and [5]

M_{st} = Saint Venant twisting moment = $GI_d\,\theta_z'$

I_d = Saint venant torsional constant of the section

2.4.2 Free Vibrations :

2.4.2.1 Basic Equations :

Out-of-plane vibrations of the plane frame are being studied. The governing equations of motion for this case are Eqns. (18) to (21). These four second order differential equations can be combined to two fourth order differential equations. Neglecting the shear one gets these equations as,

$$EI_{xx}\frac{\partial^4\bar{u}_y}{\partial\bar{z}^4} - \rho I_{xx}\frac{\partial^4\bar{u}_y}{\partial\bar{z}^2\partial t^2} + \rho A\frac{\partial^2\bar{u}_y}{\partial t^2} - \rho Ax_B\frac{\partial^2\bar{\theta}_z}{\partial t^2} = 0 \qquad \ldots\ (125)$$

$$EI_{\omega\omega}\frac{\partial^4\bar{\theta}_z}{\partial\bar{z}^4} - GI_d\frac{\partial^2\bar{\theta}_z}{\partial\bar{z}^2} - \rho I_{\omega\omega}\frac{\partial^4\bar{\theta}_z}{\partial\bar{z}^2\partial t^2} + \rho I_B\frac{\partial^2\bar{\theta}_z}{\partial t^2} - \rho Ax_B\frac{\partial^2\bar{u}_y}{\partial t^2} = 0$$

.... (126)

2.4.2.2 FEM Equations :

Equations (125) and (126) are the two differential equations for the free vibration analysis of a plane frame. These two differential equations are solved by Galerkin finite element method.

The displacements over the typical finite element, e , Fig. 3, are approximated as in Eqn. (108).

Substituting these in Eqns. (125) and (126), two residues $Re^{\bar{u}_y}$, $Re^{\bar{\theta}_z}$ are obtained. These two residues are minimized by the Galerkin method.

Here also C_1 elements are needed to satisfy the compatibility and completeness requirements. The shape function for the C_1 elements are as in Eqn. (49). The nodal variables are $\bar{u}_y$, $\bar{u}_y'$ and $\bar{\theta}_z$, $\bar{\theta}_z'$.

The minimized residual equations are put in a matrix form, using Eqn. (108) as,

$$[\bar{M}]^{(e)}\{\ddot{\bar{u}}\}^{(ne)} + [\bar{K}]^{(e)}\{\bar{u}\}^{(ne)} = \{\bar{F}\}^{(ne)}$$

.... (127)

Matrices $[\bar{K}]^{(e)}$, $\{\bar{u}\}^{(ne)}$ and $\{\bar{F}\}^{(ne)}$ are same as in Eqns. (111) to (114), and matrix $[\bar{M}]^{(e)}$ is

$$[\bar{M}]^{(e)} = \text{Mass matrix of the element in the local axes} = \begin{bmatrix} [\bar{M}_1]^{(e)} & [\bar{M}_2]^{(e)} \\ [\bar{M}_2]^{(e)} & [\bar{M}_3]^{(e)} \end{bmatrix} \quad \ldots\ldots (128)$$

where

$$[\bar{M}_1]^{(e)} = \rho A \int_0^h \{N\}[N]\,d\bar{z} + \rho I_{xx} \int_0^h \{N'\}[N']\,d\bar{z}$$

$$[\bar{M}_2]^{(e)} = -\rho A x_B \int_0^h \{N\}[N]\,d\bar{z} \quad \ldots\ldots (129)$$

$$[\bar{M}_3]^{(e)} = \rho I_B \int_0^h \{N\}[N]\,d\bar{z} + \rho I_{\omega\omega} \int_0^h \{N'\}[N']\,d\bar{z}$$

2.4.2.3 Transformation to Global axes :

Equation (128) is applicable to the elements in the local axes $(\bar{x},\bar{z})$, Fig.4. This equation can be transformed to the global axes (x,z), following the procedure of section 2.4.1.3, as

$$[M]^{(e)} \{\ddot{u}\}^{(ne)} + [K]^{(e)} \{u\}^{(ne)} = \{F\}^{(ne)} \quad \ldots\ldots (130)$$

Here $[K]^{(e)}$, $\{u\}^{(ne)}$ and $\{F\}^{(ne)}$ are same as in Eqn. (117) and

$[M]^{(e)} = [T]^{T} [M]^{(e)} [T]$ = Mass matrix of the element in the global axes, and

$[T]$ is the transformation matrix, and is same as in Eqn. (115)

After assembling for all the elements and applying the boundary conditions, Eqns. (118) to (120), one gets,

$$[M] \{\ddot{u}\}^{n} + [K] \{u\}^{n} = \{0\} \quad \ldots\ldots (131)$$

which are solved for the natural frequencies of vibration.

CHAPTER- III

RESULTS AND DISCUSSION

This chapter deals with the numerical results, obtained by Galerkin finite element method, of the coupled equations of thin walled beams for free vibration, static and buckling cases, for various boundary conditions. The results for free vibration and static analysis of a plane frame are also presented.

3.1. NUMBER OF FINITE ELEMENTS :

First of all one should decide the number of finite elements to be used in the analysis. For various boundary conditions, the problems were solved for two, four and six finite elements. It was observed that with six finite elements, first five frequencies were fairly accurate in all the cases. Sample results for pinned-pinned thin-walled beam of unequal channel cross section, Fig, 7 , are shown in Table 1.

3.2 FREE VIBRATIONS :

For a beam of doubly-symmetric cross-section, shear center B and the centroid 0 coincide.

Thus

$$X_B = Y_B = I_{pq} = I_{qr} = I_{pr} = 0 \qquad \ldots\ (132)$$

Table 1 : Comparision of exact and FEM solutions for a pinned-pinned beam of unequal channel Section.

Mode No. n	Natural frequencies			
	Finite element method solution			Exact solution [9]
	2 elements	4 elements	8 elements	
1	400.10	398.93	398.86	398.84
2	592.73	590.60	590.47	590.44
3	1615.44	1469.26	1464.99	1463.84
4	1805.11	1798.51	1798.12	1798.06
5	2603.11	2355.36	2348.03	2346.14

With this governing equations , (31) to (36), become uncoupled.

A beam having one axis of symmetry, the shear centre lie on the axis of symmetry. In this case the bending vibration equations about the axis of symmetry become uncoupled. If the x-axis is the axis of symmetry, Fig. 5, then

$$Y_B = I_{qp} = I_{qr} = 0 \qquad \ldots\ (133)$$

Bending vibration equations about y-axis (31) and (32), become uncoupled ; and Eqns. (33) to (36) remain coupled. This is known as double coupling of bending vibration about x-axis and the torsional vibration.

In the case of beam with no axis of symmetry, shear centre does not lie on any axis. Governing equations remain coupled and this is known as triple coupling of two bending vibration about the x- and y-axes and torsional vibration about z-axis.

3.2.1 Mono-axis symmetric beam :

For this, thin walled beam of semi-circular cross-sections having x-axis symmetry Fig. 5, case 1 of [14] and case 2 of [16] are chosen in this work. The dimensions, section properties and other parameters are given in Fig. 5.

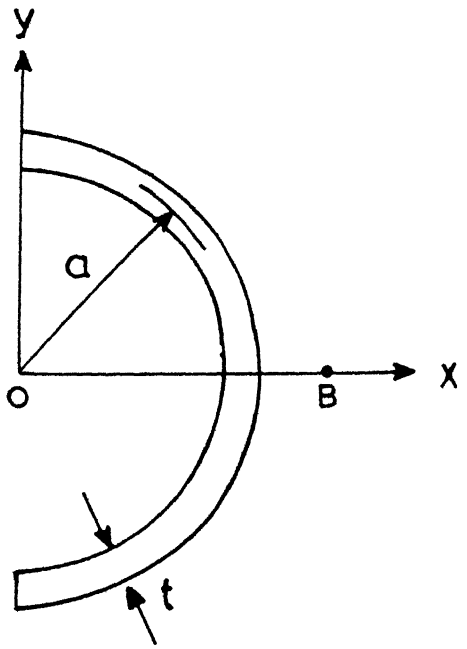

Case. 1

$a = 24.5 \times 10^{-3}$ m , $t = 4.0 \times 10^{-3}$ m

$E = 68.9$ Gpa, $G = 26.5$ Gpa, $\rho = 2711.039$ Kg/ m^3

$Ixx = 92.6 \times 10^{-9}\ m^4$, $I_{\omega\omega} = 1.52 \times 10^{-12}\ m^6$

$I_B = 0.1848 \times 10^{-6}\ m^4$, $A = 308 \times 10^{-6}\ m^2$, $l = 0.820$ m

$X = 15.5\ 10^{-3}$ m , $Y_B = 0.0$ m , $Ipp = 153.938 \times 10^{-6}\ m^2$

$Ipr = 1.0 \times 10^{-25}\ m^3$, $Irr = 0.035 \times 10^{-6}\ m^4$, $I_d = 0.8210 \times 10^{-9}\ m^4$

Case. 2

$a = 50.8 \times 10^{-3}$ m, $t = 1.5875 \times 10^{-3}$ m

$I_{XX} = 0.3269 \times 10^{-6}\ m^4$, $I_{\omega\omega} = 20.0 \times 10^{-12}\ m^6$

$I_B = 0.6538 \times 10^{-6}\ m^4$, $A = 253.35 \times 10^{-6}\ m^2$, $l = 0.90$ m

$X_B = 0.03234$ m , $Y_B = 0.0$ m , $Ipp = 126.677 \times 10^{-6}\ m^2$

$Ipr = 1.0 \times 10^{-25}\ m^3$, $Irr = 0.1238 \times 10^{-6}\ m^4$, $I_d = 0.2128 \times 10^{-9}\ m^4$

Fig. 5 Thin-Walled Semicircular Section.

The governing equations are (33) to (36) and (133). These equations are solved for pinned-pinned, fixed-fixed and contilever cases and the results are given in Tables 2,3, and 4 respectively.

First, case 1 is studied and results are obtained neglecting rotary inertia and shear. In this case Eqns. (33) and (34) become a fourth order differential equation, and Eqns. (35) and (36) become another fourth order differential equation. These two fourth order coupled equations are solved using C_1 elements with boundary conditions as,

$$\begin{aligned}
&\text{Pined end} && U_y = 0 \;;\; U_y'' = 0 \;;\; \theta_z = 0 \;;\; \theta_z'' = 0 \\
&\text{Fixed end} && U_y = 0 \;;\; U_y' = 0 \;;\; \theta_z = 0 \;;\; \theta_z' = 0 \qquad \ldots.(134) \\
&\text{Free end} && U_y'' = 0 \;;\; U_y''' = 0 \;;\; \theta_z'' = 0 \;;\; \theta_z''' = 0
\end{aligned}$$

Next, results are calculated including rotary inertia terms (but neglecting shear). In this case also one gets two coupled fourth order equations and are solved using same elements and boundary conditions, Eqns. (134).

Lastly, results are calculated including both the rotary inertia and shear terms. In this case there are four coupled second order equations. These are solved using C_1 elements with boundary conditions,

Table 2 : Coupled frequencies of a thin walled pinned-pineed beam of semi circular cross section.

Mode No.	Exact solution [10, 9]	Present FEM results			% Decrease in frequency due to Rotary inertia and shear
	Excluding Rotary inertia and shear	Excluding Rotary inertia and shear	Including Rotary inertia	Including Rotary inertia and shear	
1	945.25	945.30	944.79	939.78	0.58
2	2012.66	2012.72	2006.19	1993.09	0.98
3	2298.47	2298.87	2298.03	2286.08	0.64
4	3795.87	3800.52	3798.24	3772.23	0.74
5	5560.73	5588.57	5583.05	5522.08	1.19
6	6952.94	6958.02	6857.66	6603.65	5.09

Table 3 : Coupled frequencies of a thin walled fixed-fixed beam of semicircular cross section.

Mode No.	Present FEM results			% Decrease in frequency due to Rotary inertia and shear
	Excluding Rotary inertia and shear	Including Rotary inertia	Including Rotary inertia and shear	
1	1252.75	1252.63	1240.42	0.98
2	2679.87	2679.07	2645.12	1.30
3	3889.55	3872.86	3698.02	4.92
4	4393.25	4389.37	4300.68	2.11
5	6362.06	6355.16	6199.17	2.56

Table 4 : Coupled frequencies of a Thin-walled cantilever beam of semicircular cross section.

Mode No.	Results of [14]	Present FEM results			% Decrease in Frequency due to Rotary inertia and shear
	Including Rotary inertia	Excluding Rotary inertia and shear	Including Rotary inertia	Including Rotary inertia and shear	
1	400.62	400.95	400.73	399.08	0.47
2	863.94	866.18	865.18	861.73	0.51
3	1747.98	1750.95	1750.17	1731.82	1.09
4	3040.43	3054.45	3048.77	3017.40	1.21
5	4129.94	4172.96	4131.75	4016.05	3.71

Pinned end $U_y = 0 \; ; \; \theta_x' = 0 \; , \; ; \; \theta_z = 0 \; ; \; \Phi' = 0$

Fixed end $U_y = 0 \; , \; \theta_x = 0 \; , \; \theta_z = 0 \; , \; \Phi = 0$

Free end $\theta_x' = 0 \; , \; \dfrac{U_y' + \theta_x}{Se_{pp}^2} + \dfrac{\theta_z' - \Phi}{Se_{pr}^2} = 0$, and

$$\Phi' = 0 \; , \; \frac{\theta_z' - \Phi}{Se_{rr}^2} + \frac{U_y' + \theta_x}{Se_{rp}^2} + \frac{\Phi}{\omega e^2} = 0$$

..... (135)

Study of the results in Tables 2 to 4 shows that frequencies decrease due to rotary inertia and further decrease on inclusion of shear, as expected. For pinned-pinned beams without rotary inertia and shear, exact results of [9,10] are also given in Table 2. Present FEM results compare well. Error in FEM results increases with increase in mode number, as expected. For cantileverbeam, Friberg [14], obtained the frequencies including rotary inertia (but neglecting shear) by dynamic stiffness matrix method. The results are shown in Table 4 and present FEM results match well with them.

Next, semi-circular cross-sectional beam, Fig. 5, case 2, is studied. The ratio of frequencies (ω_{R+S}/ω_N) for this case is shown in Fig. 6 as a function of Re_{xx}. ω_{R+S} is the frequency of vibration including the effect of rotary inertia and shear. ω_N is the frequency of vibration excluding the effect of rotary inertia and shear.

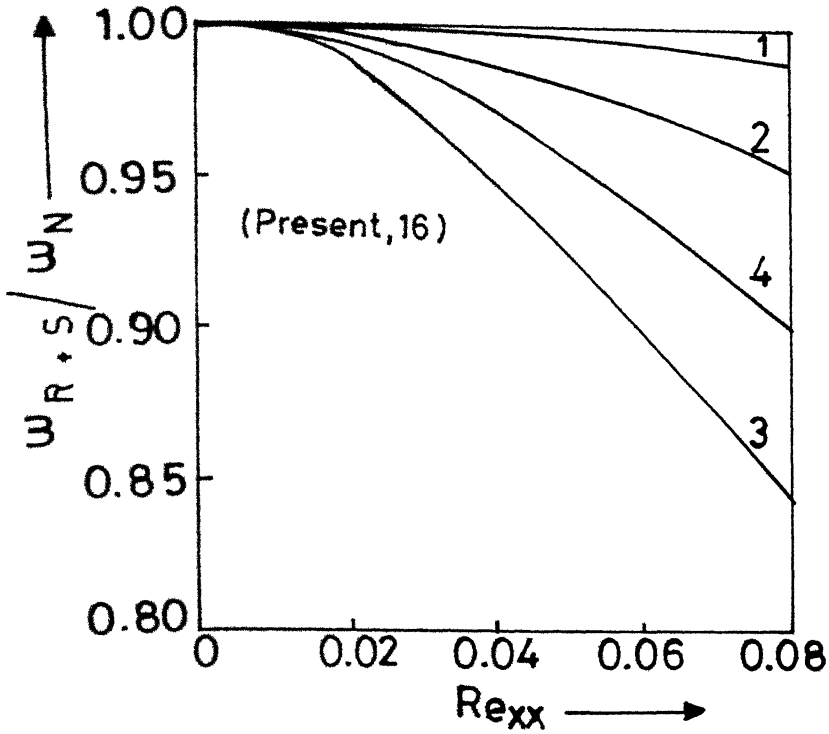

(a) Pinned-Pinned Beam

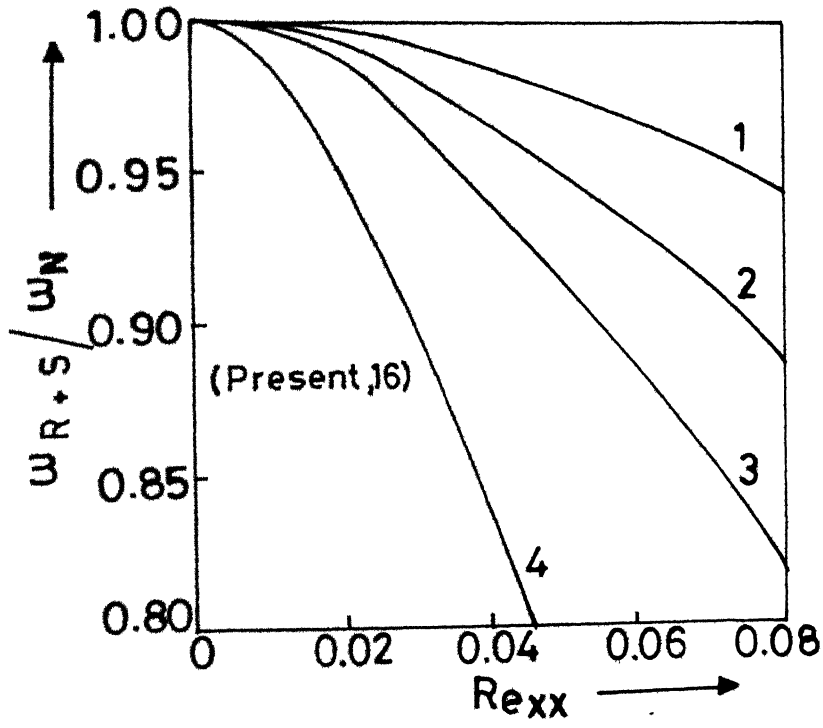

(b) Fixed-Fixed Beam

Fig. 6 Frequencies of Semi-circular Cross-section Beam as Functions of R_{exx}.

Tso [16] obtained the results analytically. Present results match well. It is not possible to see any difference in the results in this figure.

For case 1, it is seen that decrease in frequency is not always larger for the higher modes than for the lower modes. This was observed by [16] also. Study of mode shapes for pinned-pinned beam shows that first, third, fourth and fifth are torsion dominated modes ; and second and sixth are bending dominant. Parameters for this section are

$$Re^2_{xx} = .000447 \quad , Se^2_{pp} = .002326 \quad , \quad Se^2_{pr} = 2.9361$$

$$Re^2_{\omega\omega} = .00001223, \; Se^2_{rr} = .00016789, \quad Se^2_{rp} = .0000716762$$

.... (136)

Parameters Re_{xx}, Se_{pp}, Se_{pr} of bending are larger than the parameters $Re_{\omega\omega}$, Se_{rr}, Se_{rp} of torsion, hence the decrease in frequency is larger in bending dominant mode than in torsion dominant modes.

For fixed-fixed beam first, second, fourth and fifth are torsion deminant modes and third is the bending-dominant mode, thus more decrease in frequency in third mode. For cantilever beam, first, third and fourth are torsion dominant modes, second and fifth modes are bending dominant modes. In both these beams, decrease in frequencies is large in bending dominant modes than in torsion dominant modes.

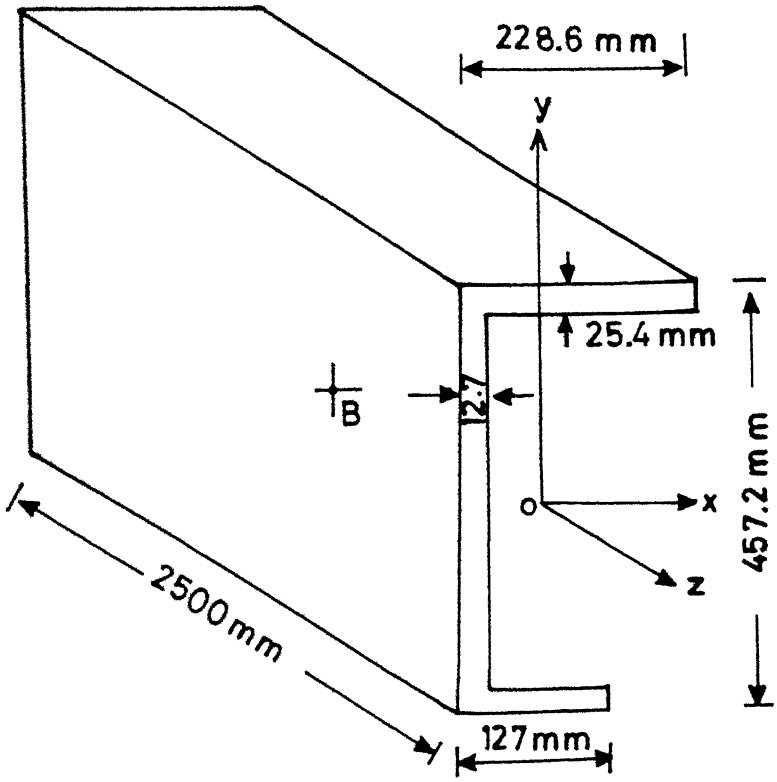

$E = 68.9$ Gpa, $G = 26.5$ Gpa, $\rho = 2711.039$ Kg/m^3

$A = 0.01483562$ m^2, $I_{\omega\omega} = 1.8403 \times 10^{-6}$ m^6, $I_{xx} = 545.263 \times 10^{-6}$ m^4

$I_{yy} = 73.673 \times 10^{-6}$ m^4, $I_P = 618.936 \times 10^{-6}$ m^4, $I_B = 886.91 \times 10^{-6}$ m^4

$X_B = -0.121793$ m, $Y_B = 0.0567944$ m, $I_{qq} = 9.03224 \times 10^{-3}$ m^2

$I_{qp} = 10^{-21}$ m^2, $I_{qr} = 0.283004 \times 10^{-3}$ m^3, $I_{pp} = 5.80644 \times 10^{-3}$ m^2

$I_{pr} = 0.36768 \times 10^{-3}$ m^3, $I_{rr} = 0.465625 \times 10^{-3}$ m^4, $I_d = 2.25459 \times 10^{-6}$ m^4

Fig.7 Thin-Walled Beam of Unequal Channel Section.

3.2.2 Unsymmetric section beam :

For this, a thin walled beam of unequal channel cross section, Fig. 7, of [5] is chosen. The dimensions, section properties and other parameters are also given in the figure.

The governing equations are (31) to (36). Results for pinned-pinned, fixed-fixed and cantilever beams are obtained and are given in Tables 5,6 and 7 respectively.

Firstly, results are obtained neglecting the effects of rotary inertia and shear. In this case the six coupled second order differential equations (31) to (36) reduce to three coupled fourth order differential equations. These three coupled differential equations are solved by Galerkin finite element method using C_1 elements with the boundary conditions as,

Pinned end $U_x = 0$; $U_x'' = 0$;, $U_y = 0$; $U_y'' = 0$; $\theta_z = 0$; $\theta_z'' = 0$

Fixed end $U_x = 0$; $U_x' = 0$; $U_y = 0$; $U_y' = 0$; $\theta_z = 0$; $\theta_z' = 0$

Free end $U_x'' = 0$; $U_x''' = 0$; $U_y'' = 0$; $U_y''' = 0$; $\theta_z'' = 0$; $\theta_z''' = 0$

.... (137)

Next, results are obtained by including the effect of rotary inertia (neglecting shear). In this case also there are three coupled fourth order differential equations. These are solved using the same elements and boundary conditions,

Table 5 : Coupled frequencies of a Thin-walled pinned-pinned beam of unequal channel section.

Mode No.	Exact solution [9]	Present FEM solution			% Decrease in Frequency due to Rotary inertia and shear
	Excluding Rotary inertia and shear [9]	Excluding Rotary inertia and shear	Including Rotary inertia	Including Rotary inertia and shear	
1	398.84	398.86	397.15	394.44	1.10
2	590.44	590.47	586.93	578.38	2.04
3	1463.84	1464.99	1443.71	1400.91	4.30
4	1798.06	1798.12	1638.16	1489.90	17.14
5	2346.14	2348.03	2232.46	2171.26	7.45

Table 6 : Coupled frequencies of a thin-walled fixed-fixed beam of unequal channel section

Mode n	Present FEM results			% Decrease in Frequency due to Rotary inertia and shear
	Excluding Rotary inertia and shear	Including Rotary Inertia	Including Rotary inertia and shear	
1	828.97	827.35	787.68	4.98
2	1329.89	1322.84	1222.44	8.03
3	2252.26	2236.03	2017.50	10.42
4	3668.58	3597.53	2332.39	36.42
5	4069.09	3879.51	3072.08	24.50

Table 7 : Coupled frequencies of a Thin-walled cantilever beam of unequal channel section

Mode n	Present FEM results			% Decrease in Frequency due to Rotary inertia and shear
	Excluding Rotary inertia and shear	Including Rotary inertia	Including Rotary inertia and shear	
1	169.97	169.14	167.83	1.26
2	218.12	217.76	214.32	1.74
3	644.27	632.50	618.74	3.96
4	858.71	854.33	837.14	2.51
5	1314.14	1296.14	1272.62	3.15

Finally, results are obtained including the effects of rotary inertia, and shear. In this the governing equations are six second order coupled differential equations. These six equations, Eqns. (30) to (34), are solved by FEM using C_1 elements with the boundary conditions as

Pinned end $U_x = 0$; $\theta'_y = 0$; $U_y = 0$; $\theta'_x = 0$; $\theta_z = 0$; $\Phi' = 0$

Fixed end $U_x = 0$; $\theta_y = 0$; $U_y = 0$; $\theta_x = 0$; $\theta_z = 0$; $\Phi = 0$

Free end $\theta'_y = 0$; $\dfrac{U'_x - \theta_y}{Se^2_{qq}} + \dfrac{U'_y + \theta_x}{Se^2_{qp}} + \dfrac{\theta'_z - \Phi}{Se^2_{qr}} = 0$

$$\theta'_x = 0 \; ; \; \frac{U'_y + \theta_x}{Se^2_{pp}} + \frac{U'_x - \theta_y}{Se^2_{pq}} + \frac{\theta'_z - \Phi}{Se^2_{pr}} = 0 \quad \text{and} \quad \ldots.(138)$$

$$\Phi' = 0 \; ; \; \frac{\theta'_z - \Phi}{Se^2_{rr}} + \frac{U'_y + \theta_x}{Se^2_{rp}} + \frac{U'_x - \theta_y}{Se^2_{rq}} + \frac{\Phi}{\omega e^2} = 0$$

It is clear from the results in Tables 5 to 7 that frequencies decrease due to the rotary inertia and decrease further with the inclusion of shear as expected. Excluding shear and rotary inertia exact results can be obtained using, Gere [9] . Exact results for pinned-pinned case are also given in Table 5 and present FEM results match well. In the three beams studied effect of shear and rotary inertia is least in cantilever and highest in fixed-fixed beam.

In this example it is observed that decrease in frequency is not always larger for higher modes than the lower modes. Study of mode shapes for pinned-pinned beam shows that second and fifth modes are bending dominant about the y-axis direction, fourth mode is bending dominant about the x-axis, first and third modes are torsion dominant. Parameters for this section are

Re^2_{yy} = 0.0007943 ; Se^2_{qq}= 0.003393 ; Se^2_{qp}= 0.3064E+17;Se^2_{qr}=0.2707

Re^2_{xx} = 0.005879 ; Se^2_{pp}=0.039 ; Se^2_{pq}=0.2268E+18 ;Se^2_{pr}=1.5423

$Re^2_{\omega\omega}$ = 0.0003319 ; Se^2_{rr}=0.001644 ; Se^2_{rp}=0.001082 ; Se^2_{rq}=0.30833

.... (139)

Derivation of these parameters is given Appendix III. Parameters Re_{xx}, Se_{pp}, Se_{pq} and Se_{pr} of bending about x-axis are larger than the parameters Re_{yy}, Se_{qq}, Se_{qp} and Se_{qr} of bending about y-axis. These parameters Re_{yy}, Se_{qq}, Se_{qp} and Se_{qr} are larger than the parameters $Re_{\omega\omega}$, Se_{rr}, Se_{rp} and Se_{rq} of torsion. Hence the decrease in frequency is larger in bending about x-axis dominant modes than in bending about y-axis dominant modes. The decrease in frequency of bending y-axis dominant modes, inturn, is more than that in torsion dominant modes.

For fixed-fixed beam, second, fifth modes are bending y-axis dominant modes, fourth mode is bending about x-axis dominant mode and first, third modes are torsion dominant modes. For cantilever beams, second, fifth modes are bending about y-axis dominant, third mode is bending about x-axis dominant, and first, fourth modes are torsion dominant, For both these beams, decrease in frequencies is more in bending about x-axis dominant modes than in bending about y-axis dominant modes. Inturn the decrease in frequencies is more in bending about y-axis dominant modes than in torsion dominent modes. For a better understanding of this, the %. decrease in frequencies as a function of Re_{xx} is shown in Fig. 8 for pinned-pinned and fixed-fixed beams. Symbol T-j stands for torsion dominant j^{th} mode, B-x-j for bending about x-axis dominant j-th mode and B-y-j for bending about y-axis dominant j-th mode.

3.3 STATIC ANALYSIS :

For beams of doubly-symmetric cross-section, Eqn.(132) holds and the governing Eqns. (66) to (71) become uncoupled and can be solved independent of each other. For beams of mono-axis symmetric cross-sections, Eqn. (133) holds and the Eqn. (66)to (67) become uncoupled and the Eqn. (68) to (71) remain coupled.

If the beam cross section has no axis of symmetry then all the equations (66)to(71) remain coupled and have to

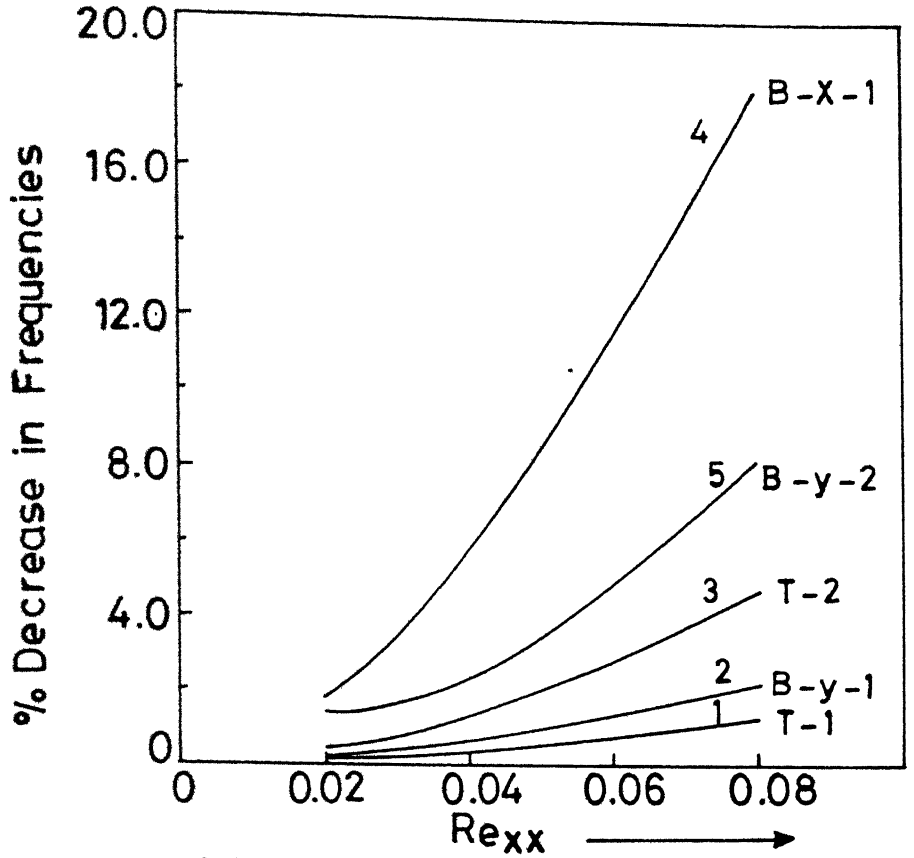

(a) Pinned-Pinned Beam

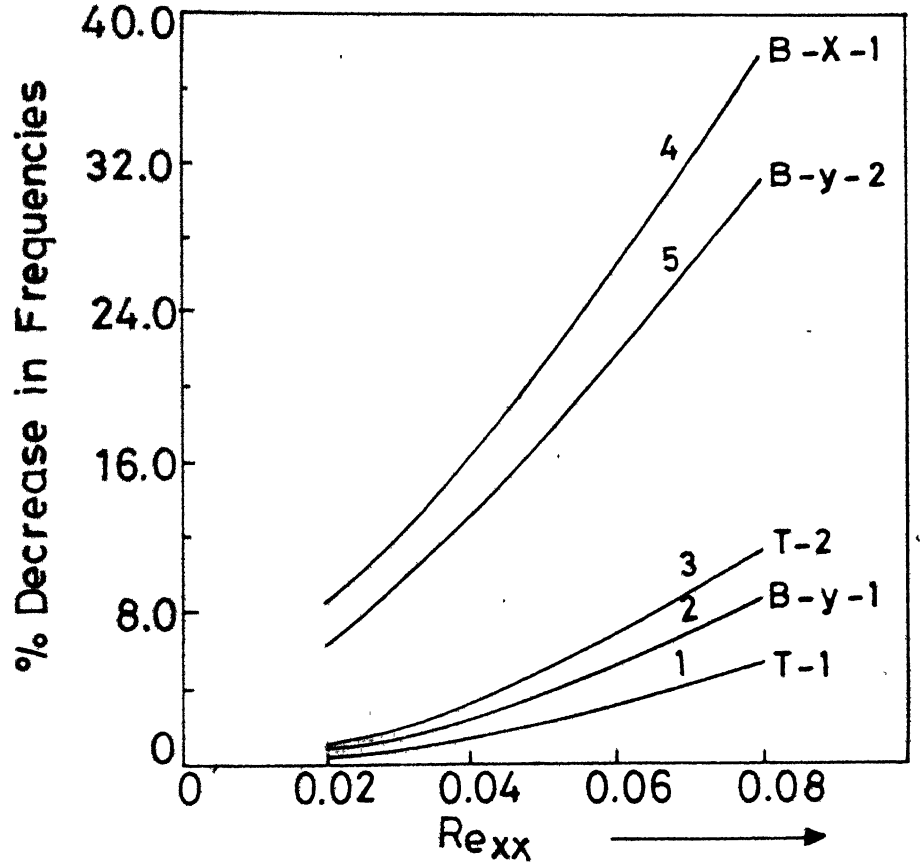

(b) Fixed-Fixed Beam

Fig.8 % Decrease in Frequencies of an Unequal Channel Section Beams as Functions of Re_{xx}.

3.3.1 Cantilever of box cross-section :

Here a thin-walled cantilever of box cross section, which is doubly symmetric, Fig.9, used by [7] is considered. The dimensions and the section properties of the beam are given in Fig. 9. Derivation of these section properties is given in Appendix III. As this cross section is doubly symmetric, governing Eqns. (66) to (71) are uncoupled. The static analysis of beams in bending is well known in the literature. Hence the static analysis of thin-walled beams in torsion, using warping-torsion theory is given in this work. Thus governing equations are Eqns. (70)to(71). It is noted that the formulation of Chapter 2 does not include the strain energy due to St.Venant shear stresses, Chen and Hu [7], which is

$$V_s = \frac{1}{2}\int_0^l GJ_s \phi^2 \, dz \qquad \ldots\ (140)$$

where

$$J_s = \frac{1}{3}\int_A t^2 \, dA \qquad \ldots\ (141)$$

is the St Venant torsional constant corresponding to St Venant shear stress.

Inclusion of this term will give rise to the following term in Eqn. (70)

$$\frac{1}{S\nu^2}\frac{\partial}{\partial z}\left(J_{s_n}\bar{\phi}\right) \qquad \ldots\ (142)$$

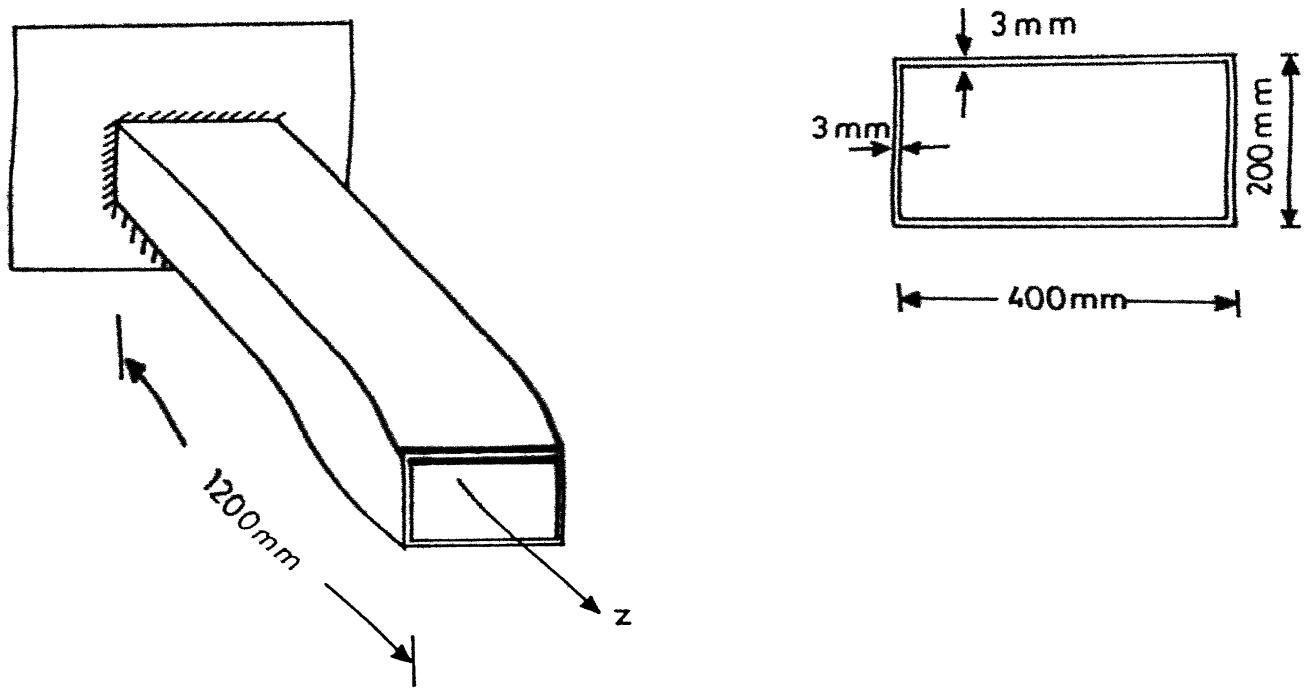

E = 200 Gpa, G = 75Gpa, ρ = 7860 Kg / m^3, Js = 0.1333 x 10^{9} m^4

Id = 64.0 x 10^{-6} m^4, Irr = 72.0 x 10^{-6} m^4, $I_{\omega\omega}$ = 0.48 x 10^{-6} m^6, Sv = 81.66

Fig. 9 Thin-Walled Cantilever of Box Cross-Section.

where

$$Sv^2 = \frac{EI_{\omega\omega_o}}{GJ_{s_o} l^2} \qquad \ldots\ (143)$$

Thus the results in this section are based on Eqns. (70)to(71), with Eqn. (142) included in Eqn. (70). Loading is uniformly distributed torque, m_T = 0.0216. The boundary canditions are

$$\text{Fixed end} \quad \theta_z = 0 \ , \quad \Phi = 0$$

$$\text{Free end} \quad \Phi' = 0 \ , \quad \frac{\theta_z' - \Phi}{Se_{rr}^2} + \frac{\Phi}{\omega e^2} + \frac{\Phi}{Sv^2} = 0 \qquad \ldots\ (144)$$

Results for angle of twist (θ_z), warping measure (Φ) and bimoment (M_ω) are given in Fig. 10. Chen and Hu [7] results are also given and present results match well.

3.3.2 Tapered cantilever of I section :

In this case a thin-walled tapered cantilever of I section used by [8] , Fig. 11, is chosen. This section is a doubly symmetric cross-section. Thus for torsion analysis governing equations are Eqns. (70)to(71) with Eqn. (132) and boundary conditions are Eqn. (144). The dimensions and section properties are also given in Fig. 11. Equations (70)to(71), which can be used for variable cross-sections, are solved for a end torque of M_T = 224.65E03 (1 kN.m). Ten elements are taken in this case.

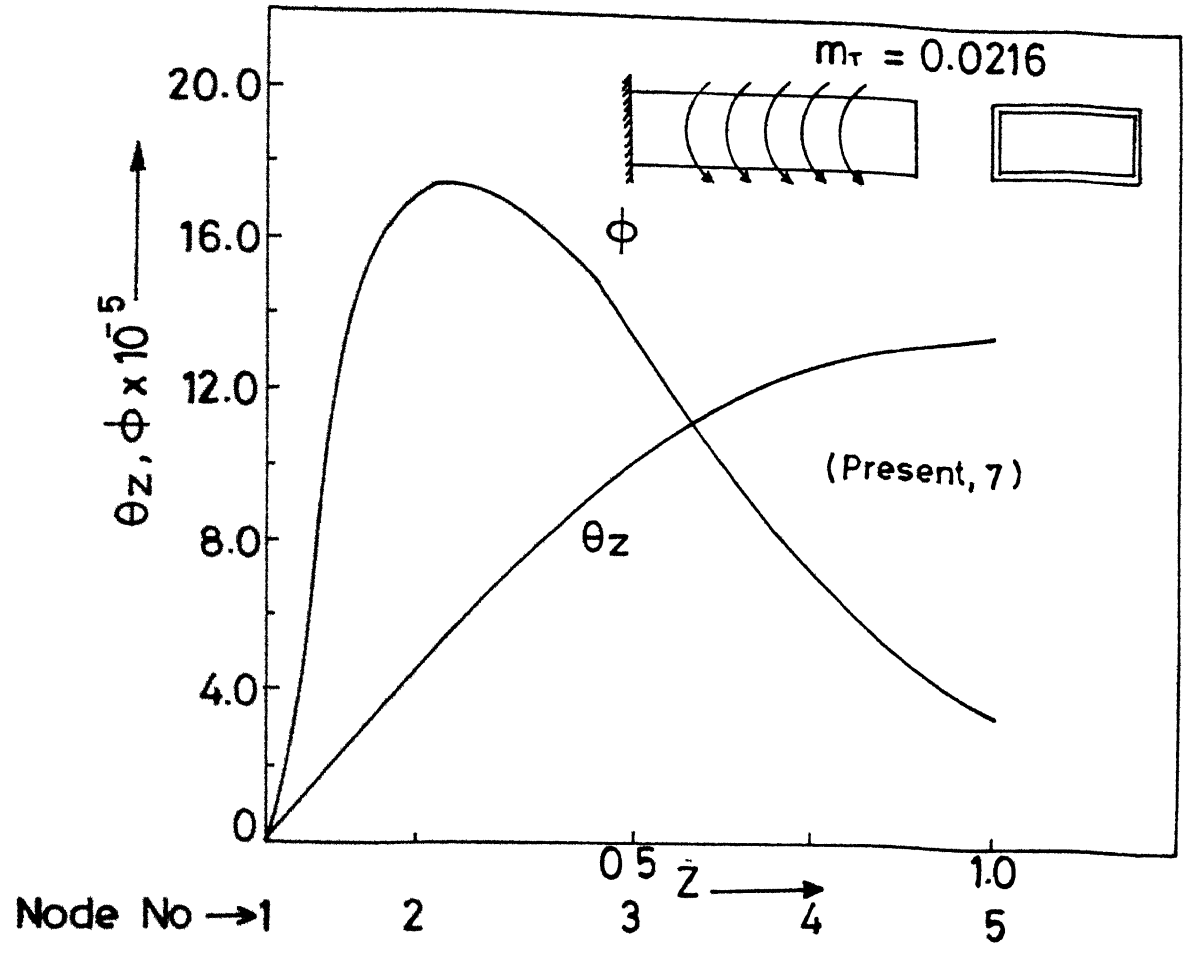

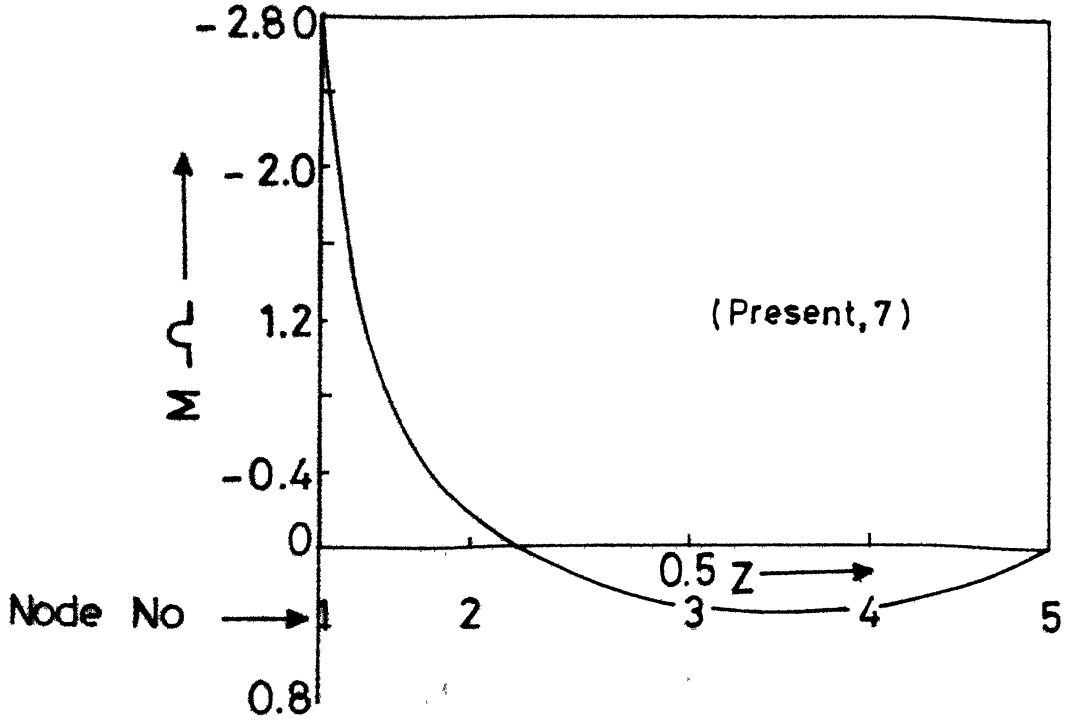

Fig.10 Variation of the Nodal Variables of a Cantilever of Rectangular Cross Section Along the Length of the Beam.

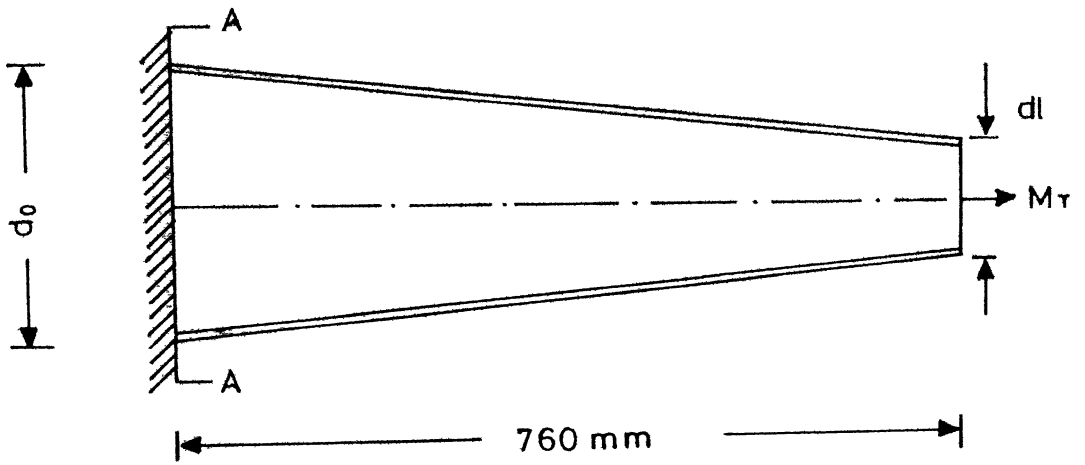

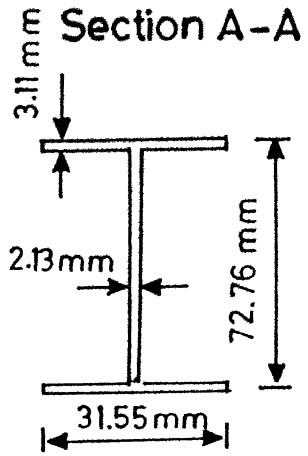

$E = 68.9$ Gpa, $G = 26.5$ Gpa, $\rho = 2711.039$ Kg / m^3

$Irr_o = 0.25973 \times 10^{-6}\ m^4$, $I_{\omega\omega_o} = 21.5443 \times 10^{-12}\ m^6$, $I_d = 0.86706 \times 10^{-9}\ m^4$

Fig.11 Thin-Walled Tapered Cantilever of I Section .

The results for angle of twist (θ_z) and bimoment (M_ω) are given in Fig. 12 as function of taper ($\alpha = d_1/d_o$). For uniform cantilever (α=1) close form results are available in [2] and present results match well with them. Results for angle of twist obtained by [8] are also included, and present results match well with them. It may be noted that [8] divided the beam into elements along its length and then, a shell mid surface of the element is approximated by arbitrary triangular subelements. It is seen that bimoment is maximum at the fixed and it increases with α, as expected.

Warping stresses (normal and shear) at the fixed and free ends are given in Table 8. These are calculated from bimoments and twisting moments (at the nodes) obtained from the element equations and further using the following relations [2].

$$\sigma_\omega = \frac{M_\omega(z)\ \omega(s)}{I_{\omega\omega}}\ ,\quad \tau_\omega = \frac{M_t I_\omega(S_E)}{t\ I_{\omega\omega}} \qquad \ldots\ (145)$$

where $I_\omega(S_E) = \int_A \omega\, dA$ and S_E is the distance from the edge.

For uniform cantilever (α=1) close-form solution of [2] is also given in the table. Present results agree well with them.

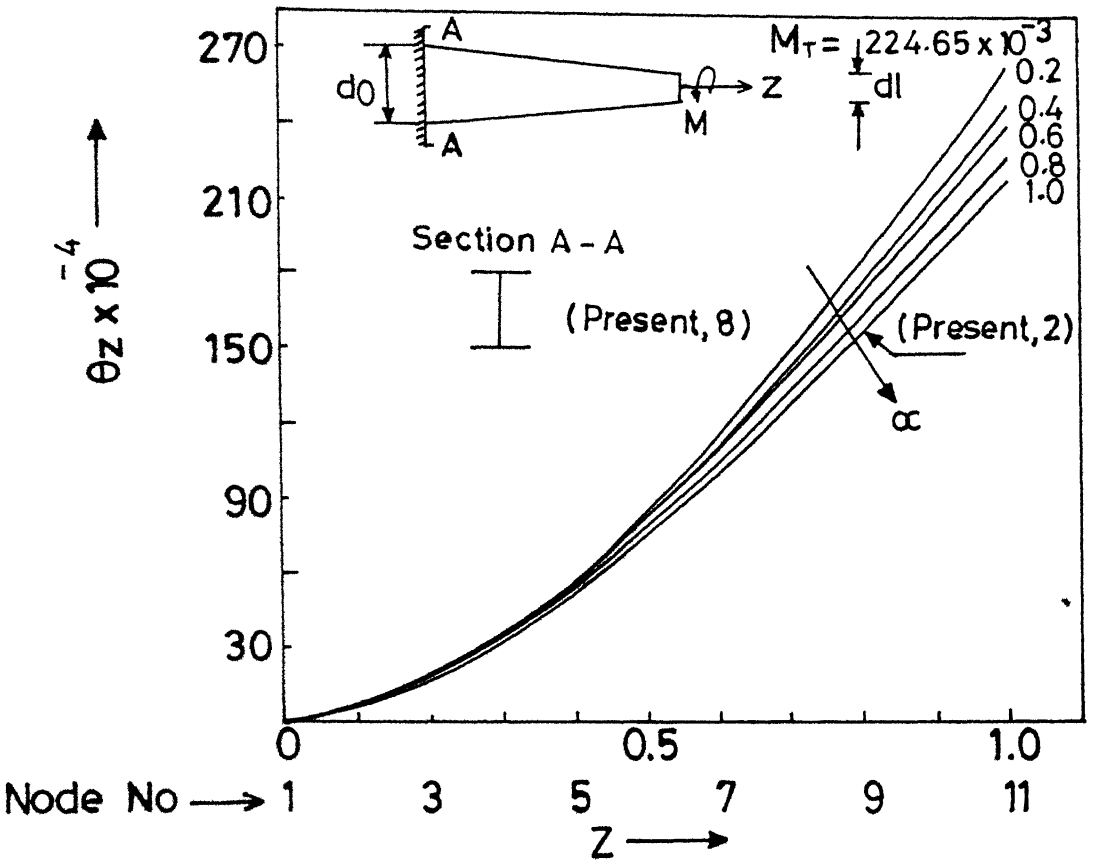

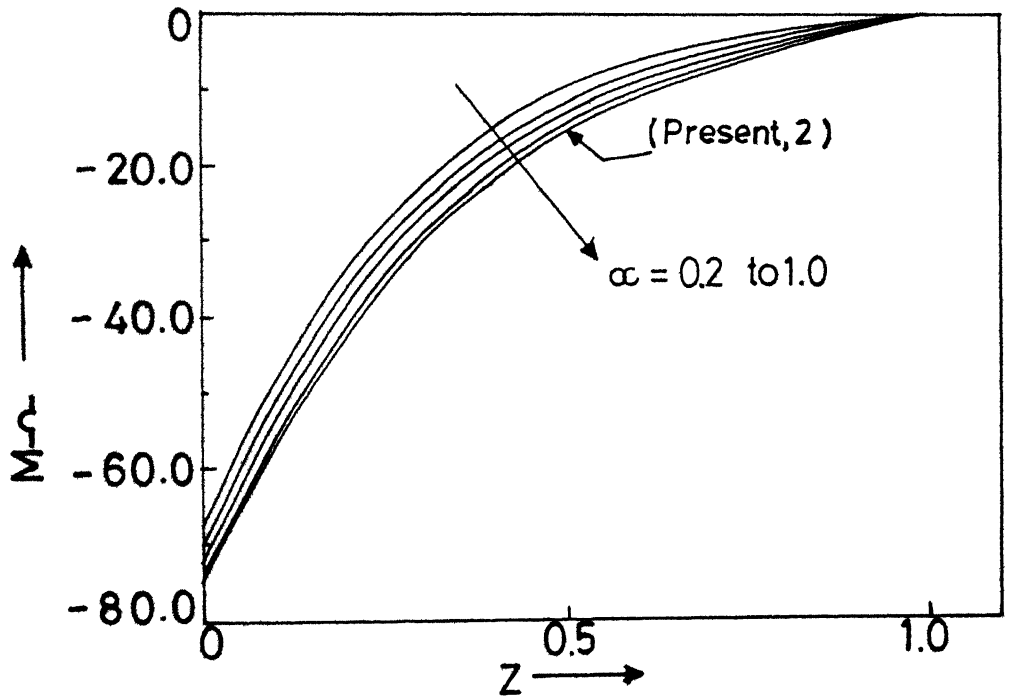

Fig.12 Angle of Twist and Bimoment Diagrams of a Tapered Cantilever of I Section.

Table 8 : Warping stresses in a Tapered Cantilever of I-section

Stresses (Mp_a)	Present Results					Results of [2]
	α					
	0.2	0.4	0.6	0.8	1.0	1.0
			Z = 0			
σ_ω	-6.1431	-6.3326	-6.4617	-6.6042	-6.7364	-6.7365
τ_ω	0.2101	0.2101	0.2101	0.2101	0.2101	0.2101
			Z = 1			
σ_ω	0.130×10^{-5}	-0.624×10^{-5}	-0.694×10^{-6}	-0.104×10^{-4}	-0.1249×10^{-4}	0.0
τ_ω	0.0456	0.0359	0.0291	0.0245	0.0211	0.0211

3.3.3 Mono-axis symmetric beam :

For this study a thin-walled beam of semicircular section, Fig. 5, is chosen. For this mono-axisymmetric beam, as said earlier the governing equations are Eqns. (68)to(71) with Eqn. (133). The boundary conditions are Eqn. (135). This beam is subjected to a uniformly distributed load., $q_Y = -1.0$. It is solved for pinned- pinned, fixed-fixed and cantilever cases. Results for displacement in the y-direction (U_y), angle of twist (θ_z) and warping measure(θ)are given in Figs. 13 to 15.

Figure 13 gives the results for pinned-pinned beam. Displacement and angle of twist are maximum, and warping measur is zero at the center of beam as expected. Maximum displacement is 0.013313 compared with elementary strength of material value of 0.013021.

Results of Fig. 14 and 15 for fixed-fixed and cantilever beams are also as expected. Maximum displacements are 0.0028963 and 0.125168 compared to elementary strength of material values of 0.0026041 and 0.125.

3.3.4 Unsymmetric section beam :

For this, a thin-walled beam of unsymmetric channel cross section, Fig. 7, is chosen. As the cross section is unsymmetric, all the equations (66)to(71) are coupled. These coupled equations are solved for pinned-pinned, fixed-fixed, and cantilever cases. The boundary conditions are same as in

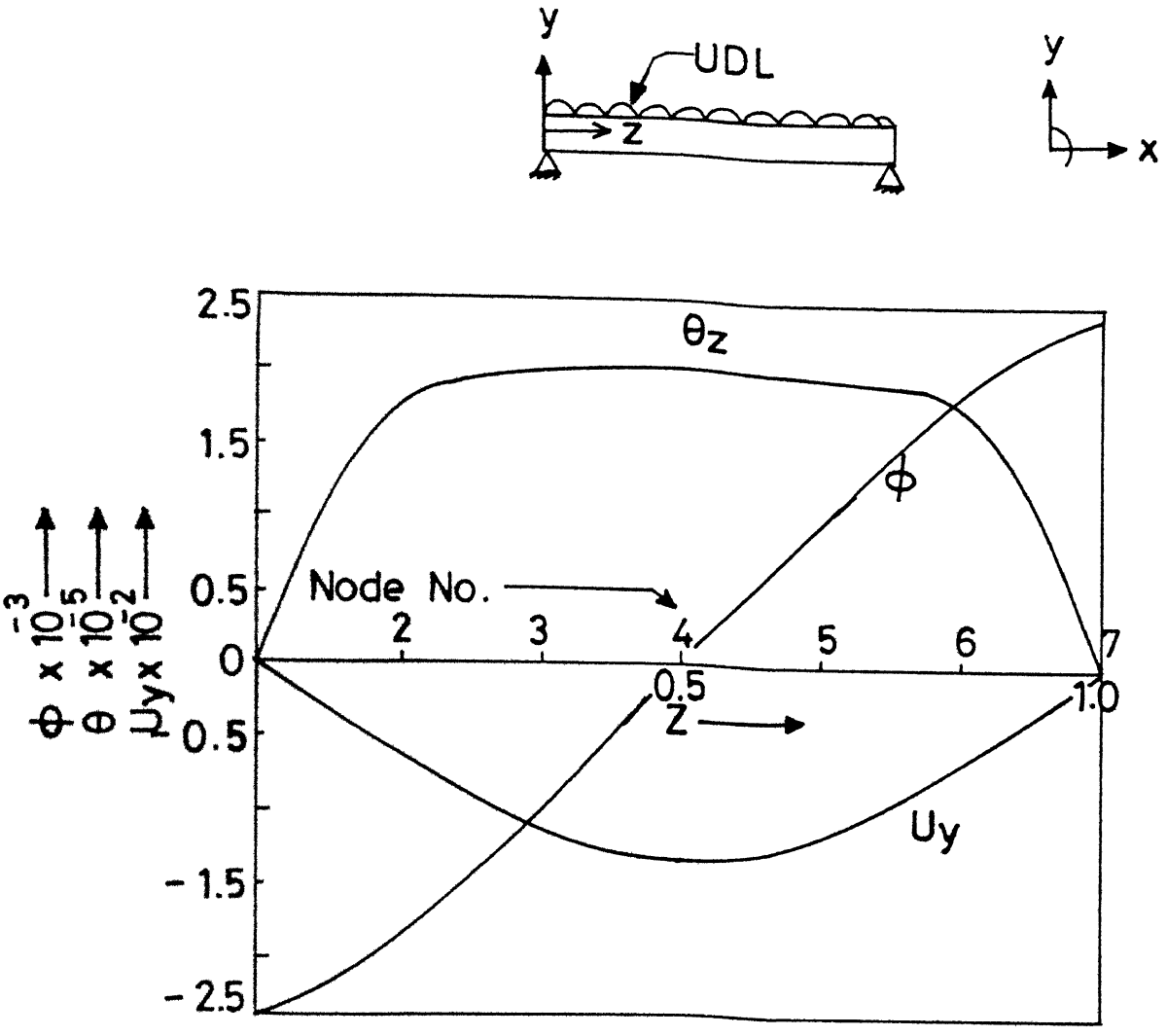

Fig.13 Variation of the Nodal Variables of a Pinned-Pinned Beam of Semicircular Section Along the Length of the Beam.

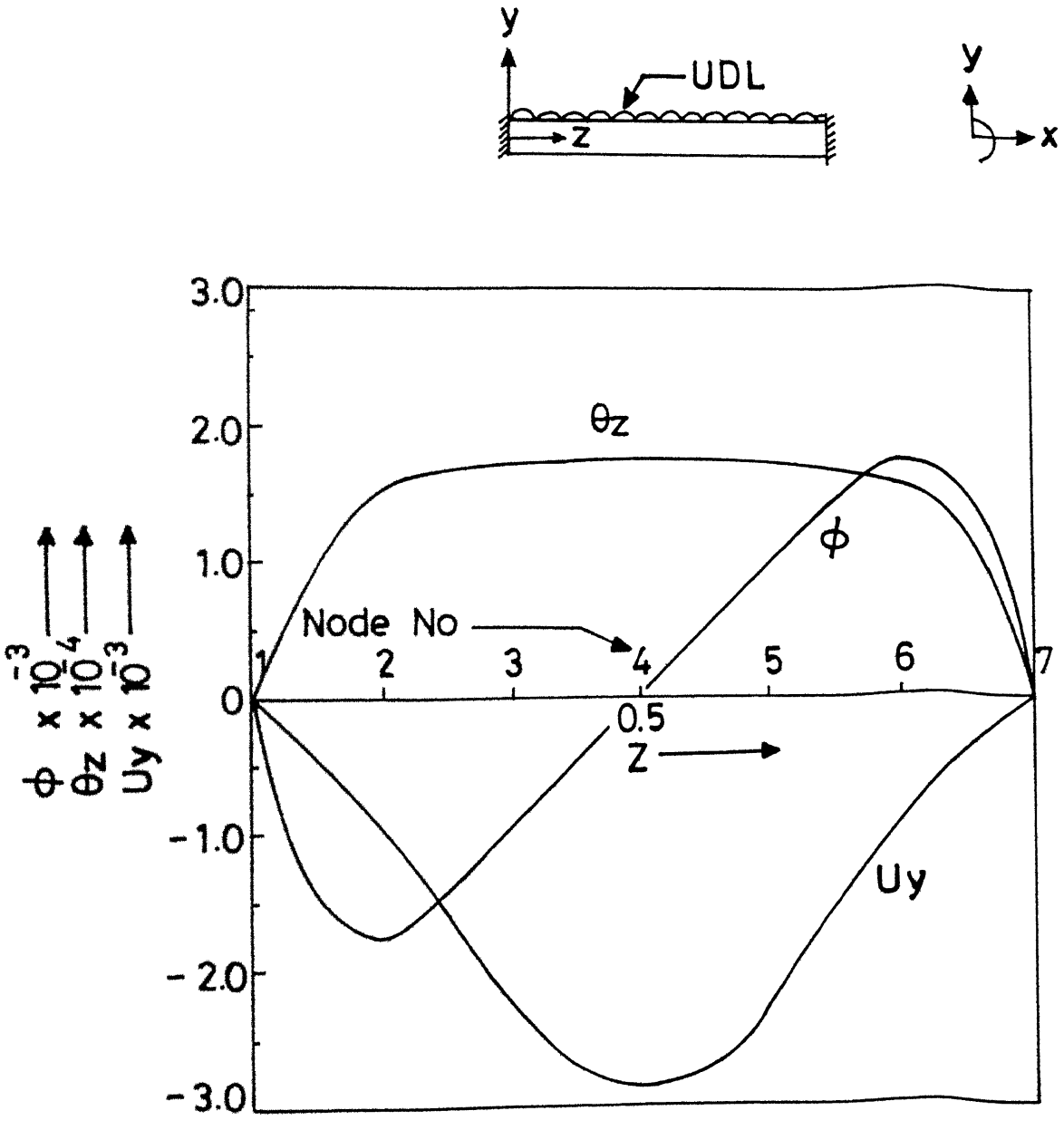

Fig.14 Variation of the Nodal Variables of a Fixed-Fixed Beam of Semicircular Section Along the Length of Beam.

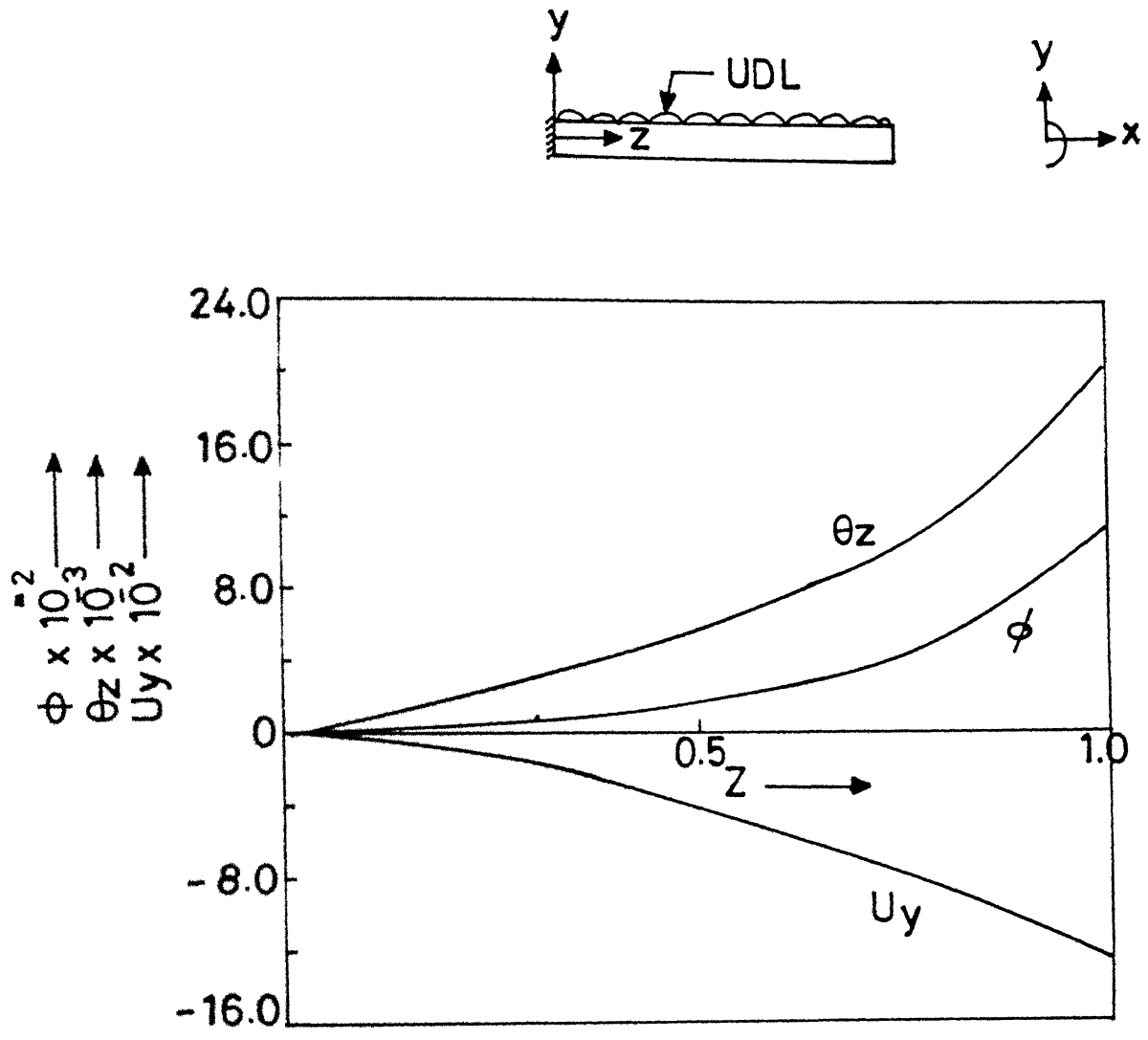

Fig. 15 Variation of the Nodal Variables of a Cantilever of Semicircular Section Along the Length the Beam.

Eqn. (138). These beams are subjected to a uniformly distributed load, $q_Y = -1.0$

The results for displacements (U_x, U_y), angle of twist (θ_z) and warping measure (Φ) are given in Figs. 16 to 18 for these beams. Results are as expected. Displacements U_x are less than the displacements U_y. Maximum displacements U_y are 0.013372, 0.0029552 and 0.12588 compared to the elementary strength of material values of 0.013021, 0.0026041 and 0.125 for pinned-pinned, fixed-fixed and cantilever cases respectively.

3.4 BUCKLING ANALYSIS :

For a column with doubly symmetric cross section, the shear center B and the centroid O coincide.

Thus

$$X_B = Y_B = 0 \qquad \ldots\ (146)$$

Hence the equations (93) to (95) become uncoupled and can be solved independent of each other. For a column with monoaxisymmetric cross section, shear center lies on the axis of symmetry. If the x-axis is the axis of symmetry, Fig. 5, then

$$Y_B = 0 \qquad \ldots\ (147)$$

Hence the Eqn. (93) becomes uncoupled from the rest of the equations. Eqns. (94) to (95) remain coupled. This is known as double coupling of flexural buckling about y-axis and the torsional buckling.

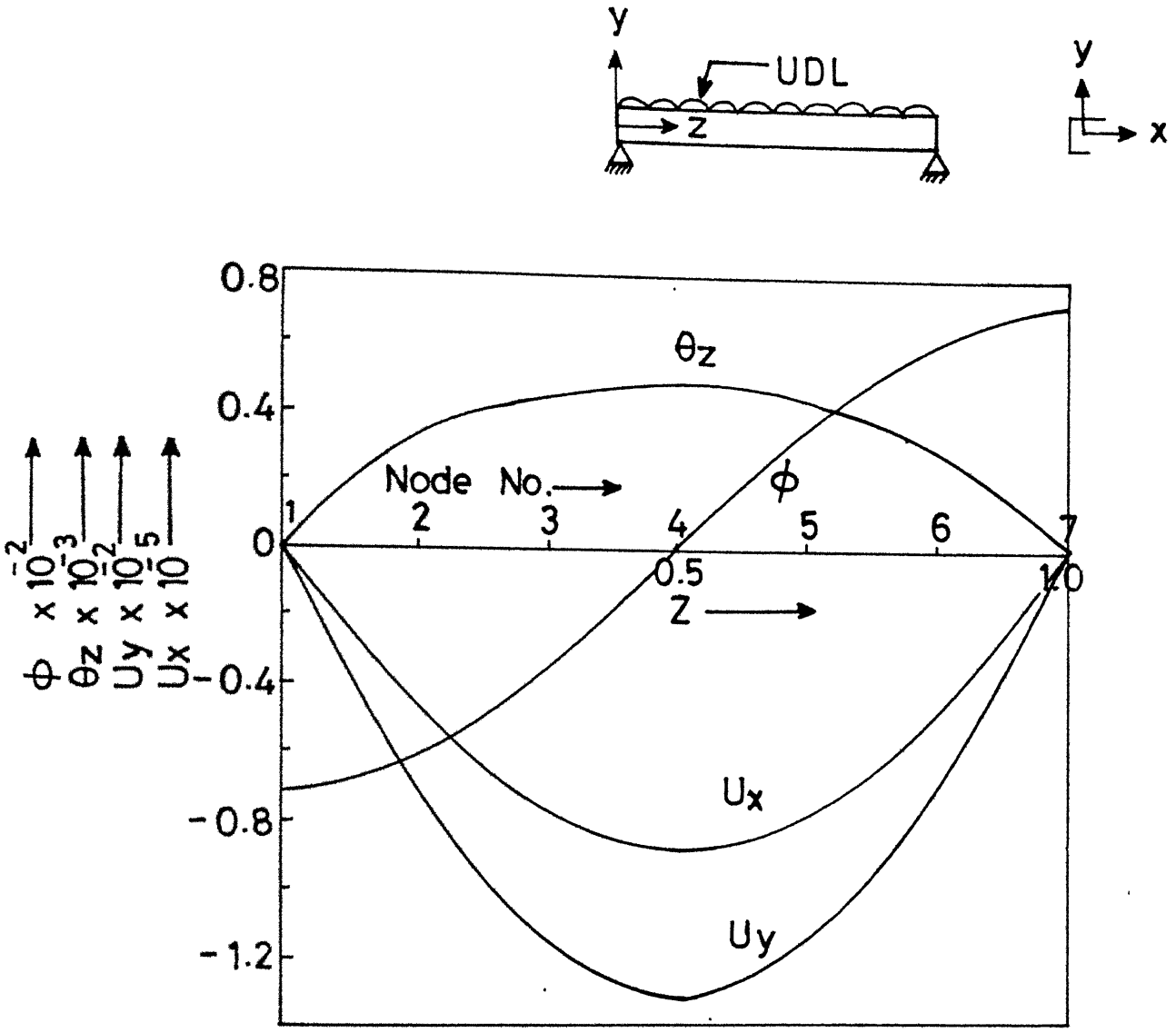

Fig.16 Variation of the Nodal Variables of a Pinned-Pinned Beam of Unequal Channel Section Along the Length of the Beam.

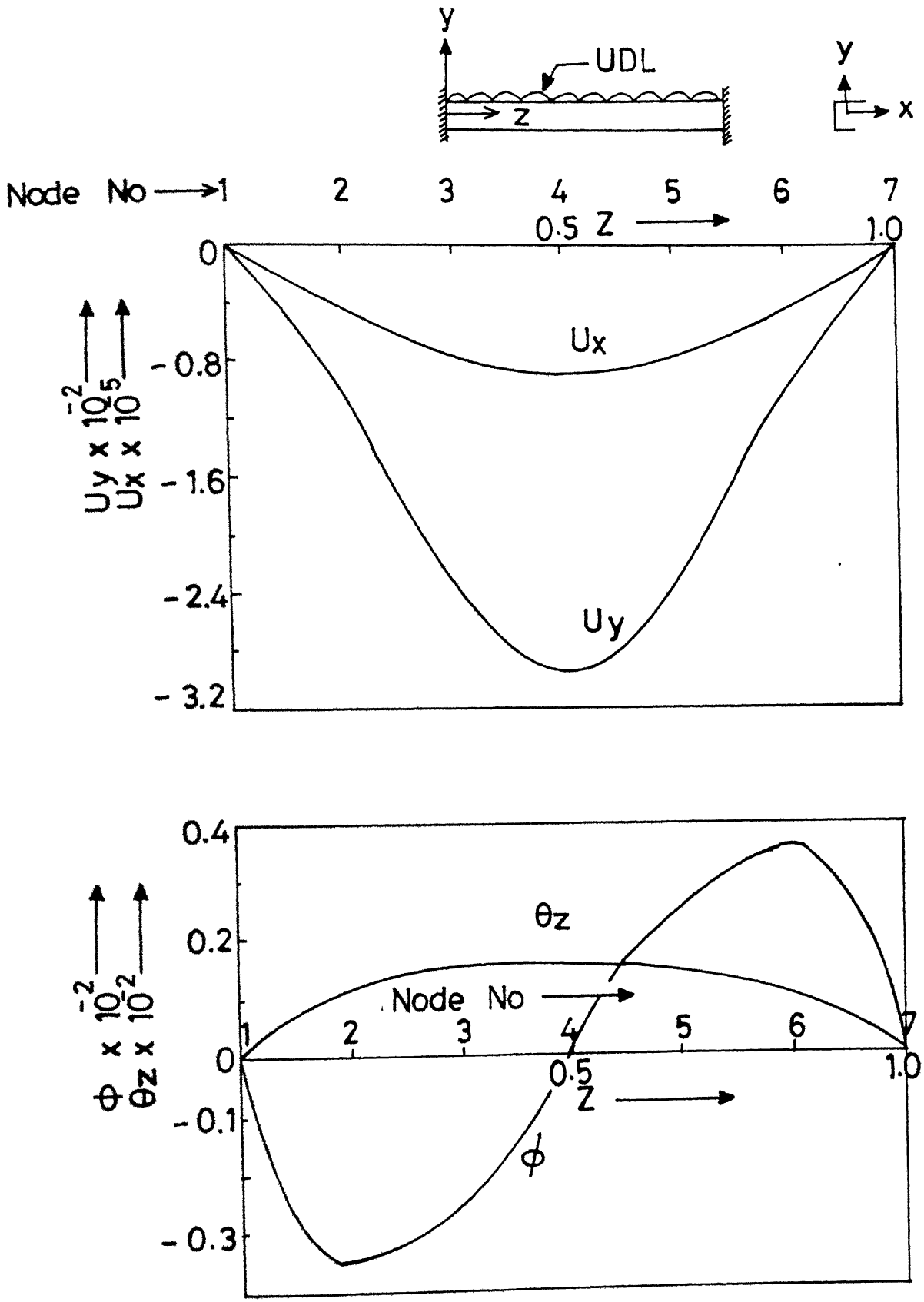

Fig.17 Variation of the Nodal Variables of a Fixed-Fixed Beam of Unequal Channel Section Along the Length of the Beam.

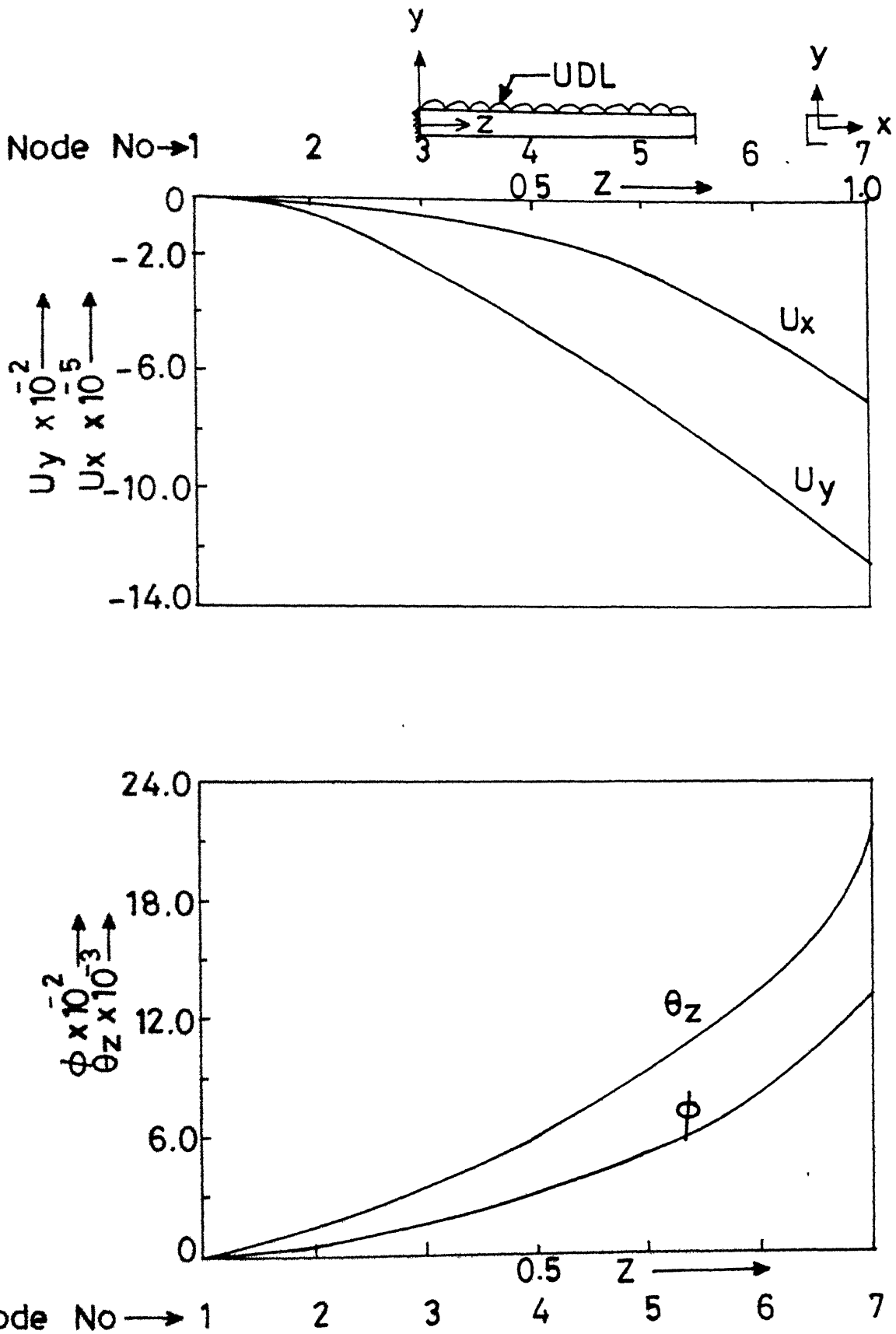

Fig.18 Variation of the Nodal Variables of a Cantilever of Unequal Channel Section Along the Length of the Beam.

In the case of a column with no axis of symmetry, shear center does not lie on any axis and hence the governing equations, Eqns. (93) to (95), remain coupled. This is known as triple coupling of flexural bucklings about x and y-axes and torsional buckling about z-axis. Boundary conditions are Eqns. (97) to (99).

For buckling analysis, unsymmetric channel section, Fig. 7, is chosen. Critical loads are obtained for pinned-pinned, fixed-fixed and cantilever columns as function of Re_{xx} and are given in Figs. 19 to 21 respectively. Close form results for pinned-pinned and fixed-fixed beams of [17] are also given in the figures. Present results match well with them.

The critical buckling load P increases with increase of Re_{xx} as expected. It is observed that this increase is not uniform. In some modes the increase is small and in some modes it is very large. This is because in coupled buckling, there will be some modes which are flexural dominant and some other modes are torsion dominant. Study of mode shapes, for pinned-pinned column shows that the first and third modes are torsion dominant, second and fourth are flexure about y-axis dominant, fifth mode is flexure about x-axis dominant.

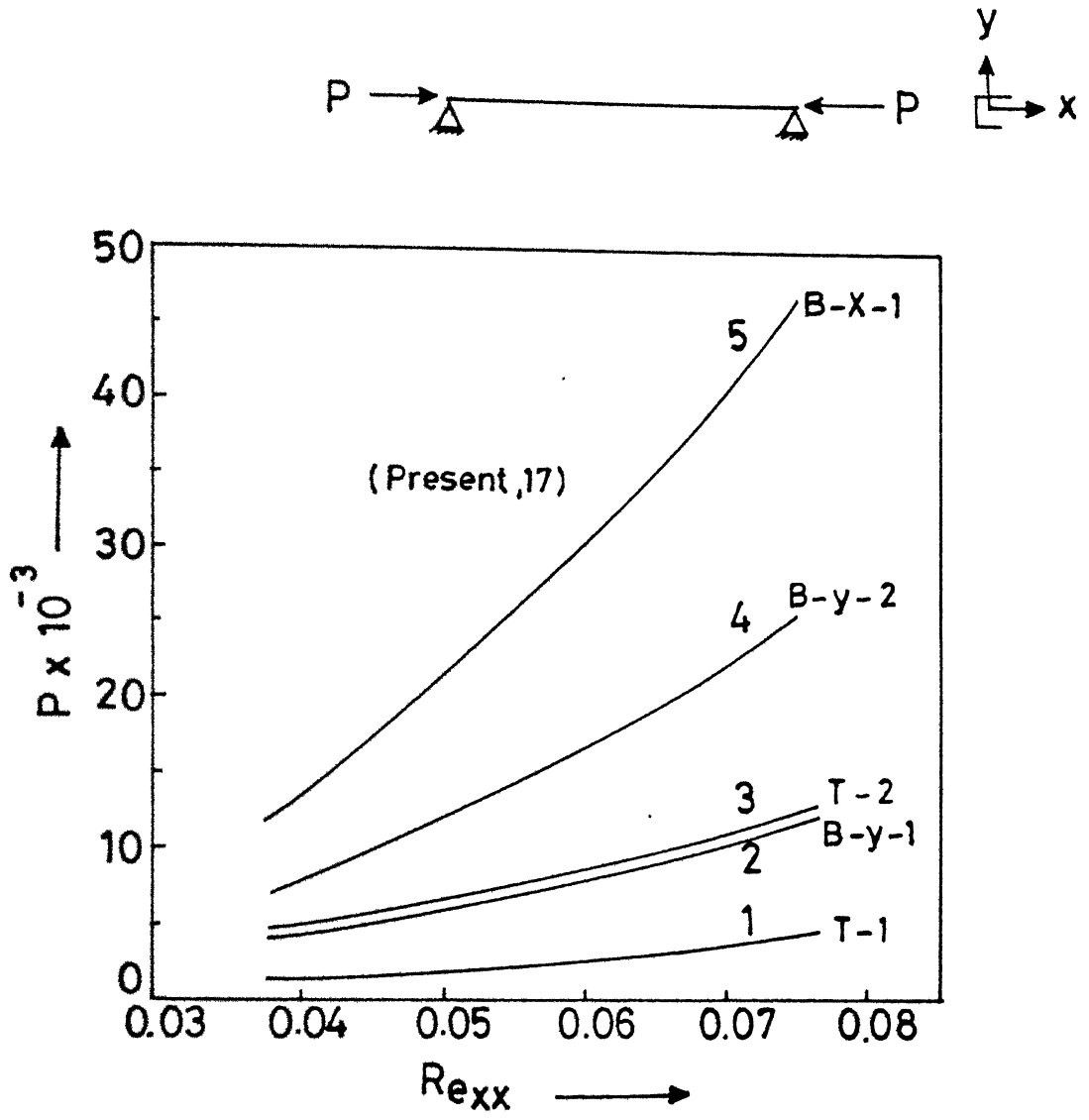

Fig. 19 Critical Buckling Loads of a Pinned-Pinned Column of Unequal Channel Section.

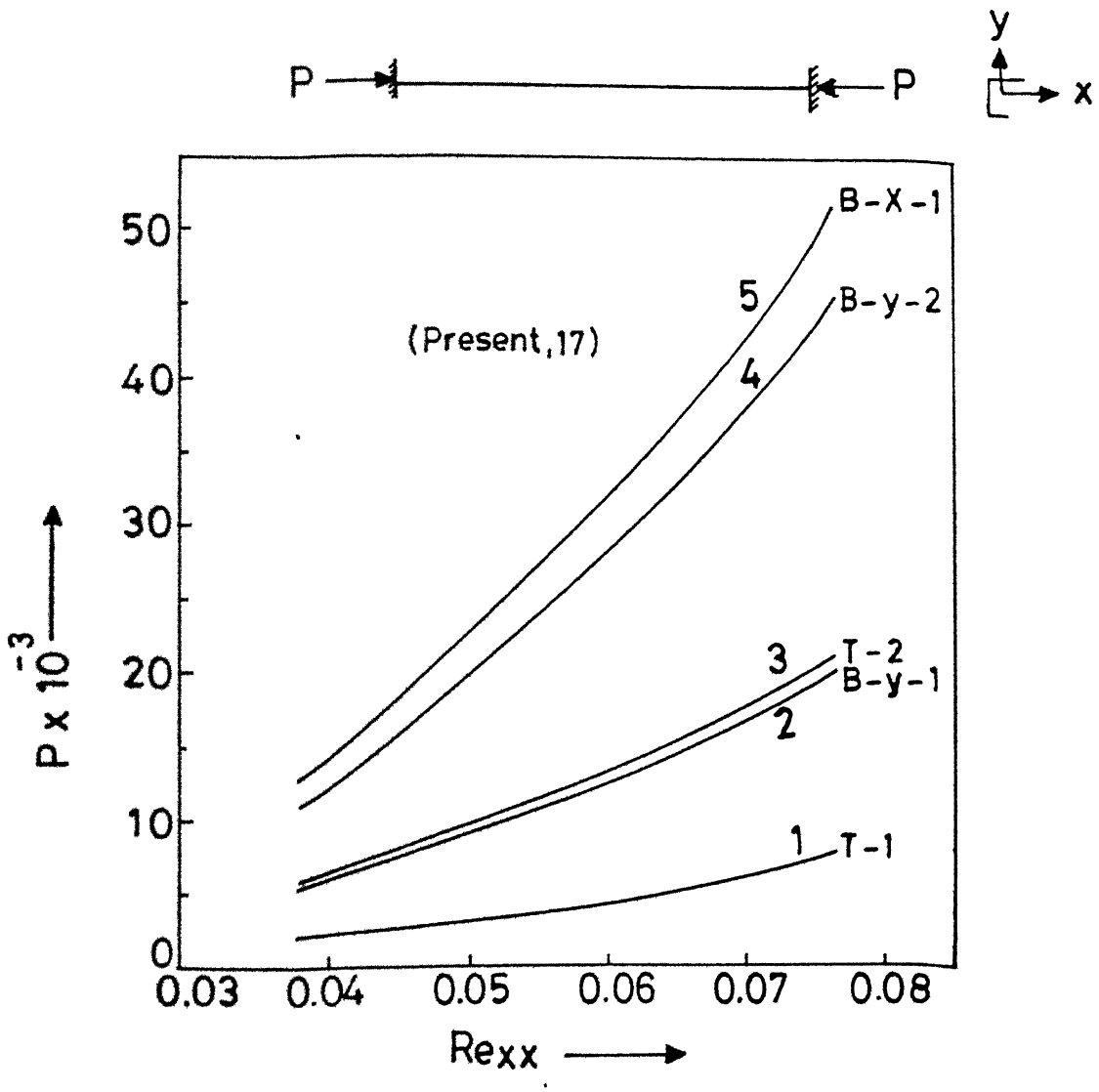

Fig.20 Critical Buckling Loads of a Fixed-Fixed Column of Unequal Channel Section.

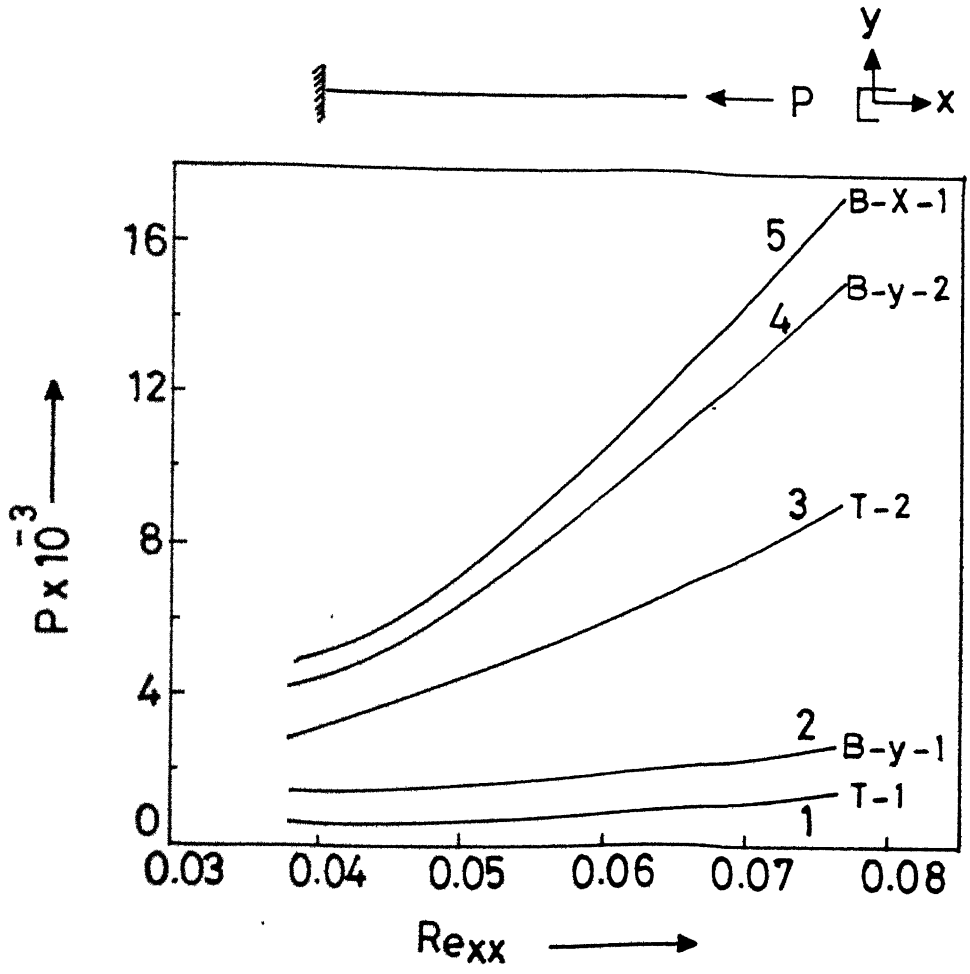

Fig. 21 Critical Buckling Loads of a Cantilever Column of Unequal Channel Section.

The non-dimensionalised parameters for this section are

$$Re_{xx} = 0.0757 \; ; \; Re_{yy} = 0.0282 \; ; \; Re_{\omega\omega} = 0.001782$$

Parameter Re_{xx} is greater than Re_{yy}, and in turn Re_{yy} is greater than $Re_{\omega\omega}$. Therefore increase in critical loads with increase in Re_{xx} is largest in flexure deminant modes about x-axis and smallest in torsion dominant modes. Similar trends are observed in the case of fixed-fixed and cantilever columns.

3.5 PLANE FRAME :

In this section results for the static and free vibration analyses of two plane frames, a balcony frame and a chassis frame subjected to transverse loading, Fig.22 and 24 respectively, are given. These frames lie in the xz plane. Beams of channel cross-section, shown in Fig. 23, are used in both these frames. The dimension and its section properties are also given in this figure.

3.5.1 Static analysis :

3.5.1.1 Balcony frame :

In this case a balcony frame, Fig. 22, is considered. This frame is formed by joining three thin-walled beams of channel cross-section, Fig. 23. A concentrated load of 1kN is acting at the mid point of the longer beam. It is acting at the shear centre. The frame is divided into eight finite elements. Firstly the element stiffness and load matrices are calculated in local coordinates and then transformed to the global coordinates using the transformation matrix. These are assembled for the frame. After applying the boundary conditions the displacements are obtained. Stresses are calculated from Eqns. (123) to (124), after obtaining the elemental forces and moments by back substitution from Eqn. (122).

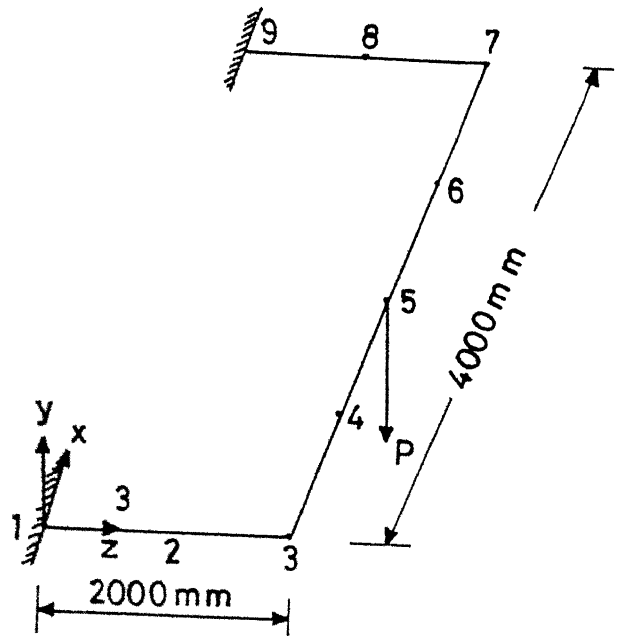

Fig.22 Balcony Frame.

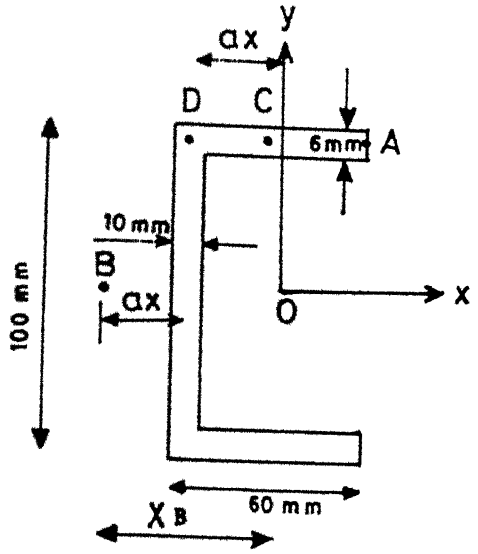

$I_{xx} = 2.4943 \times 10^{-6}\ m^4$, $I_{yy} = 0\ 4787 \times 10^{-6}\ m^4$, $A = 1.66 \times 10^{-3} \times m^2$
$X_B = -33\ mm$, $Y_B = 0.0\ mm$ $I_d = 42.0 \times 10^{-9}\ m^4$, $I_{\omega\omega} = 1.053 \times 10^{-9}\ m^6$
$I_0 = 2.973 \times 10^{-6}\ m^4$, $I_B = 4.781 \times 10^{-6}\ m^4$ $E = 200\ GPa$
$G = 75\ GPa$, $\rho = 7860\ Kg/m^3$, $a_x = 20.506\ mm$

Fig.23 Thin-Walled Channel Cross-Section.

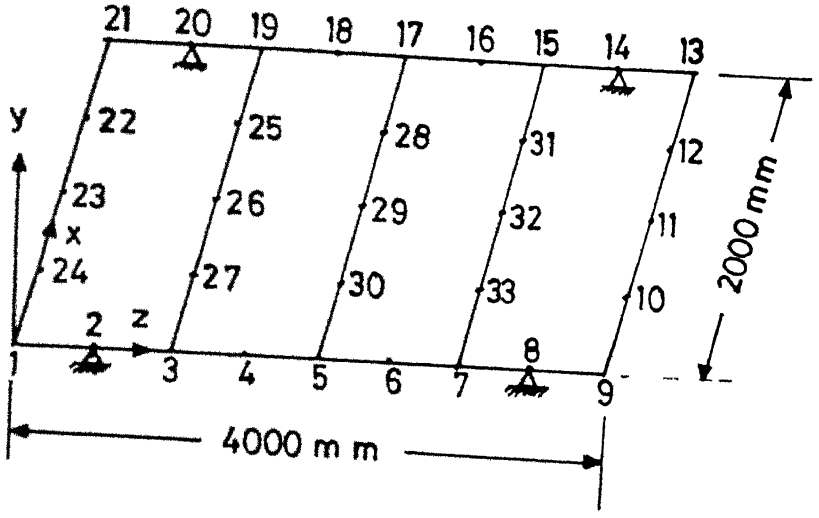

Fig. 24 Chassis Frame.

Displacements are given in Table 9 and stresses in Table 10. First results are obtained by neglecting the effect of warping, i.e. Euler beam elements are used. The basic equations for this case are Eqns. (104) and (105), with the omission of the term with warping rigidity ($EI_{\omega\omega}$) in Eqn. (105). In this case linear interpolation function is used for the twisting angle θ_z. Next results are obtained with including the effect of warping, i.e. thin-walled beam elements are used. The results of [18] obtained by direct stiffness method are also given in the Table 9.

The present results for displacements and stresses based on Euler beam match well with [18] . The displacements based on thin walled beam elements (i.e. including warping) are quite close to those based on Euler beam elements, but stresses differ quite a bit. There is not much change in displacements as the load acts through shear centre and causes no torsion. On the top flange, sectorial coordinate ω is positive maximum at A, zero at C and negative maximum at D , Fig. 23. Shear stresses are maximum at the C point. The stresses are calculated at these three points and given in Table 10. Thus warping effect changes the stresses quite a bit.

Table 9 : The nodal displacements and rotations of a balcony frame.

Node No.	Direct stiffness method: Euler beam elements			Present FEM results: Euler beam elements			Present FEM results: Thin-walled beam elements			
	u_y (mm)	u_y'	θ_z	u_y (mm)	u_y'	θ_z	u_y	u_y'	θ_z	θ_z'
1	0	0	0	0	0	0	0	0	0	0
2	-	-	-	-0.8352	-0.0015	0.0010	-0.8352	-0.0015	0.0010	0.0012
3	-2.6728	-0.0020	0.0020	-2.6728	-0.0020	0.0020	-2.6727	-0.0020	0.0020	0.0006
4	-	-	-	-4.5008	-0.0020	0.0015	-4.4984	-0.0018	0.0015	0
5	-5.3329	-0.0020	0	-5.3329	-0.0020	0	-5.3297	-0.0018	0	0
6	-	-	-	-4.5008	-0.0020	-0.0015	-4.4984	-0.0018	-0.0015	0
7	-2.6728	-0.0020	-0.0020	-2.6728	-0.0020	-0.0020	-2.6727	-0.0020	-0.0020	-0.0006
8	-	-	-	-0.8352	-0.0015	-0.0010	-0.8352	-0.0015	-0.0010	-0.0012
9	0	0	0	0	0	0	0	0	0	0

Table 10 : Maximum stresses of the balcony frame.

(All stresses in Mpa)

Node No.	Results of 18		Present FEM results				
			Euler beam element		Thin-walled beam elements		
	Normal stresses $(\sigma_z)_A$ and $(\sigma_z)_D$	Shear stresses $(\tau_{zs})_C$	Normal stress $(\sigma_z)_A$ and $(\sigma_z)_D$	Shear stresses $(\tau_{zs})_C$	Normal stress $(\sigma_z)_A$	Normal stress $(\sigma_z)_D$	Shear stress $(\tau_{zs})_C$
1	-20.0	-0.6	-20.0	-0.6	-22.1	-19.0	-0.5
2	-	-	-10.0	-0.2	-10.1	-10.0	-0.4
3	-0.0	0.3	- 0.0	0.3	1.0	-0.5	0.2
4	-	-	- 0.0	0.1	0.0	-0.0	-18.5
5	-0.0	0.6	- 0.0	0.6	0.0	-0.0	-36.3
6	-	-	- 0.0	-0.1	0.0	-0.0	-18.3
7	-0.0	-1.5	- 0.0	-1.5	-1.0	0.5	-1.4
8	-	-	-10.0	-1.0	-10.0	-10.0	-1.1
9	-20.0	-0.6	-20.0	-0.6	-18.0	-21.0	-0.7

3.5.1.2 Chassis frame :

For the analysis of a chassis frame, Fig. 24, is considered. The dimensions of the frame are given Fig. 24. The frame is made up of seven thin-walled beams of channel section Fig. 23. The dimensions and section properties of the channel section are given in this figure. The frame is divided into 36 elements with 33 nodes. The frame is simply supported at the nodes 2,8,14 and 20. In this present analysis two configurations of the chassis frame are used. Two different types of loading are considered. Results are obtained without and with warping effects. The following notation is used to identify the different loadings and configurations. In all the cases the loads (along y-axis) act through the centroid of the cross-section.

B1 - Uniformily distributed loading of 8 kN/m on circumference of the frame only. All the circumferential channels are facing inside. Beam 3 - 19 is parallel to beam 1 - 21; beams 5 - 17 and 7 - 15 are parallel to beam 9 - 13. Effect of warping is neglected in this case.

WB1 - Configuration of beams is same as in B1. Warping effects are included.

BC1 - Loading is same as in B_1 case. Longer beams face inside. Local x-axes of all shorter beam are in the direction of global negative z-axis. Warping is neglected.

WBC1 - Configuration and loadings are same as in BC1, but warping is included.

Cases B2, WB2, BC2 and WBC2 have same configuration of beams and warping effects of B1, WB1, BC1 and WBC1 respectively, but uniform loading of 8 kN/m is on all the beams.

Finite element equations for the whole frame are obtained as explained in the case of balcony frame ; displacements and stresses are obtained. The nodal displacements (of shear center) and rotations for B1, WB1, BC1 and WBC1 are given in Table 11. Studying the displacements for B1 and WB1.

It is observed that there is no change in the displacements along the nodes of the longer beams 1 - 9 and 13 - 21, a bit of change in outer shorter beam 9 - 13 and some change in the other shorter beams. Thus the change in the displacements, when warping is included, is observed along the shorter beams. Comparing the displacements of B1 and BC1 cases there is a significant change in displacements along all the beams. This is because in the BC1 case all shorter beams are in the same direction and given rise to more twist compared to B1 case where twisting gets cancelled because of four shorter beams face each other.

Table 11 : Nodal displacements and rotations, of a chassis frame.

Node No.	B1		WB1		BC1		WBC1	
	u_y(mm)	θ_z	u_y(mm)	θ_z	u_y(mm)	θ_z	u_y(mm)	θ_z
1	-0.2469	0.0051	-0.2469	0.0049	-0.9084	-0.0054	-0.9084	[illegible]
2	0.0000	0.0000	0.0000	0.0000	0.0000	0.0000	[illegible]	[illegible]
3	1.9661	-0.0004	1.9661	-0.0005	2.3704	-0.0004	[illegible]	[illegible]
4	4.1481	-0.0109	4.1481	-0.0035	4.7361	-0.0109	[illegible]	[illegible]
5	5.0425	-0.0005	5.0425	-0.0005	5.6378	-0.0005	5.6378	[illegible]
6	4.1481	-0.0109	4.1481	-0.0031	4.6185	-0.0109	4.6185	[illegible]
7	1.9671	-0.0004	1.9661	-0.0005	2.2234	-0.0004	2.2234	[illegible]
8	0.0000	0.0000	0.0000	0.0000	0.0000	0.0000	0.0000	[illegible]
9	-0.2469	0.0051	-0.2469	0.0049	-0.5115	0.0051	-0.5115	[illegible]
10	2.0595	0.0036	1.9790	0.0035	1.7949	0.0036	1.7144	[illegible]
11	2.9954	-0.0000	2.8880	0.0000	2.7308	-0.0000	2.6234	0.0000
12	2.0595	-0.0036	1.9790	-0.0035	1.7949	-0.0036	1.7144	0.0035
13	-0.2469	-0.0051	-0.2469	-0.0049	-0.5115	-0.0051	-0.5115	0.0049
14	0.0000	0.0000	0.0000	0.0000	0.0000	0.0000	0.0000	0.0000
15	1.9661	0.0004	1.9661	0.0005	2.2234	0.0004	2.2234	-0.0005
16	4.1481	0.0109	4.1481	0.0031	4.6185	0.0109	4.6185	-0.0031
17	5.0425	0.0005	5.0425	0.0005	5.6378	0.0005	5.6378	-0.0005
18	4.1481	0.0109	4.1481	0.0031	4.7361	0.0109	4.7361	-0.0033
19	1.9661	0.0004	1.9661	0.0049	2.3704	0.0004	2.3704	-0.0004
20	0.0000	0.0000	0.0000	0.0000	0.0000	0.0000	0.0000	0.0000
21	-0.2469	-0.0051	-0.2469	-0.0049	-0.9084	0.0054	-0.9084	0.0052
22	2.0595	-0.0036	1.9790	-0.0035	1.3980	0.0035	1.4410	0.0036
23	2.9954	-0.0000	2.8880	0.0000	2.3338	0.0000	2.3912	-0.0000
24	2.0595	0.0036	1.9790	0.0035	1.3980	-0.0035	1.4410	-0.0036
25	1.8188	0.0002	1.7838	0.0002	2.2237	0.0002	2.2155	-0.0002
26	1.7697	0.0000	1.7230	-0.0000	2.1740	-0.0000	2.1639	0.0000
27	1.8188	-0.0002	1.7838	-0.0002	2.2230	-0.0002	2.2155	0.0002
28	4.8447	0.0003	4.8397	0.0003	5.4400	0.0002	5.4334	0.0003
29	4.7787	0.0000	4.7721	-0.0000	5.3741	0.0000	5.3654	-0.0000
30	4.8447	-0.0003	4.8397	-0.0003	5.4400	-0.0002	5.4335	0.0003
31	1.8188	0.0002	1.7838	0.0002	2.0761	0.0002	2.0412	-0.0002
32	1.7697	0.0000	1.7230	-0.0000	2.0270	0.0000	1.9806	-0.0000
33	1.8188	-0.0002	1.7838	-0.0002	2.0761	-0.0002	2.0413	0.0002

Comparing the displacement of BC1 and WBC1, it is observed that there is no change in the displacements along the longer beams and the change in the displacement of the shorter beams 9 - 13 , 7-15 , 5-17 and 3-19 is of the same order as that of B1 and WB1 cases. The displacements of shorter beam 1-21 increase in contrast to their decrease between B1 and WB1 cases.

The total normal stresses at the points A and D, and shear stresses at point C are given in Table 12 for B1, WB1, BC1 and WBC1 cases. The stresses for the cases B2, WB2, BC2 and WBC2 are given in Table 13.

Referring to the Tables 12 and 13, it is observed that the stresses change when the effect of warping is considered. This change is very significant and can not be ignored.

Also the stresses in BC and WBC cases are in general higher than those in cases of B and WB, as in BC and WBC cases twisting moments of shorter beams do not oppose each other.

3.5.2 Free Vibration :

For the free vibration analysis of the chassis frame, the chassis frame of Fig. 24 is considered. The frame is simply supported at the nodes 2,8,14 and 20. The elemental mass and stiffness matrices are obtained for each element in the local coordinates using Eqn. (127). Then these elemental equations are

Table 12 : Stresses in the chassis frame for loading case 1

Node No.	B1		WB1			BC1		WBC1		
	$(\sigma_z)_{A,D}$	$(\tau_{zs})_C$	$(\sigma_z)_A$	$(\sigma_z)_D$	$(\tau_{zs})_C$	$(\sigma_z)_{A,D}$	$(\tau_{zs})_C$	$(\sigma_z)_A$	$(\sigma_z)_D$	$(\tau_{zs})_C$
	(All stresses in Mpa)									
1	5.3	-14.3	-75.6	47.3	-5.3	-5.3	-14.8	42.9	-30.3	-11.6
2	105.5	14.4	126.4	94.7	15.1	94.9	14.2	88.8	98.1	16.2
3	5.3	10.0	-24.4	20.7	14.7	-3.5	9.8	-29.8	10.1	14.4
4	-54.8	14.7	-40.8	-62.2	6.8	-61.9	14.4	-47.4	-69.4	6.6
5	-74.9	0.5	-110.3	-56.5	5.4	-80.2	0.3	-115.9	-61.6	5.2
6	-54.8	5.0	-40.8	-62.2	-2.6	-58.4	4.8	-44.3	-65.7	-2.9
7	5.3	-9.3	-21.2	19.1	-5.1	3.5	-9.5	-23.0	17.3	-5.3
8	105.5	14.4	126.4	94.7	11.7	105.5	14.4	126.3	94.7	11.7
9	5.3	5.0	-75.6	47.3	-1.3	5.3	5.0	-75.6	47.3	-1.3
10	2.6	1.6	18.5	-5.6	106.0	2.6	1.6	18.5	-5.6	106.0
11	-0.0	0.0	28.1	-14.6	140.5	-0.0	0.0	28.1	-14.6	140.5
12	-2.6	-1.6	13.2	-10.9	101.0	-2.6	-1.6	13.2	-10.9	101.0
13	-5.3	-5.0	-86.2	36.7	-13.9	-5.3	-5.0	-86.2	36.7	-13.9
14	-105.5	14.4	-84.7	-116.3	13.7	-105.5	14.6	-84.7	-116.3	14.0
15	-5.3	9.3	-35.0	10.1	4.5	-3.5	9.5	-32.2	11.9	4.7
16	54.8	-5.0	68.9	47.5	2.9	58.4	-4.8	72.4	51.1	3.1
17	74.9	-0.5	39.4	93.3	-5.4	80.2	-0.3	44.2	98.9	-5.2
18	54.8	-14.7	68.9	47.5	-7.0	61.9	-14.4	76.4	54.4	-6.9
19	-5.3	-10.0	31.8	8.5	-14.1	3.5	-9.8	-17.0	14.2	-12.6
20	-105.5	14.4	-84.7	-116.3	17.2	-94.9	14.4	-101.1	-91.8	11.1
21	-5.3	14.3	-86.2	36.7	20.5	5.3	4.8	53.4	-19.7	14.7
22	-2.6	8.0	13.2	-10.9	-96.4	-2.6	-1.5	18.2	-13.5	107.2
23	-0.0	0.0	28.1	-14.6	-140.5	-0.0	-0.0	29.5	-15.3	146.6
24	2.6	-8.0	18.5	-5.6	-110.6	2.6	1.5	23.5	-8.2	112.0
25	-0.0	-0.2	-0.5	0.2	8.8	-0.0	-0.2	0.9	-0.4	-7.8
26	-0.0	-0.0	-0.1	0.1	9.0	-0.0	0.0	0.3	-0.1	-7.6
27	-0.0	0.2	-0.5	0.2	9.1	-0.0	0.2	0.9	-0.4	-7.5
28	-0.0	-0.2	-0.0	0.0	-10.2	0.0	-0.2	0.0	0.0	-10.2
29	-0.0	-0.0	0.0	0.0	-10.0	0.0	0.0	0.0	-0.0	-10.1
30	0.0	0.2	0.0	0.0	-9.8	0.0	0.2	0.0	-0.0	-9.9
31	0.0	-0.2	-0.5	0.2	-9.1	0.0	-0.2	-0.5	0.2	-9.1
32	0.0	0.0	-0.1	0.1	-9.0	0.0	0.0	-0.1	0.1	-9.0
33	0.0	0.2	-0.5	0.2	-8.8	0.0	0.2	-0.5	0.2	-8.8

Table 13 : Stresses in the chassis frame for loading case 2.

Node No.	B2		WB2			BC2		WBC2		
	$(\sigma_z)_{A,D}$	$(\tau_{zs})_C$	$(\sigma_z)_A$	$(\sigma_z)_D$	$(\tau_{zs})_C$	$(\sigma_z)_{A,D}$	$(\tau_{zs})_C$	$(\sigma_z)_A$	$(\sigma_z)_D$	$(\tau_{zs})_C$
	(All stresses in Mpa)									
1	5.3	-14.3	-77.0	48.0	-4.8	-5.3	-14.3	38.9	-28.2	-10.3
2	105.5	28.8	136.6	89.4	28.9	94.9	28.3	117.4	83.3	25.5
3	-108.8	9.9	-175.3	-74.3	16.1	-126.4	9.5	-128.4	-125.4	14.3
4	-208.2	14.6	-202.7	-211.0	5.7	-222.3	14.2	-209.3	-229.0	6.0
5	-272.7	-9.3	-250.3	-279.2	-5.1	-283.3	-9.7	-277.8	-286.1	-5.3
6	-211.7	-4.7	-198.0	-218.8	-13.1	-218.7	-5.1	-205.9	-225.4	-13.6
7	-115.9	-28.6	-125.0	-111.1	-22.1	-119.4	-29.0	-127.7	-115.1	-22.6
8	-105.5	14.4	138.2	88.5	11.2	105.5	14.4	138.1	88.6	11.2
9	5.3	5.0	-77.3	48.2	-1.8	5.3	5.0	-77.2	48.1	-1.8
10	2.6	1.6	18.3	-5.5	105.5	2.6	1.6	18.3	-5.5	105.5
11	-0.0	0.0	28.0	-14.6	140.0	-0.0	0.0	28.0	-14.6	140.0
12	-2.6	-1.6	13.0	-10.8	100.4	-2.6	-1.6	13.0	-10,8	100.5
13	-5.3	-5.0	-87.8	37.6	-14.5	-5.3	-5.0	- 87.8	37.6	-14.5
14	-105.5	29.0	-72.8	-122.5	29.3	-105.5	29.4	-73.0	-122.4	29.7
15	110.6	18.9	30.1	152.4	11.0	114.1	19.4	34.8	155.3	11.6
16	211.7	4.7	225.3	204.6	9.5	218.7	5.1	231.6	212.1	10.3
17	267.4	-0.4	208.8	297.8	-6.2	278.0	0.1	207.4	314.7	-7.3
18	208.2	-14.6	213.6	205.3	-5.4	222.3	-14.2	235.3	215.5	-8.7
19	114.1	-19.6	114.2	114.0	-25.0	121.2	-19.1	39.1	163.8	-28.0
20	-105.5	14.4	-74.5	-121.7	17.6	-94.9	14.4	-72.5	-106.6	12.3
21	-5.3	14,3	-87.6	37.6	21.0	5.3	14.3	49.5	-17.7	15.9
22	-2.6	8.0	13.0	-10.8	-95.9	-2.6	-1.5	18.8	-13.8	105.9
23	-0.0	0.0	28.1	-14.6	-140.1	-0.0	-0.0	29.7	-15.4	145.3
24	2.6	-8.0	18.3	-5.5	-110.1	2.6	1.5	24.1	-8.5	110.7
25	-2.6	7.9	15.4	-12.0	-94.2	-2.6	-1.7	13.4	-11.0	97.3
26	0.0	0.0	28.7	-14.9	-138.3	-0.0	-0.0	28.2	-14.2	136.9
27	2.6	-7.9	20.7	-6.7	-108.4	2.6	1.7	18.7	-5.7	102.5
28	-2.6	-1.7	14.1	-11.7	100.8	-2.6	-1.7	14.0	-11.3	99.1
29	0.0	0.0	28.5	-14.8	140.3	0.0	0.0	28.3	-14.7	138.6
30	2.6	1.7	20.0	-6.4	105.8	2.6	1.7	19.3	-6.0	104.1
31	-2.6	-1.7	14.7	-11.6	96.6	-2.6	-1.7	14.7	-11.7	96.8
32	0.0	0.0	28.5	-14.8	136.2	0.0	0.0	28.5	-14.8	136.4
33	2.6	1.7	20.0	-6.3	101.8	2.6	1.7	20.0	-6.4	102.0

transformed to the global coordinates, using the transformation matrix of Eqn. (115). Assembling for all the elements in the global axes, using Eqn. (130) and applying the boundary conditions for simply supports , Eqn. (118) , the Eqn. (131) is solved for the frequencies of vibration. The first six frequencies of vibration are given in Table 14.

First the frequencies are obtained, neglecting the effects of rotary inertia and warping. The basic equations for this case are Eqn. (125) and (126) with the ommission of rotary inertia and warping terms. In this case linear polynomial approximation is made for θ_z. Next results are obtained including the effects of rotary inertia and warping. In this case the basic equations are Eqns. (125) and (126). Refering to the Table 14 it is observed that the frequencies of vibrations decrease with the inclusion of rotary inertia and warping, as expected. Decrease in the fifth frequency is very small. It seems fifth mode is twisting dominant mode.

Table 14 : Frequencies of vibration of a chassis frame.

(rad/sec)

Mode No.	Excluding warping and rotary inertia	Including warping and rotary inertia
1	289.80	279.65
2	386.31	360.80
3	412.62	364.32
4	418.57	369.39
5	423.24	416.10
6	606.69	524.86

CHAPTER- IV

CONCLUSIONS

The following conclusions are drawn from the present work.

1. The application of finite element method to the coupled equations of free vibration, static and buckling of beams and frames is very straight forward, even when the effects of warping, rotary inertia and shear deformation are taken into account. To find the exact solution in these cases is very difficult. The exact solution for frames with various types of beams does not seem to be possible.

2. When the effect of shear deformation is included, accurate results are obtained using six coupled second order differential equations with cubic polynomial approximation as geometrical and natural boundary conditions are satisfied exactly.

3. In the case of coupled vibrations, when the effects of rotary inertia and shear deformation are considered, the frequencies decrease. The percentage decrease in frequencies of higher modes is not always more than the percentage decrease in the lower modes, in contrast to

the uncoupled vibrations. This is because in coupled vibrations, there is an interaction between the bending modes and torsional modes hence some modes are bending dominant modes and some are torsion dominant modes. Since the effects of rotary inertia and shear are more for bending than for torsion, the percentage decrease in frequencies of bending dominant modes is more and that of torsion dominant modes is less.

4. Present formulation can take care of tapered beams in a straight forward way.

5. The normal and shear stresses change quite significantly when the warping effects are considered. The warping stresses can be as large as or even larger than the bending stresses, hence can not be ignored. In frames stresses will change with change of configuration of the beams.

APPENDIX -I

DISPLACEMENTS OF A POINT ON THE CROSS-SECTION

It is assumed that the cross-section of the thin-walled beam retains its shape when it bends and twists [2]. Thus the cross-section moves as a rigid body and such a movement can be considered as a rotation about a point (Vlasov's theorem).

Now a geometrical relationship which exists between displacements when a cross-section is rotated about an arbitrary point 'C', Fig. A.1, is established in this appendix.

The in-plane displacements :

The displacement $u_{x_A}(z)$ and $u_{y_A}(z)$ of a point A on the cross-section due to a rigid-body rotation are derived in terms of the displacements $u_{x_o}(z)$ and $u_{y_o}(z)$ of the origin 'O' (Fig. A.1). Points O and A move to O' and A' respectively. Body rotates about point C through angle θ_z.

It is seen from the Fig. A.1 that

$$FG = OE + O'H - G''H' - OF$$

or
$$u_{x_A} = u_{x_o} + x_A \cos\theta_z - y_A \sin\theta_z - x_A \qquad \ldots\ (A\text{-}1)$$

and
$$AF''' = FF' + HH' + G''A' - FA$$

or
$$u_{y_A} = u_{y_o} + x_A \sin\theta_z + y_A \cos\theta_z - y_A \qquad \ldots\ (A\text{-}2)$$

Assuming angle of rotation θ_z as small (i.e. first order theory, $\sin \theta_z \simeq \theta_z$ and $\cos \theta_z \simeq 1$), one gets

$$u_{x_A} = u_{x_o} - y_A \theta_z \quad \ldots\ (A\text{-}3)$$

$$u_{y_A} = u_{y_o} + x_A \theta_z \quad \ldots\ (A\text{-}4)$$

Similarly displacement of any other point B can be expressed as

$$u_{x_B} = u_{x_o} - y_B \theta_z \quad \ldots\ (A\text{-}5)$$

$$u_{y_B} = u_{y_o} + x_B \theta_z \quad \ldots\ (A\text{-}6)$$

Thus displacements of point A on the body can be expressed in terms of the displacement of any other point B, as

$$u_{x_A} = u_{x_B} - (y_A - y_B) \theta_z \quad \ldots\ (A\text{-}7)$$

$$u_{y_A} = u_{y_B} + (x_A - x_B) \theta_z \quad \ldots\ (A\text{-}8)$$

The above displacements u_{x_A} ; u_{y_A} etc. are in the directions of the coordinate axes. It is desirable to know the displacements in the tangential and normal directions of the section. A section VA is shown in Fig. A-2. Tanget at A is making an angle α with the x-axes. Displacement in the tangential direction is v and in the normal direction is w. It may be noted that both these are in-plane displacements. It is seen from the Fig. A-2 that

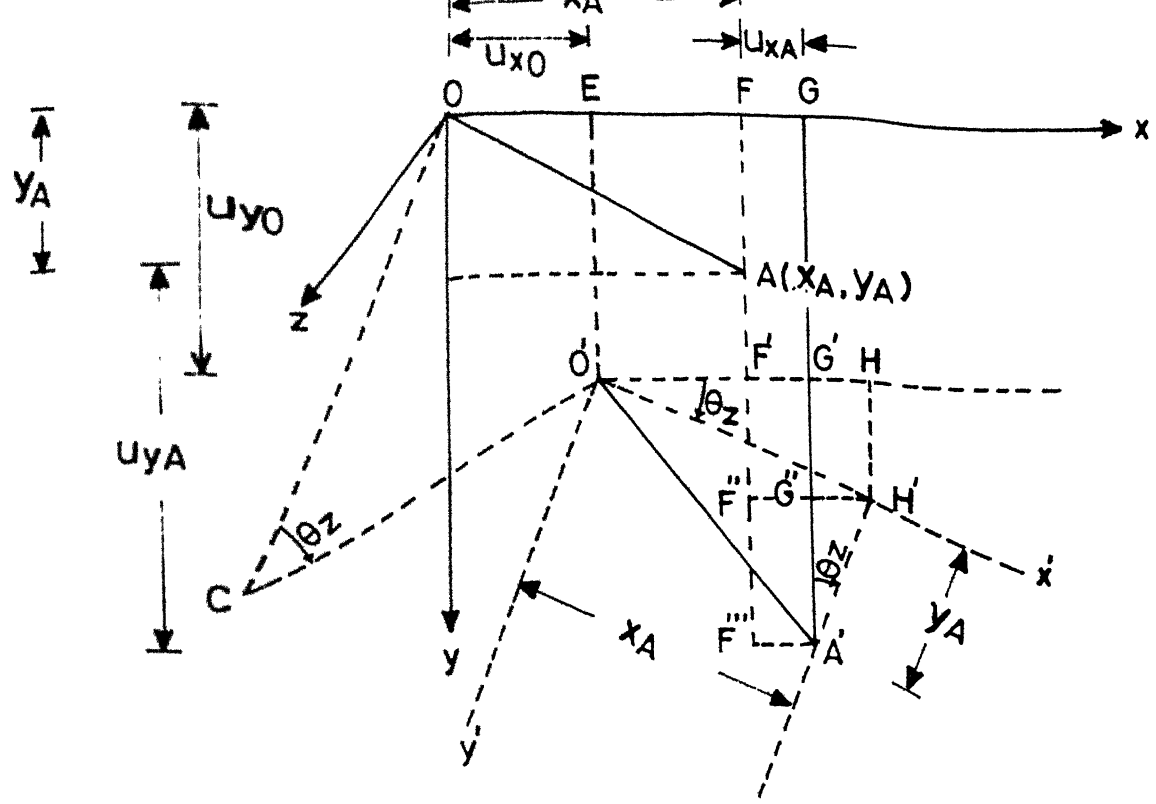

Fig. A-1 Displacements u_{xA} and u_{yA} of an Arbitrary Point A.

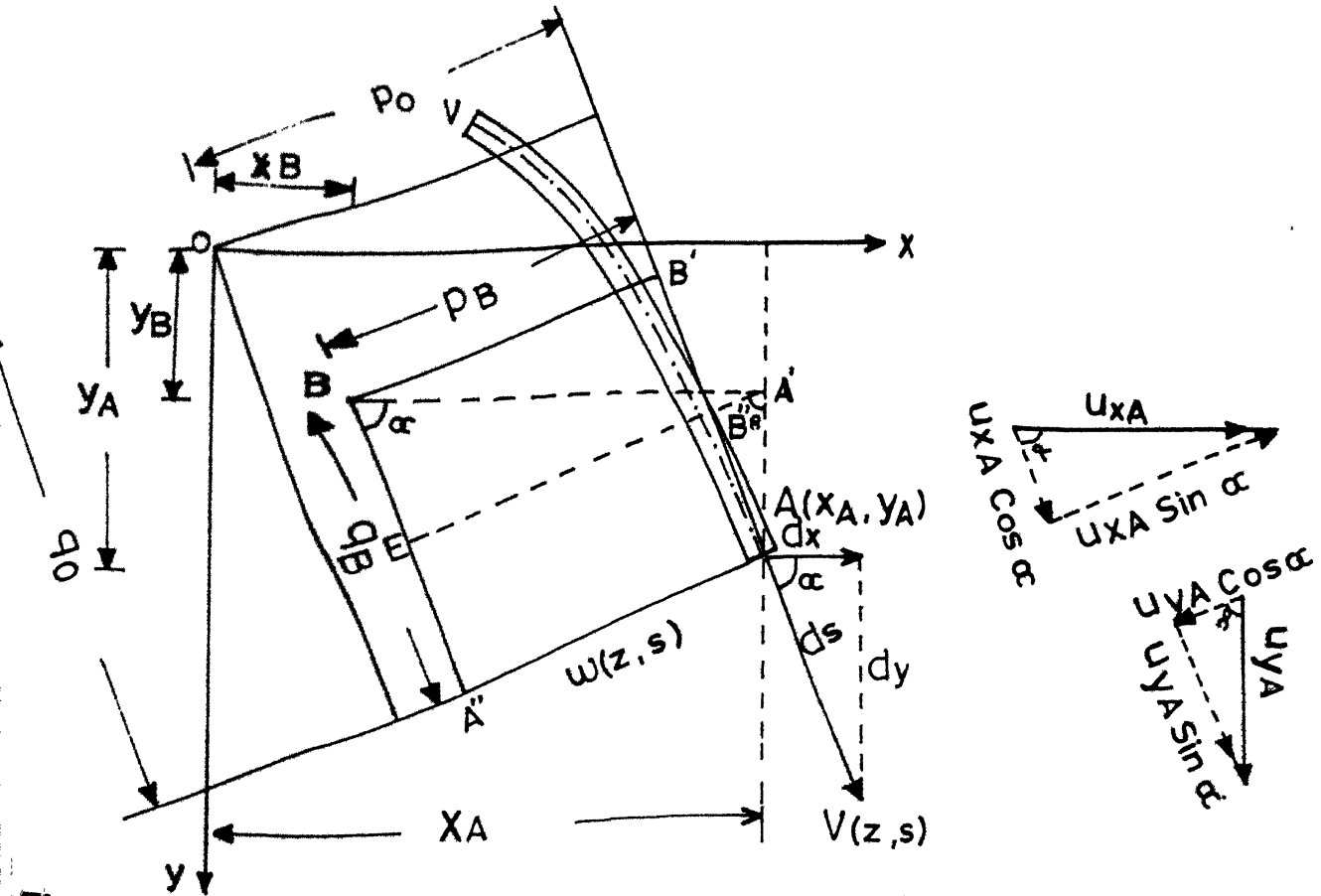

Fig. A-2 The Inplane Displacements v and w of the Point A on the Thin Walled Cross-Section.

$$v(z,s) = u_{x_A} \cos \alpha + u_{y_A} \sin \alpha$$

$$w(z,s) = -u_{x_A} \sin \alpha + u_{y_A} \cos \alpha \qquad \ldots\ (A\text{-}9)$$

Using Eqns. (A-7) and (A-8), these equations become

$$v(z,s) = u_{x_B} \cos \alpha + u_{y_B} \sin \alpha + ((x_A - x_B)\sin \alpha - (y_A - y_B)\cos \alpha)\theta_z$$

$$w(z,s) = -u_{x_B} \sin \alpha + u_{y_B} \cos \alpha + ((x_A - x_B)\cos \alpha + (y_A - y_B)\sin \alpha)\theta_z$$

$$\ldots\ (A\text{-}10)$$

From Fig. A-2, it is seen that perpendicular distances (p_B and q_B) from B to the tangent and normal can be written as

$$BB' = EA' - B''A'$$

or $$p_B = (x_A - x_B)\sin \alpha - (y_A - y_B)\cos \alpha \qquad \ldots\ (A\text{-}11)$$

Similarly $$BA'' = BE + B''A$$

or $$q_B = (x_A - x_B)\cos \alpha + (y_A - y_B)\sin \alpha \qquad \ldots\ (A\text{-}12)$$

Also $$dx = ds \cos \alpha$$

or $$\cos \alpha = \frac{dx}{ds} = \bar{x} \qquad \ldots\ (A\text{-}13)$$

Similarly $$\sin \alpha = \frac{dy}{ds} = \bar{y} \qquad \ldots\ (A\text{-}14)$$

Here bar (-) denotes differentiation with respect to s-coordinate.

Using these Eqns. (A-11) to (A-14), Eqns. (A-10) become

$$v(z,s) = u_{x_B} \bar{x} + u_{y_B} \bar{y} + p_B \theta_z \qquad \ldots\ (A\text{-}15)$$

$$w(z,s) = -u_{x_B} \bar{y} + u_{y_B} \bar{x} + q_B \theta_z \qquad \ldots\ (A\text{-}16)$$

The out-of-plane displacement for open profile sections :

The shear strain γ_{zs} is

$$\gamma_{zs} = \gamma_{\omega} + \gamma_{s}$$

Where γ_{ω} is the shear strain due to warping and γ_{s} is the shear strain due to Saint Venant torsion. For open profiles γ_{ω} is of secondary nature and is assumed to be zero at the middle surface of the profile (Vlasov's theorem). The Saint Venant shear strain γ_{s} is also zero according to Saint Venant torsion theory for the open profiles, thus

$$\gamma_{zs} = \frac{\partial u(z,s)}{\partial s} + \frac{\partial v(z,s)}{\partial z} = 0 \qquad \ldots\ldots (A\text{-}17)$$

Here u(without any subscript) is the out of plane displacement i.e. longitudinal displacement.

By integrating the Eqn.(A-17) between an arbitrary starting point V and point A on the profile distance s from V, Fig. A-2 and substituting v from Eqn. (A-15), the following expression for the displacement in the longitudinal, direction is obtained.

$$u(z,s) = u_V(z) - u'_{x_B}(z)\,(x(s) - x(0)) - u'_{y_B}(z)(y(s)-y(0)) - \theta'_z(z)\,\omega_B(s) \qquad \ldots\ldots (A\text{-}18)$$

where $\omega_B(s)$ is the warping function and is

$$\omega_B(s) = \int_0^s p_B(s)\,ds \qquad \ldots\ldots (A\text{-}19)$$

Obviously values x(o) and y(o) are constant for a given value of z. We can, therefore, incorporate their products with constant $u_y(z)$ into one constant [5] and rewrite the above equation (A-18) into a general form :

$$u(z,s)= u_a(z)-u'_{x_B}(z)\ x(s)-u'_{y_B}(z)\ y(s)-\theta'_z(z)\ \omega_B(s) \qquad \ldots\ (A\text{-}20)$$

Displacements u_x,u_y u_a and rotation θ_z can be considered to have two parts. One part with subscript b denotes the part of solution in which shear strain has been neglected and the subscript s denotes the contribution of the shear strain. Thus

$$\begin{aligned} u_{x_B} &= u_{x_{B\ b}} + u_{x_{B\ s}} \\ u_{y_B} &= u_{y_{B\ b}} + u_{y_{B\ s}} \qquad \ldots\ (A\text{-}21) \\ \theta_z &= v_{z_b} + \theta_{z_s} \\ u_a &= u_{a_b} + u_{a_s} \end{aligned}$$

Using the Eqn. (A-21), Eqn. (A-20) becomes

$$u(z,s)= u_b(z,s)+u_s(z,s)=(u_{a_b}-u'_{x_{B\ b}}x(s)- u'_{y_{B\ b}}y(s)- \theta'_{z_b}\ \omega_B(s)\ )$$

$$+(u_{a_s}-u'_{x_{B\ s}}\ x(s)- u'_{y_{B\ s}}\ y(s) - \theta'_{zs}\ \omega_B(s)\ ) \qquad \ldots\ (A\text{-}22)$$

Where $u_b(z,s)$ is the out-of-plane displacement at point A neglecting the shear strain and $u_s(z,s)$ is the out-of-plane displacement at point A due to shear strain. Displacement $u_s(z,s)$ is small compared with $u_b(z,s)$ and can be neglected [16] . Thus

$$u(z,s)= u_b(z,s)= u_{a_b} - u'_{x_{B\ b}}\, x(s) - u'_{y_{B\ b}}\, y(s) - \theta'_{z_b}\, \omega_B(s) \qquad \ldots\ (A\text{-}23)$$

$u'_{x_{B\ b}}$ and $u'_{y_{B\ b}}$ in Eqn. (A-23) are

$$u'_{x_{B\ b}} = \frac{\partial u_{x_{B\ b}}}{\partial z} \text{ and } u'_{y_{B\ b}} = \frac{\partial u_{y_{B\ b}}}{\partial z}$$

From Fig. (A-3) it is seen that above derivatives can be written as

$$u'_{x_{B\ b}} = \theta_y \text{ and } u'_{y_{B\ b}} = -\theta_x \qquad \ldots\ (A\text{-}24)$$

$\theta'_{z_b}(z)$ in Eqn. (A-23) is measure of warping and now onwards it will be denoted as $\phi(z)$.

Now onwards u_{a_b} in Eqn. (A-22) is denoted as u_a for the sake of simplicity. Thus Eqn. (A-23) becomes

$$u(z,s) = u_a(z) - \theta_y\, x(s) + \theta_x\, y(s) - \phi(z)\omega_B(s) \qquad \ldots\ (A\text{-}25)$$

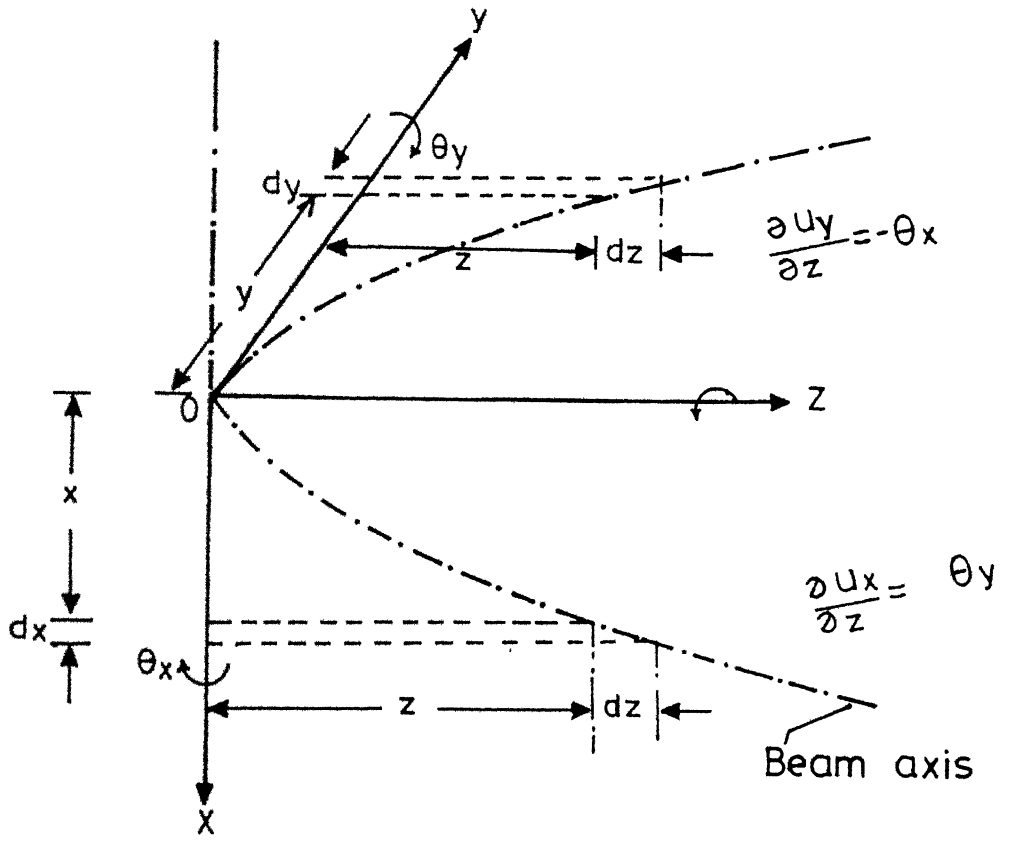

Fig. A-3 Variations of the Displacement u_x and u_y along the Beam Axis.

Where $\Psi_i(z)$ is the torsional function, independent of the material and external loading of the beam.

Hence

$$\gamma_{zs} = \frac{\partial u(z,s)}{\partial s} + \frac{\partial v(z,s)}{\partial z} = \frac{\Psi_i(z)}{t(s)} \theta'_z(z) \quad \ldots. \text{(A-30)}$$

Now integrating Eqn. (A-30) between an arbitrary starting point V and point A on the profile, distance s from V, and substituting v from the Eqn. (A-15) and using the Eqn. (A-21) and neglecting the out of plane displacement at A due to shear and using Eqn. (A-24) the following expression for the displacement in the longitudinal i.e. z direction is obtained,

$$u(z,s) = u_a(z) - \theta_y(z)\, x(s) + \theta_x(z)\, y(s) - \phi(z) \int_0^s \left(p_B(s) - \frac{\Psi_i(z)}{t(s)}\right) ds$$

$\ldots.$ (A-31)

Here $\int_0^s \left(p_B(s) - \frac{\Psi_i(z)}{t(s)}\right) ds$ is defined as the warping function $\omega_B(s)$ for the closed profile

$$\omega_B(s) = \int_0^s \left(p_B(s) - \frac{\Psi_i(z)}{t(s)}\right) ds \quad \ldots. \text{(A-32)}$$

Now Eqn. (A-31) becomes,

$$u(z,s) = u_a(z) - \theta_y(z)\, x(s) + \theta_x(z) y(s) - \phi(z)\omega_B(s)$$

$\ldots.$ (A-33)

summarizing, out of plane displacement u and in-plane tangential and normal displacements v and w for thin walled section are

$$u(z,s) = u_a - \theta_y x + \theta_x y - \phi\omega$$

$$v(z,s) = u_x \bar{x} + u_y \bar{y} + p\,\theta_z \qquad \ldots\ (A\text{-}34)$$

$$w(z,s) = -u_x \bar{y} + u_y \bar{x} + q\,\theta_z$$

where $\omega = \int_0^s p\,ds$ for open profiles

$$\omega = \int_0^s (p - \frac{\Psi_i}{t})ds \text{ for close profiles} \qquad \ldots\ (A\text{-}35)$$

Here u_x, u_y, θ_x, θ_y, θ_z, ϕ, p, q and ω all are of point B chosen.

APPENDIX- II

DERIVATION OF PRINCIPAL POLE AND PRINCIPAL ORIGINS

Consider a thin-walled cross-section , Fig. B-1,[3] which is having two contour coordinate systems s and s^* and corresponding origins O and O^*.

$p(x_p, y_p)$ is the pole of the cross section in the contour coordinate system s and

$p^*(x_p^*, y_p^*)$ is the pole of the cross section in the contour coordinate system s^*

The perpendicular distance from the point p to the tangent at any point A(x,y) on the cross section of the beam is r and the perpendicular distance to the normal at A is q. Similarly the perpendicular distance from the point p^* to the tangent at any point A(x,y) on the cross section of the beam is r^* and the perpendicular distance to the normal at A is q^*.

The coordinate of O^* in the s contour coordinate system is s_o^*.

There will be two contour warping functions $\omega(s)$ and $\omega^*(s^*)$ associated with the points pAO and p^* AO^* respectively.

By the definition of contour warping function

$$\omega(0) = 0$$
$$\omega^*(0) = 0 \qquad \ldots\ldots (B\text{-}1)$$

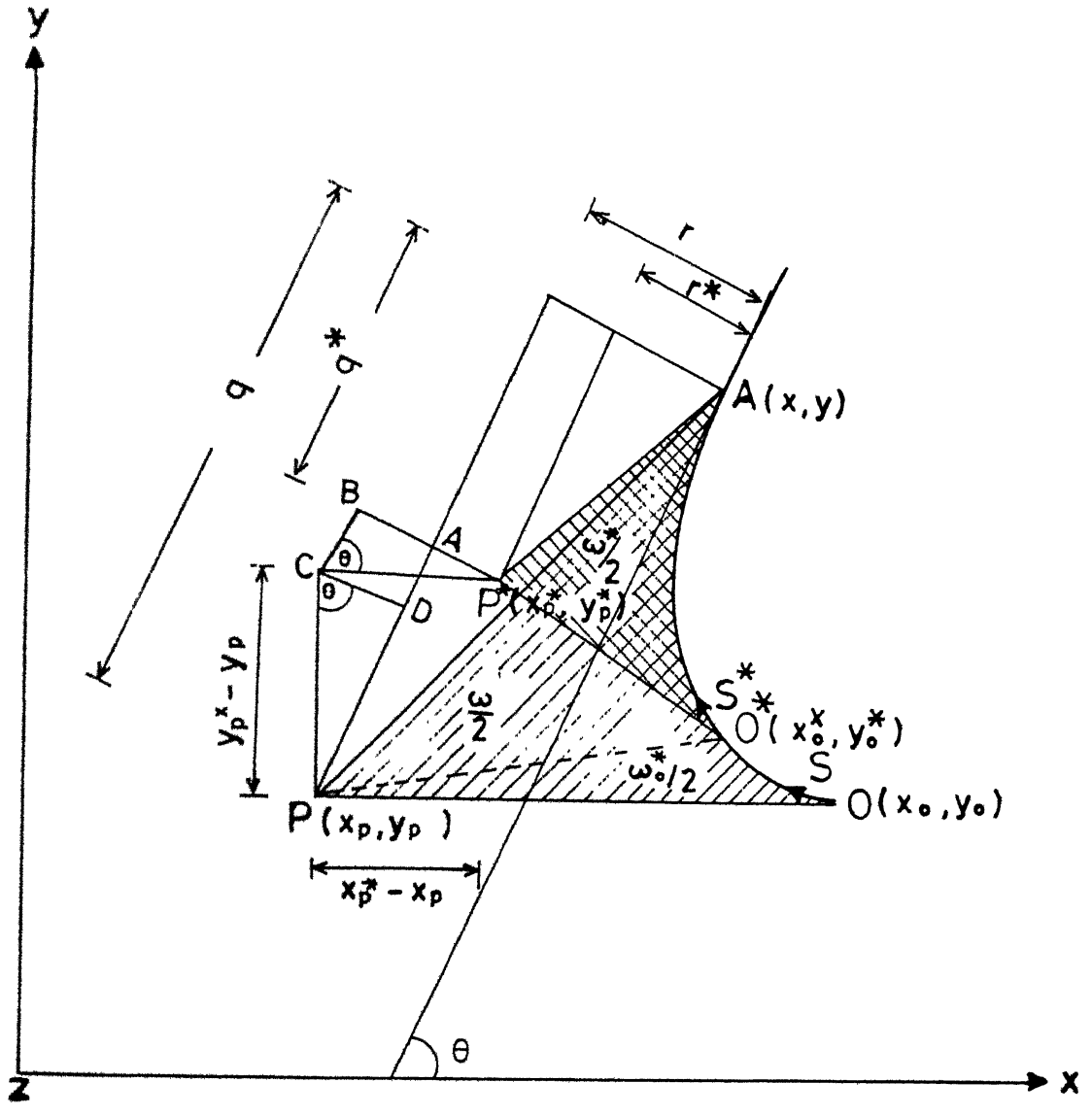

Fig.B.1 Principal Pole and Principal Origin of a Thin-Walled Cross Section.

Since the perpendicular distances r and q are dependent on the position of the pole, if the pole is changed from p to p^*, r changes to r^*.

It is seen from the Fig. B-1 that

$$r^*(s^*) = r(s) - AP^*$$

$$= r(s) - BP^* + BA = r(s) - BP^* + CD$$

$$r^*(s^*) = r(s) - (x_{p^*} - x_p)\sin\theta + (y_{p^*} - y_p)\cos\theta \quad \ldots\ (B\text{-}2)$$

$$q^*(s) = q(s) - AP$$

$$= q(s) - AD - DP = q(s) - BC - DP \quad \ldots\ (B\text{-}3)$$

$$q^*(s^*) = q(s) - (x_{p^*} - x_p)\cos\theta - (y_{p^*} - y_p)\sin\theta$$

since $\omega^* = \int_0^{s^*} r^*\, ds^*$

a change in ω^* is $\quad \ldots\ (B\text{-}4)$

$$d\omega^* = r^*\, ds^*$$

Since a change in s^*, is equal to change in s i.e. $ds^* = ds$, Fig. B-1,

$$d\omega^* = r^*\, ds \quad \ldots\ (B\text{-}5)$$

substituting for r^* from Eqn. (B-2) in (B-5) one gets,

$$d\omega^* = r(s)\,ds - (x_{p*}-x_p)\sin\theta\,ds + (y_{p*}-y_p)\cos\theta\,ds \quad \ldots\ (B\text{-}6)$$

We know that $\sin\theta\,ds = dy$, $\cos\theta\,ds = dx$ [2]

also $$r(s)\,ds = d\omega(s) \quad \ldots\ (B\text{-}7)$$

Substituting Eqn. (B-7) in Eqn. (B-6) one gets

$$d(\omega^*-\omega) = -(x_{p*}-x_p)\,dy + (y_{p*}-y_p)\,dx \quad \ldots\ (B\text{-}8)$$

Integrating Eqn. (B-8) w.r.t s between the limits s_{o*} and s i.e. between the origin O* and point A one gets

$$\omega^* = \omega-\omega_{o*}-(x_{p*}-x_p)(y-y_{o*})+(y_{p*}-y_p)(x-x_{o*}) \quad \ldots\ (B\text{-}9)$$

where

$$\omega_{o*} = \omega(s_{o*}) \quad \ldots\ (B\text{-}10)$$

ω_{o*} is the value of ω at O* and it gives the difference in the origins O and O* (Fig. B-1).

Now the properties of the cross-section w.r.t. the contour coordinate system s* can be expressed as

$$I_{\omega^*} = \int_A \omega^*\,dA$$

$$I_{\omega^* x} = \int_A \omega^* y\,dA \quad \ldots\ (B\text{-}11)$$

$$I_{\omega^* y} = \int_A \omega^* x\,dA$$

On substituting the value of ω^* from Eqn. (B-9) in (B-11) and simplyfying one gets,

$$I_{\omega^*} = \int_A [\omega - \omega_{o^*} - (x_{p^*} - x_p)(y - y_{o^*}) + (y_{p^*} - y_p)(x - x_{o^*})]\, dA$$

$$= \int_A \omega dA - \omega_{o^*} \int_A dA - (x_{p^*} - x_p)\left(\int_A y dA - y_{o^*} \int_A dA\right) + (y_{p^*} - y_p)\left(\int_A x dA - x_{o^*} \int_A dA\right)$$

$$I_{\omega^*} = I_\omega - \omega_{o^*} A - (x_{p^*} - x_p)(I_x - y_{o^*} A) + (y_{p^*} - y_p)(I_y - x_{o^*} A)$$

.... (B-12)

$$I_{\omega^* x} = \int_A \omega^* y dA = \int_A (\omega_y - \omega_{o^*} y - (x_{p^*} - x_p)(y^2 - y_{o^*} y) + (y_{p^*} - y_p)(xy - x_{o^*} y))dA$$

$$= \int_A \omega y dA - \omega_{o^*} \int_A y dA - (x_{p^*} - x_p)\left(\int_A y^2 dA - y_{o^*} \int_A y dA\right) + (y_{p^*} - y_p)\left(\int_A xy dA - x_{o^*} \int_A y dA\right)$$

$$I_{\omega^* x} = I_{\omega x} - \omega_{o^*} I_x - (x_{p^*} - x_p)(I_{xx} - y_{o^*} I_x) + (y_{p^*} - y_p)(I_{xy} - x_{o^*} I_x)$$

....(B-13)

similarly

$$I_{\omega^* y} = \int_A \omega^* x\, dA$$

$$= I_{\omega y} - \omega_{o^*} I_y - (x_{p^*} - x_p)(I_{xy} - y_{o^*} I_y) + (y_{p^*} - y_p)(I_{yy} - x_{o^*} I_y)$$

.... (B-14)

The Eqns. (B-12)to (B-14) give the change in the sectional properties when the pole and origin are changed. In the above equations, x,y axes are arbitrary.

When the axes x,y are the principal axes and the origin is located at the centroid of the cross-section, one has

$$I_x = \int_A ydA = 0$$

$$I_y = \int_A xdA = 0 \qquad \ldots\ (B\text{-}15)$$

$$I_{xy} = \int_A xy\, dA = 0$$

By making use of Eqn. (B-15) the Eqns. (B-12)to (B-15) reduce to

$$I_{\omega^*} = I_\omega - A\,(\omega_{o^*} - y_{o^*}(x_{p^*} - x_p) + x_{o^*}(y_{p^*} - y_p)) \qquad \ldots\ (B\text{-}16)$$

$$I_{\omega^* x} = I_{\omega x} - (x_{p^*} - x_p)\, I_{xx} \qquad \ldots\ (B\text{-}17)$$

$$I_{\omega^* y} = I_{\omega y} + (y_{p^*} - y_p) I_{yy} \qquad \ldots\ (B\text{-}18)$$

Eqns. (B-17) and (B-18) are independent of the position of the contour origin. From Eqns. (B-17) and (B-18) one can see that

When $x_{p^*} = x_p + \dfrac{I_{\omega x}}{I_{xx}}$ $\qquad \ldots\ (B\text{-}19)$

$I_{\omega x} = 0$

$$y_{p^*} = y_p - \frac{I_{\omega y}}{I_{yy}} \qquad \text{.... (B-20)}$$

$$I_{\omega^* y} = 0$$

The pole $p^*(x_{p^*}, y_{p^*})$ where the quantities $I_{\omega^* x}$ and $I_{\omega^* y}$ are becoming zero is called the principal pole (center of shear).

Hence when the pole of the cross-section is the principal pole (center of shear) then

$$I_{\omega^* x} = 0$$

$$I_{\omega^* y} = 0 \qquad \text{.... (B-21)}$$

From Eqn. (B-16) one knows that

when the two poles p and p* are placed at the principal pole and

$$\omega_{o^*} = \frac{I_\omega}{A} \qquad \text{.... (B-22)}$$

then

$$I_{\omega^*} = 0$$

The position of the origin O* which gives the value of ω_{o^*} (Eqn. B-22) is said to be at the principal position, i.e., O* is the principal origin of the contour coordinate system.

Hence when the origin (starting point) of the contour is the principal contour origin then

$$I_{\omega^*} = 0 \qquad \ldots. \text{(B-23)}$$

The s* contour coordinate system is the principal contour coordinate system and all the section properties with a * symbol are calculated with reference to this system.

APPENDIX- III

C.1 Section Properties of a channel section :

A channel section of breadth b and depth h, Fig. C-1 is considered. The thickness of the web is t_w and that of flange is t_f. In calculating the warping function $\omega(s)$ of the cross section, clock wise sense is taken as positive.

Consider the pole and starting point to be at the point D, Fig. C.1(a). For finding the warping function of this open profile the following equation is used,

$$\omega(s) = \int_s p \, ds \qquad (C-1)$$

where p is the perpendicular distance from the pole to the targent to the middle line of the profile at the point of consideration.

At the starting point D, s = 0. Since p is zero for both DA and DE the warping function $\omega(s)$ is zero from E to A. From E to a point lying at a distance s_1 to the right of E is

$$\omega(s_1) = - \int_0^{s_1} h \, ds = - hs_1 \qquad (C-2)$$

Here the minus sign appears because from E to F the sense of ω is anticlock wise, ie negative. Thus from E to F $\omega(s)$ is a linear function and at F it is given as

$$\omega_{FD} = - h b \qquad (C-3)$$

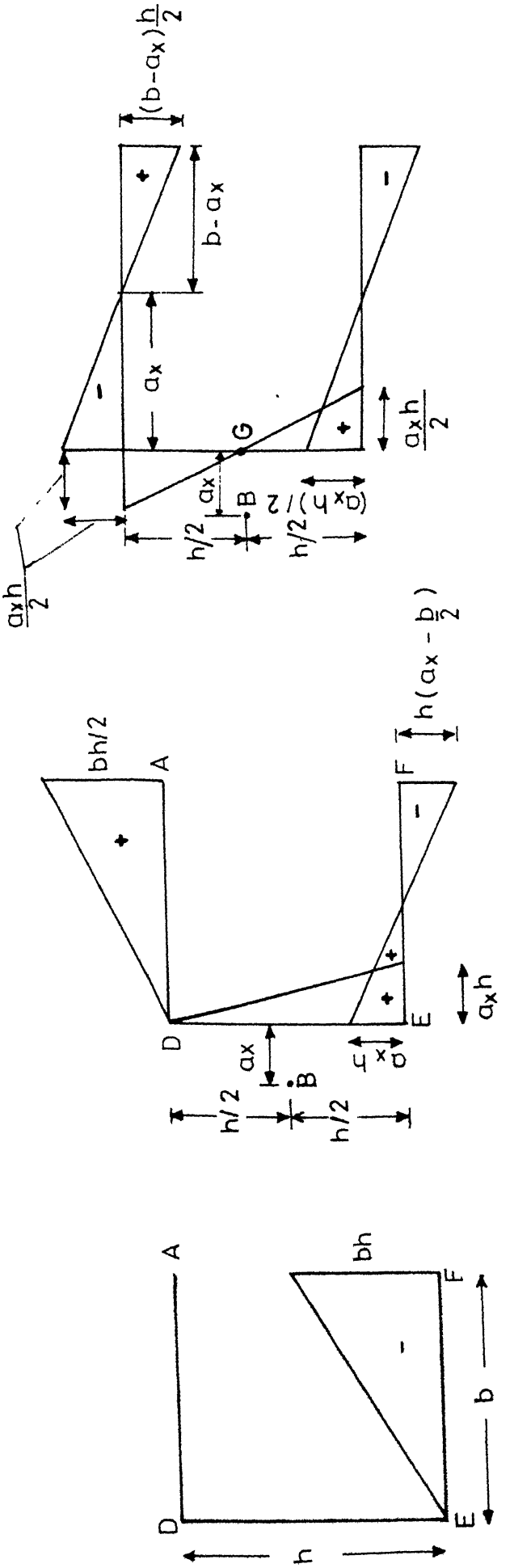

Fig. C.1 Warping Function (ω) Diagram of a Channel Section.

Refering to Fig. C.1(b) , where the starting print is at D and the pole is at B. By following the above procedure for calculating $\omega(s)$, one gets $\omega(s)$ as a linear function from D to A and at A it is

$$\omega_{AB} = \frac{bh}{2} \qquad (C-4)$$

From D to E again it is linear and at E its value is

$$\omega_{EB} = a_x h \qquad (C-5)$$

when the integration is continued up to F, the value of $\omega(s)$ becomes

$$\omega_{FB} = a_x h - \frac{bh}{2} \qquad (C-6)$$

When the starting point is at G , pole is at B, Fig. C.1(c), $\omega(s) = 0$ at G. Integrating from G to D gives a anticlockwise rotation hence $\omega(s)$ at D is

$$\omega_{DB} = - a_x \frac{h}{2} \qquad (C-7)$$

Integration from D to A involves a clockwise rotation and hence $\omega(s)$ at A is

$$\omega_{AB} = -a_x \frac{h}{2} + \frac{hb}{2} \qquad (C-8)$$

At F $\omega(s)$ is same as at A but with a negative sign.

While moving from D to A $\omega(s)$ changes its sign from -ve to +ve through a point where $\omega(s) = 0$. This point at which $\omega(s) = 0$ is at a distance of a_x from the web. At this point

where $\omega(s) = 0$, it will have maximum value of statical sectorial moment I_ω.

Hence the maximum value of I_ω at this point distant a_x from the web is

$$I_\omega(a_x) = \int_A \omega(s)\, dA = \int_S \omega(s)\, ds.\ t = \int_0^{b-a_x} t\, \omega(s)\, ds : \frac{(b-a_x)^2}{4} \cdot h\, t_f \qquad (C\text{-}9)$$

similarly $I_{\omega\omega} = \int_A \omega^2(s)\, dA$ can be obtained and can be given a

$$I_{\omega\omega} = \left(\frac{t_f\, b^3 h^2}{12}\right) \frac{3b\, t_f + 2h\, t_w}{6b\, t_f + h\, t_w} \qquad (C\text{-}10)$$

The distance a_x is given as

$$a_x = \frac{3b^2 t_f}{6b\, t_f + h\, t_w} \qquad (C\text{-}11)$$

Similarly

$$X_B = \frac{t_f\, b^2}{h\, t_w + 2b\, t_f} + \frac{3t_f\, b^2 h^2}{t_w h^3 + 2b\, t_f^3 + 6b\, t_f h^2} \qquad (C\text{-}12)$$

C-2. Section properties of an unequal channel section.

For the thin-walled beam of unequal channel section, Fig. 7, the warping function $\omega(s)$ can be calculated as describ for channel section, in the previous section. Similarly the oth section properties can be calculated.

For this section the contour coordinate of the profile of the cross-section, s is equal to -x, -y and x for the top flange, web and the bottom flange respectively.

Hence the section properties I_{qq}, I_{qp}, I_{qr}, I_{pp}, I_{pr} and I_{rr} of the unequal channel section are

$$I_{qq} = \int_A \bar{x}^2 \, dA = \int_A \left(\frac{dx}{ds}\right)^2 dA = 9.03224 \times 10^{-3} \ m^2$$

$$I_{qp} = \int_A \bar{x}\bar{y} \, dA = 0$$

$$I_{qr} = \int_A p \, \bar{x} \, dA = 0.283004 \times 10^{-3} \ m^3 \qquad (C\text{-}13)$$

$$I_{pp} = \int_A \bar{y}^2 \, dA = \int_A \left(\frac{dy}{ds}\right)^2 dA = 5.80644 \times 10^{-3} \ m^2$$

$$I_{pr} = \int_A p \, \bar{y} \, dA = 0.36768 \times 10^{-3} \ m^3$$

and $$I_{rr} = \int_A p^2 dA = 0.465625 \times 10^{-3} \ m^4$$

The non dimensionalised parameters are obtained using the properties given in Fig. 7, and Eqn. (37).

C.3 Section Properties of a box section :

Considering a thin-walled box section, of length 2a, and breadth 2b, Fig. 9 the torsional function Ψ is 2

$$\Psi = \frac{2A}{\oint \frac{ds}{t}} = \frac{2x4abxt}{4(a+b)} = \frac{2ab\ t}{(a+b)}$$

$$\frac{\Psi}{t} = \frac{2ab}{(a+b)}$$

$$I_{rr} = \int_A p^2\, dA = 2b^2x\ 2at + 2a^2x\ 2bt \qquad (C-14)$$

$$I_d = \int_A \frac{\Psi^2}{t^2}\, dA = \frac{4A^2}{\oint \frac{ds}{t}} = \frac{16a^2b^2t}{(a+b)}$$

Because of the symmetry the starting points V lie at the mid point of each side. The value of ω is same for all the corners, but they differ in signs. The value of ω at a corner of the cross section can be given as

$$\omega = \int_0^s (p - \frac{\Psi}{t})\, ds = \int_0^s (b - \frac{2ab}{a+b})\, ds = \frac{-ab(a-b)}{a+b}$$

(C-15)

Using this warping function, the sectorial moment of inertia, can be obtained as,

$$I_{\omega\omega} = \int_A \omega^2 dA = \frac{4}{3}\, t\, \frac{a^2b^2(a-b)^2}{(a+b)} \qquad (C-16)$$

REFERENCES

1. Vlasov, V.Z., "Thin-walled Elastic Beams", U.S. Department of Commerce, National Technical Information Service, 1961.

2. Murray, N.W., "Introduction to the theory of thin-walled structures," Oxford engineering science series, Oxford 1984.

3. Gjelsvik, A., "The theory of thin-walled bars", John Wiley and Sons, New York, 1981.

4. Megson, T.H.G., "Linear analysis of Thin-Walled Elastic Structures", John Wiley and Sons, New York, 1974.

5. Zbirohowski, K. and Koscia, "Thin walled beams", crosby Lockwood and Sons Ltd., London, 1967.

6. Gunnlaugsson, G.A., "A Finite Element formulation for Beams with Thin-Walled cross-sections", Computers and structures, Vol. 15, No.6, 1982, pp 691-699.

7. Bo-Zhen Chen and Yu-Ren Hu, "The torsional stiffness matrix of a Thin-walled beam and its application to beams under combined Loading", Computers and structures, vol. 28, No.3, 1988, pp 421-431.

8. Wekezer, J.W., "Elastic Torsion of Thin-walled bars of variable cross-section", Computers and Structures, vol. 19, No.3, 1984, pp 401-407.

9. Gere, J.M. and Lin, Y.K., "Coupled Vibrations of Thin-Walled Beams of Open cross sections", Journal of Applied Mechanics, vol. 25, 1958, pp 373-378.

10. Timoshenko, S., Young, D.H., and W. Weaver, JR. "Vibration problems in Engineering," John Wiley and Sons, New York, 1974.

11. Mei, C., "Coupled Vibrations of thin-walled beams of open section using the finite element method", Int. J. Mech. Sci, 12, 1970, pp 883-891.

12. Friberg, P.O., "Coupled Vibrations of Beams- An exact Dynamic Element Stiffness Matrix", Int. Journal for Numerical Methods in Engineering, Vol. 19, 1983, pp 479-493.

13. Hallauer, W.L., Jr and Liu, R.Y.L., "Beam Bending - Torsion Dynamic stiffness Method for calculations of Exact Vibration Modes", Journal of Sound and Vibration, 85(1), 1982, pp 105-113.

14. Friberg, P.O., "Beam element Matrices Derived from Vlasov's Theory of open thin-walled Elastic Beams", Int. Journal for Numerical Methods in Engineering, vol.21, 1985, pp 1205-1228.

15. Bishop, R.E.D., and Price, W.G., "Coupled Bending and Twisting of a Timoshenko Beam", Journal of Sound and Vibration, 50(4), 1977, pp 469-477.

16. Tso, W.K., " Coupled Vibrations of thin-walled elastic bars", J. Engineering Mechanics Division, ASCE, 91(EM3), 1965, pp 33-52.

17. Timoshenko, S.P. and Gere, J.M. "Theory of Elastic stability," McGraw-Hill book Company, New York, 1963.

18. Martin, H.C. "Introduction to the matrix methods of structural analysis", McGraw-Hill, New York, 1966.

19. Nosseir, T.A. and Dickinson, S.M. "The Free Vibration of a model of a car body", Journal of Sound and Vibration 15(2), 1971, pp 257-268.

20. Ali, R., Hedges, J.L., Mills, B., Norville, C.C. and Gurdogan, O. " The application of finite element techniques to the analysis of an automobile structure ", (a three-part paper dealing with the static, stress and dynamic analyses of a chassis frame). IME Proc., vol. 185,44/71, 1970-71, pp 665-690.

21. Zhang, S.H., and Lyons, L.P.R., "A thin-walled Box Beam Finite element for curved Bridge Analysis", Computers and Structures, vol. 18, No.6, 1984, pp 1035-1046.

22. Hildebrand, F.B. "Advanced calculus for applications", Prentice-Hall, INC., New Jersey, 1948.

23. Gallagher, R.H., "Finite Element Analysis", Prentice Hall, Inc. 1975.

24. Singh, K., Ph.D. Thesis, "Free Vibrational analysis of some structural components with Timoshenko effects using finite element methods". Indian Institute of Technology, Kanpur, 1982.

25. Reddy, J.N. "An introduction to the Finite Element Method", McGraw-Hill Book Company, New York, 1985.

26. Timoshenko, S. "Strength of Materials," Part 1 , D.Van Nostrand Company, INC. Princeton, 1930.

ME - 1988 - M - MUR - ANA